



Title	High-Pressure Stability of Pure Gas Hydrates
Author(s)	Sugahara, Keisuke
Citation	大阪大学, 2012, 博士論文
Version Type	VoR
URL	https://hdl.handle.net/11094/2609
rights	
Note	

The University of Osaka Institutional Knowledge Archive : OUKA

<https://ir.library.osaka-u.ac.jp/>

The University of Osaka

High–Pressure Stability of Pure Gas Hydrates

A dissertation submitted to

THE GRADUATE SCHOOL OF ENGINEERING SCIENCE

OSAKA UNIVERSITY

in partial fulfillment of the requirements for the degree of

DOCTOR OF PHILOSOPHY IN SCIENCE

by

Keisuke Sugahara

March 2012

Preface

This dissertation was carried out under the direction of Professor Kazunari Ohgaki at Division of Chemical Engineering, Department of Materials Engineering Science, Graduate School of Engineering Science, Osaka University at the period from April 2001 to September 2005 and from April 2008 to March 2009.

The purpose is to study the high-pressure stabilities of seven pure gas hydrate systems to obtain the some scientifically efficient information about fundamental properties (thermodynamic stabilities, cage occupancies, and structures) of pure gas hydrates. As a result, the scientific information may contribute to attractive engineering applications of gas hydrates.

The author hopes that the present study will be able to clarify the unknown scientific mechanisms of gas hydrates and these mechanisms will be an answer to improve some problems of environments of the earth, in addition, to lead to achievement of “Integrated EcoChemistry”.

Keisuke Sugahara



Completed the course work part of the Doctoral program (March 31, 2009) in
Division of Chemical Engineering
Graduate School of Engineering Science
Osaka University
1-3 Machikaneyama, Toyonaka, Osaka 560-8531, Japan

Contents

Summary

General Introduction	1
Gas hydrates	1
Histories of gas hydrate studies	3
Pure Gas Hydrates	4
The purpose for this thesis	9
Literature Cited	11

Chapter-I: Thermodynamic Stability and Structure of N₂ Hydrate Crystal

Abstract	15
Introduction	15
I-1 Experimental	16
I-1-1 Materials	16
I-1-2 Experimental Apparatus	16
I-1-3 Experimental Procedure	17
I-2 Results and discussion	18
Summary	23
Nomenclature	23
Literature Cited	24

Chapter-II: High-Pressure Phase Equilibrium and Raman Spectroscopic Studies on N₂O Hydrate System

Abstract	26
Introduction	26
II-1 Experimental	27
II-1-1 Materials	27
II-1-2 Experimental Apparatus	27
II-1-3 Experimental Procedure	28
II-2 Results and discussion	30

Summary	35
Nomenclature	35
Literature Cited	36

Chapter-III: Thermodynamic and Raman Spectroscopic Studies on Kr and Xe Hydrates

Abstract	38
Introduction	38
III-1 Experimental	39
III-1-1 Materials	39
III-1-2 Experimental Apparatus	39
III-1-3 Experimental Procedure	39
III-2 Results and discussion	40
Summary	47
Nomenclature	47
Literature Cited	48

Chapter-IV: Thermodynamic and Raman Spectroscopic Studies of Ar Hydrate System

Abstract	50
Introduction	50
IV-1 Experimental	52
IV-1-1 Materials	52
IV-1-2 Experimental Apparatus	52
IV-1-3 Experimental Procedure	52
IV-2 Results and discussion	54
Summary	61
Nomenclature	61
Literature Cited	62

Chapter-V: High-Pressure Phase Behavior and Cage Occupancy for the CF₄ Hydrate System

Abstract	64
-----------------	-----------

Introduction	64
V-1 Experimental	65
V-1-1 Materials	65
V-1-2 Experimental Apparatus	65
V-1-3 Experimental Procedure	65
V-2 Results and discussion	66
Summary	74
Nomenclature	74
Literature Cited	75
Chapter-VI: Thermodynamic and Raman Spectroscopic Studies on Pressure-Induced Structural Transition of SF₆ Hydrate	
Abstract	77
Introduction	77
VI-1 Experimental	78
VI-1-1 Materials	78
VI-1-2 Experimental Apparatus	78
VI-1-3 Experimental Procedure	79
VI-2 Results and discussion	80
Summary	87
Nomenclature	87
Literature Cited	88
General Conclusion	90
Literature Cited	92
List of Publications and Presentations	93
Acknowledgements	95

Summary

In this thesis, the high-pressure stabilities (structures, cage occupancies, and thermodynamics properties) of seven pure gas hydrate systems (Ar, Kr, Xe, N₂, N₂O, CF₄, and SF₆) are clarified under the three-phase coexisting conditions (hydrate, aqueous, and guest fluid phases) based on the high-pressure phase equilibrium measurements and Raman spectroscopy.

First of all, the background and the purpose of this thesis are summarized in General Introduction. In Chapter-I, thermodynamic stability of N₂ hydrate was measured in the pressure region up to 439 MPa. Based on the Raman shift of the N–N vibration, the occupancy of N₂ molecules in the L-cage was discussed. The pressure dependence of the O–O vibration of structure-II N₂ hydrates was compared with those of the structure-I hydrates. In Chapter-II, thermodynamic stability of N₂O hydrate was measured in the pressure range up to 305 MPa in order to be compared with the phase behavior of CO₂ hydrate. The cage occupancy of N₂O molecule in the structure-I N₂O hydrate phase was discussed based on the Raman spectroscopic analysis. In Chapter-III, thermodynamic stabilities of Kr and Xe hydrates were measured in the pressure region up to approximately 500 MPa. The pressure dependences of the Raman shifts of O–O vibrations were compared with those of other hydrates. In Chapter-IV, thermodynamic stability of Ar hydrate was precisely measured in the pressure region up to 485 MPa. In addition, the largest single crystals (2 mm) of Ar hydrates were prepared along stability boundary and analyzed using a laser Raman microprobe spectrometer. Based on the change of Raman shifts of the O–O vibration mode between water molecules, hydrate structural transitions were discussed. In Chapter-V, thermodynamic stability of CF₄ hydrate was measured in the pressure region up to 454 MPa and the phase behavior was compared with that of the methane hydrate. In addition, the S-cage (void, 0.51 nm in diameter) occupancy of CF₄ (van der Waals diameter, 0.52 nm) at high pressures was discussed. In Chapter-VI, six three-phase coexisting curves of SF₆ hydrate were measured in the pressure region up to 155 MPa. The location of two quadruple points Q₂ (hydrate + liquid SF₆ + gas + aqueous) and Q₃ (hydrate + liquid SF₆ + solid SF₆ + aqueous) was decided based on the extrapolation of the three-phase coexisting curves. The structural phase transition was discussed based on the discontinuousness of dp/dT on the hydrate stability curve and Raman spectra. Finally, the results obtained in this work are summarized in General Conclusion.

General Introduction

Gas hydrates [1]

Gas hydrate is one kind of inclusion compounds, which appearance is an ice-like solid. It consists of hydrogen-bonded water molecules and guest molecules, for example H_2 , noble gases, and relatively small hydrocarbons. The water molecules make frameworks with hydrogen bond and construct some small cavities, so called “hydrate cages”. In order to stabilize gas hydrates, guest molecules occupy each hydrate cage. Generally, a guest molecule occupies a hydrate cage. Schematic illustration of the enclathration of a guest molecule is shown in **Figure 1**.

Gas hydrates have three typical lattice (unit-cell) structures, that is, they are structure-I (s-I), structure-II (s-II), and structure-H (s-H), which belong to the cubic $Pm\bar{3}n$, $Fd\bar{3}m$, and hexagonal $P6/mmm$, respectively. Schematic illustration of three lattice structures is shown in **Figure 2**. The s-I is composed of two kinds of hydrate cages; one is the S-cage of pentagonal dodecahedron (5^{12}), the other is the M-cage of tetrakaidecahedron ($5^{12}6^2$). A combination of the S-cage and L-cage (hexakaidecahedron, $5^{12}6^4$) constitutes the s-II. The s-H is made from three types of cages, S-cage, S'-cage (dodecahedron, $4^35^66^3$), and U-cage (icosahedron, $5^{12}6^8$). Three S-cages, two S'-cages, and one U-cage construct the s-H. Each of five cages is illustrated in **Figure 3**. Summary on the lattice structures is listed in **Table 1**.

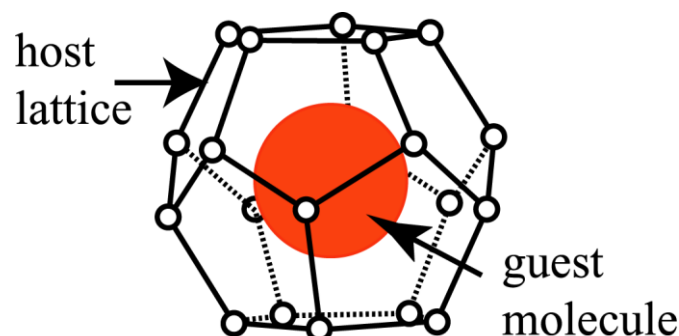


Figure 1 Schematic illustration of a molecule (for example; Xe) occupying a hydrate cage (for example; S-cage of structure-I): \bigcirc , oxygen atom; $-$, hydrogen bond.

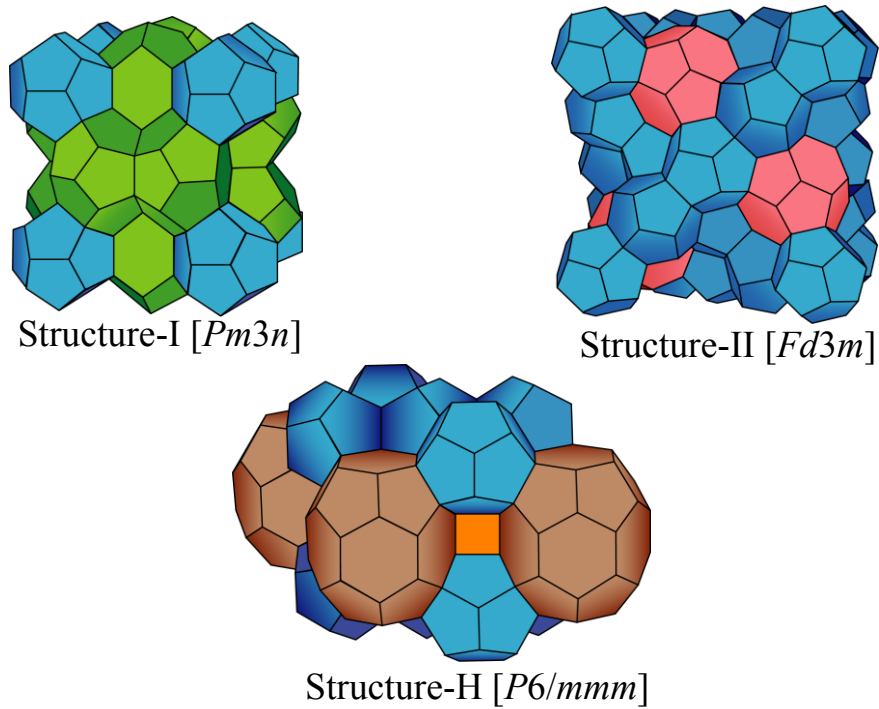


Figure 2 Schematic illustration of hydrate unit-cell structures, s-I, s-II, and s-H.

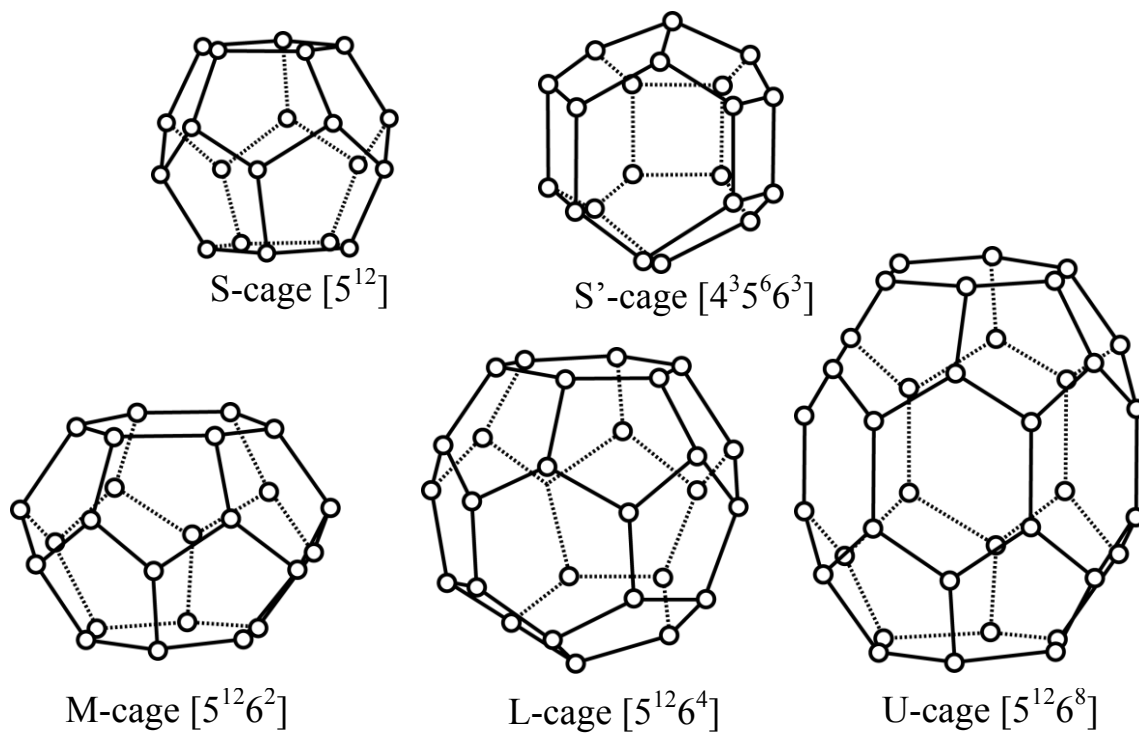


Figure 3 Schematic illustration of five hydrate cages.

Table 1 Summary on hydrate unit-cell and cages

Structures of gas hydrates							
Type of unit cell	Structure-I		Structure-II		Structure-H		
Water molecules in a unit cell	46		136		34		
Types of cages constructing unit cell	5^{12}	$5^{12}6^2$	5^{12}	$5^{12}6^4$	5^{12}	$4^35^66^3$	$5^{12}6^8$
Tag of cages in this thesis	S	M	S	L	S	S'	U
Number of cages	2	6	16	8	3	2	1
Diameter of cages / nm	0.795	0.860	0.782	0.946	0.788	0.808	1.158
Coordination number	20	24	20	28	20	20	36
Diameter of free cavities / nm	0.51	0.58	0.50	0.67	0.50*	0.53*	0.87*
Crystal type	Cubic		Cubic		Hexagonal		
Lattice constant a / nm	1.20**		1.73**		1.22***		
c / nm	-		-		1.01***		

*Subtract the diameter of water molecules (0.28 nm) from that of cage for the structure-H.

**Lattice constant for the structure-I and structure-II from Parrish and Prausnitz (1972) [2].

***Lattice constant for the structure-H from Udachin et al. (1997) [3].

Histories of gas hydrate studies

In 1810, Davy [4] discovered important facts, which overturn the former common sense about chlorine compounds. The one was that he pointed out that hydrogen chloride was an acid. Before this, the definition of an acid was that it includes an oxygen atom as the name for example sulphuric acid and nitric acid. When oxide gas (called chlorine gas) cooled under the existence of water, he found that vivid yellow "chlorine crystal" generates. This has been said to be an origin of a study on gas hydrates. After, Faraday (1823) [5] who was an assistant of Davy found out that the mole ratio of chlorine water is $\text{Cl}_2 \cdot 10\text{H}_2\text{O}$ about "chlorine crystal". 130 years later from his study, Pauling and Marsh (1952) [6] cleared that the "chlorine crystal" consists of host water molecules and guest chloride molecules using X-ray analysis

and after his study, this compound has been called chlorine hydrate. Based on an X-ray diffraction experiment, Stackelberg and Müller (1954) [7] indicated the structural models of s-I and s-II. Moreover, he has clarified that the hydrate structures depend on size of guest molecules. After that, Ripmeester et al. (1987) [8] discovered a structure-H hydrate. Now, the s-I, s-II, and s-H have been well known as the structures of gas hydrates.

Thermodynamic studies of gas hydrates represented by natural gas hydrates were rapidly developed in the middle of the 20th century. Especially, to solve the accidents in petroleum industry promotes the studies on gas hydrates; the blockage accidents of the pipeline, which were discovered by Hammerschmidt (1934) [9], were often caused by natural gas hydrates generated in the petroleum and natural gas transport pipelines at the cold areas (Russia, North America). In order to prevent the pipeline blockage, the industries requested to clarify the precise stability boundaries of natural gas hydrates in the pipelines. The researchers have clarified those stability boundaries of natural gas hydrates depend on the mixed compositions of natural gases and the addition of salts and alcohols, etc.

The methane hydrate has been regarded as potential energy resources by several researches since the 1970's. Ohgaki et al. (1994) [10] have proposed CO₂ storage method combining with methane exploitation from methane hydrate. In this process, CO₂ is poured into the methane hydrate layers for the sake of the substitute reaction from methane hydrate to CO₂ hydrate. Our researches were started to clarify the fundamental properties of gas hydrates to obtain the scientific acquaintances and the information for applied techniques of gas hydrates.

Pure Gas Hydrates

Generally the structure of gas hydrate depends on van der Waals diameter of guest molecule. Historically, van der Waals diameter has been persistently used as a standard. The classification of the hydrate structure by van der Waals diameter of guest molecule is shown in **Figure 4**.

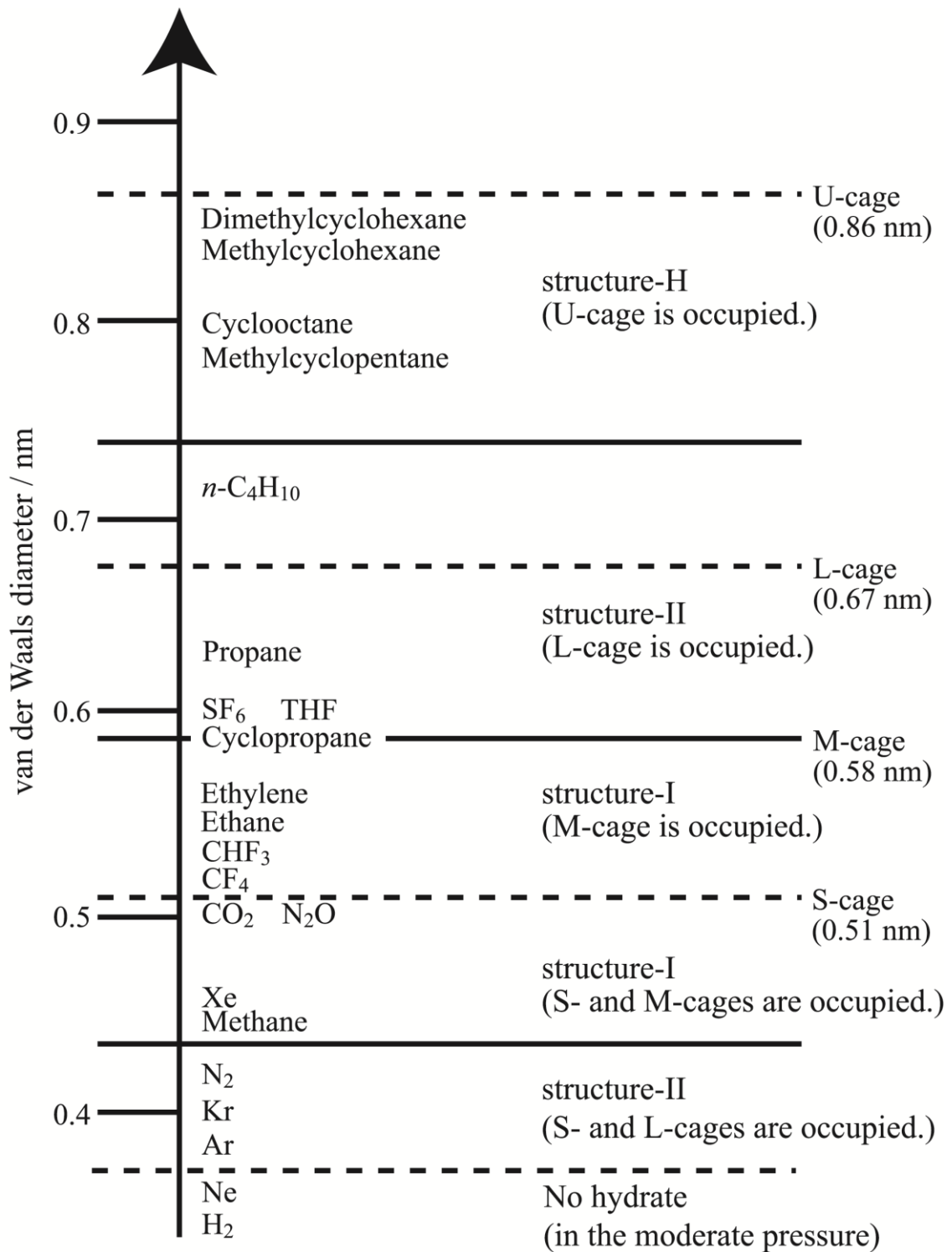


Figure 4 Molecular diameter dependence on hydrate structures and cage occupancies.

The details of the classification are as follows:

- Below 0.35 nm

Under moderate pressure conditions, He, H₂, and Ne are included into a solid ice, which resembled the ice-Ih lattice structure (Dyadin et al. 1999 [11]), which is one kind of “interstitial solid solution”. It is impossible to sweepingly say that these are forming gas hydrates because they do not have the cage structure. Dyadin et al. (1999) [11] have reported that H₂ (0.27 nm) constructs hydrate lattice (later, Mao et al. 2002 [12] have clarified the structure is s-II based on X-ray diffraction experiments).

- 0.38-0.41 nm

Ar, Kr, N₂, and O₂ hydrates belong to s-II type. Before Stackelberg and Müller (1954) proposed, it had been believed that they cannot generate hydrates or they belong to the s-I type. These guest molecules, according to the experiment by Davidson et al. (1984) [13] based on the X-ray and the neutron diffractions, occupy both S- and L-cages of the s-II.

- 0.41-0.51 nm

Methane, Xe, and CO₂ form s-I hydrate and they occupy S- and M-cages. The upper limit size (0.51 nm) is equivalent to the free-space diameter inside S-cage (0.51 nm).

- 0.52-0.58 nm

CHF₃, ethane, ethylene, and cyclopropane form s-I hydrate. These guest molecules occupy only M-cage because they are larger than the free-space diameter of S-cage. Cyclopropane is the upper limit size (0.58 nm) and equivalent to the free-space diameter of M-cage (0.58 nm). Recently, it has been cleared that ethane, ethylene, and cyclopropane occupy S-cage under high-pressure conditions. (The S-cage occupancy is later described).

- 0.59-0.70 nm

SF₆, THF, and propane form s-II hydrate and they occupy only L-cage. The existence of the vacant S-cages may result in the pressure-induced structural phase transition of hydrates. Because the S-cage occupancy of small guest species, such as H₂, methane, and CO₂, leads to the large stability of s-II hydrates. The equilibrium pressure-temperature relation of the mixed-gas hydrate is shifted to a condition milder than that of pure s-II hydrate without small guest species.

- 0.71-0.74 nm

For example, *n*-butane and benzene form s-II hydrate in the presence of help gases (methane, Xe etc.). Without help gas, *n*-butane and benzene cannot form any hydrates. Help gases occupy S-cage and large guest species like *n*-butane and benzene occupy L-cage.

- 0.75-0.86 nm

Methylcyclohexane, cycloheptane, methylcyclopentane, and *cis*-1,2-dimethylcyclohexane generate s-H hydrate in the presence of help gases. Help gases occupy S-cage and S'-cage and large guest species occupy U-cage, respectively. Nakamura et al. (2003, 2004) [14, 15] have reported that the limit for the U-cage occupancy of s-H hydrate helped by methane is laid between 1,2-dimethylcyclohexane stereo-isomers and between 1,4-dimethylcyclohexane stereo-isomers.

The molecular size of guest species has an effect upon the hydrate structure and cage occupancy as mentioned above. It has been argued that some molecules such as ethane (0.53 nm), ethylene (0.55 nm), and cyclopropane (0.58 nm) can not occupy the S-cage since they have molecular sizes larger than the S-cage. However, the direct evidences on S-cage occupancy of ethane (Morita et al. 2000 [16]), ethylene (Sugahara et al. 2000 [17]), and cyclopropane (Suzuki et al. 2001 [18]) hydrate systems have been reported based on the Raman spectroscopic analysis in a pressure range up to 500 MPa under the three-phase (hydrate + aqueous + liquid) coexisting conditions. Especially, cyclopropane hydrate shows the most characteristic S-cage occupancy by pressurization. The Raman peak intensity of the cyclopropane molecule in the S-cage increases with pressurization under the three-phase coexisting curve. The cyclopropane molecule occupies the S-cage in the pressure range above 200 MPa while the S-cage is vacant below 200 MPa. We have called these phenomena as “pressure oppressive cage occupancy”.

The lattice structure of a gas hydrate depends on the pressure, the temperature and the composition and so on. Dyadin et al. (1997) [19] have reported that the methane hydrate changes to new lattice structure at 620 MPa under the three-phase (methane hydrate + aqueous + gas) coexisting conditions.

In early 2000's, some studies on the physical properties (for example, phase transition) of methane hydrate have been reported. Hirai et al. (2000) [20] have indicated that the cubic s-I

remains stable up to *ca.* 2 GPa and that the hydrate cage decomposes into ice-VII and solid methane in the higher-pressure region. The X-ray diffraction measurement using a diamond anvil cell (DAC) was applied at room temperature in their study. Chou et al. (2000) [21] have claimed that the phase transition from the s-I to the s-II was observed at 0.1 GPa and the second transitions from the s-II to the hexagonal s-H was located at 0.6 GPa based on the X-ray diffraction and Raman spectroscopy with DAC at room temperature. Loveday et al. (2000) [22] have also studied by use of the neutron and X-ray measurements. According to their results, the s-I hydrate remains stable up to 1 GPa and a new structure (expediently MH-II, being very close to the hexagonal s-H) appears in the pressure interval of 1-2 GPa. In the higher-pressure region, an additional new structure (MH-III) becomes stable up to at least 10 GPa without further transition. The MH-III has no hydrate cage, in the sense; this crystal does not belong to the “classical” gas hydrate. Shimizu et al. (2002) [23] have studied using Raman spectroscopy with DAC. They stated that there are two transition points, s-I changes to MH-II and MH-II changes to MH-III at 0.9 and 1.9 GPa, respectively. Their results seem to be consistent with those of Loveday et al. (2000). In a pressure range of 1.9-5.2 GPa, the Raman spectra of MH-III shift to the lower energy than those of pure solid methane. Hirai et al. (2001) [24] have reported that an additional transition is laid at *ca.* 1.6 GPa. Excluding this additional transition, their results are roughly consistent with those of Loveday et al. (2000) and Shimizu et al. (2002).

Similarly, many investigators have widely studied some gas hydrate systems of small guest species. Hirai et al. (2004) [25] have summarized the results of these pressure-induced hydrate phase transitions (H₂, Ar, Kr, N₂, methane, and Xe hydrate systems). The details are not mentioned here, because these results have focused over 500 MPa (In this thesis, the maximum experimental pressure is *ca.* 500 MPa) and most of them have carried out by DAC at room temperature, which is away from three-phase coexisting conditions (hydrate + aqueous + gas). Therefore, the transition pressures have large discrepancy from the results of Dyadin’s group (hydrates decomposition curves up to 1.5 GPa), the precise measurements along the stability boundaries are needed.

As the above mentioned, the guest molecules that construct s-II hydrate can roughly divide to two groups; the one is comparatively small size molecules (Ar, Kr, N₂ etc.) and the larger molecules (SF₆, THF, propane etc.). N₂, which is a representation of smaller guests, occupies

S-cage and L-cage. However, L-cage is too large for single N₂ molecule, a possible double occupancy of N₂ in L-cage has been reported (Kuhs et al. 1997 [26]). On the other hand, the phase behavior of the larger guest molecules (for example, THF) that form s-II has been well summarized in Dyadin's book (1991) [27]. Because of the existence of vacant S-cages, there is high possibility of structural phase transition of hydrate lattice at a pressure lower than that of the smaller guest molecule (ex. methane). In the mixed-gas hydrate systems containing methane, some remarkable phenomena have been reported. According to reports, methane + ethane (Subramanian et al. 2000 [28], Hashimoto et al. 2008 [29]), methane + cyclopropane (Makino et al. 2005 [30]), and methane + CF₄ (Kunita et al. 2007 [31]) mixed-gas hydrates construct the s-II hydrate lattice at a particular composition. These guest molecules usually generate s-I hydrate lattice. The mechanism of phase transition to the s-II hydrates in certain composition regions is still unclear. A lot of unclear properties in the s-II hydrate system still remain. Therefore, the more fundamental research on the s-II hydrates is essential.

The purpose of this thesis

The purpose of this thesis is to clarify the stability of pure gas hydrates based on temperature and pressure as the operational variables. One of the factors, that dominate stabilities of gas hydrates, is cage occupancy, and the cage occupancy depends on the size and the shape of guest species. In order to clarify the effects of the pressure and the size of guest species, I have selected three noble gases (Ar, Kr, and Xe) and four pure gases (N₂, N₂O, CF₄, and SF₆) as approximately spherical molecules, and I have clarified the thermodynamic stabilities of these seven pure gas hydrate systems in the pressure region up to 500 MPa. In this thesis, first of all, I report the results of the N₂ and N₂O hydrate systems. N₂ and N₂O molecules have relatively linear shape. N₂ (0.41 nm) is the typical small guest molecule, which forms the s-II hydrate. N₂O (0.51 nm) molecule has almost the same diameter as CO₂ (0.50 nm) molecule and both molecules construct the s-I hydrate lattice as above described. Next, I have studied to study three kinds of noble gas hydrate systems. They have simple sphere shape from the smallest Ar (0.38 nm) to Kr (0.40 nm) and Xe (0.43 nm). Finally, I have studied two fluorine compounds for guest species. CF₄ (0.52 nm) was used for the guest that is substituted for all the hydrogen atoms of methane (0.41 nm) molecule in fluorine atoms. Moreover, SF₆ (0.59 nm; SF₆ forms the s-II) hydrate system has been studied. CF₄ and SF₆ are relatively

spherical shape. As a result, thermodynamics and Raman spectroscopic data for seven pure gas hydrate systems have been clarified. The thermodynamic datum is one of the most important fundamental data for understanding the properties of pure gas hydrates, such as solid phase transition of gas hydrates at high-pressures. In addition, the Raman spectroscopic studies confirm hydrate structures and the cage occupancy of guest species.

Literature Cited

- [1] Sloan, E. D. Jr.; Carolyn, C. A. "Clathrate Hydrate of Natural Gases: *Third Edition, Revised and Expanded*", Taylor & Francis / CRC Press (2008).
- [2] Parrish, W. R.; Prausnitz, J. M. "Dissociation Pressure of Gas Hydrates Formed by Gas Mixtures", *Industrial & Engineering Chemistry Process Design and Development*, **11**, 26-35 (1972).
- [3] Udachin, K. A.; Ratcliffe, C. I.; Enright, G. D.; Ripmeester, J. A. "Structure H Hydrate : A Single Crystal Diffraction Study of 2,2-dimethylpentane·5(Xe, H₂S)·34H₂O". *Supramolecular Chemistry*, **8**, 173-176 (1997)
- [4] Davy, H. "On a Combination of Oxymuriatic Gas and Oxygen Gas", *Philosophical Transactions of the Royal Society*, **101**, 155 (1811).
- [5] Faraday, M. "On Fluid Chlorine", *Philosophical transactions of the Royal Society of London*, **113**, 160 (1823)
- [6] Paulling, L; Marsh, R. E. "The Structure of Chlorine Hydrate", *Proceedings of National Academy Science*, **38** (1952).
- [7] Stackelberg, M; Müller, H. R. "Feste Gashydrate II Struktur und Raumchemie", *Zeitschrift für Elektrochemie*, **58**, 25-29 (1954).
- [8] Ripmeester, J. A.; Tse, J. S.; Ratcliffe, C. I; Powell, B. M. "A New Clathrate Hydrate Structure", *Nature*, **325**, 135-136 (1987).
- [9] Hammerschmidt, E. G. "Formation of Gas Hydrates in Natural Gas Transmission Lines", *Industrial and Engineering Chemistry*, **26**, 851 (1934).

- [10] Ohgaki, K.; Takano, T.; Moritoki, M. “Exploitation of CH₄ Hydrates under the Nankai Trough in Combination with CO₂ Storage”, *Kagaku Kogaku Ronbunshu*, **20**, 121-123 (1994).
- [11] Dyadin, Y. A.; Larionov, E. G.; Aladko, E. Y.; Manakov, A. Y.; Zhurko, F. V.; Mikina, T. V.; Komarnov, V. Y.; Grachev, E. V. “Clathrate Formation in Water-Noble Gas (Hydrogen) Systems at High Pressures”, *Journal of Structural Chemistry*, **40**, 790-795 (1999).
- [12] Mao, W. L.; Goncharov, A. F.; Struzhkin, V. V.; Guo, Q.; Hu, J.; Shu, J.; Hemley, R. J.; Somayazulu, M.; Zhao, Y. “Hydrogen Clusters in Clathrate Hydrate”, *Science*, **297**, 2247-2249 (2002).
- [13] Davidson, D. W.; Handa, Y. P.; Ratcliffe, C. I.; Tse, J. S. “The Ability of Small Molecules to Form Clathrate Hydrates of Structure II”, *Nature*, **311**, 142-143 (1984).
- [14] Nakamura, T.; Makino, T.; Sugahara, T.; Ohgaki, K. “Stability Boundaries of Gasd Hydrates Helped by Methane – Structure-H Hydrates of Methylcyclohexane and *cis*-1,2-Dimethylcyclohexane”, *Chemical Engineering Science*, **58**, 269-273 (2003)
- [15] Nakamura, T.; Sugahara, T.; Ohgaki, K. “Stability Boundary of the Structure-H Hydrate of *cis*-1,4-Dimethylcyclohexane Helped by Methane”, *Journal of Chemical and Engineering Data*, **49**, 99-100 (2004).
- [16] Morita, K.; Nakano, S.; Ohgaki, K. “Structure and Stability of Ethane Hydrate Crystal”, *Fluid Phase Equilibria* **169**, 167-175 (2000).
- [17] Sugahara, T.; Morita, K.; Ohgaki, K. “Stability Boundaries and Small Hydrate-Cage Occupancy of Ethylene Hydrate System”, *Chemical Engineering Science* **55**, 6015-6020 (2000)

- [18] Suzuki, M.; Tanaka, Y.; Sugahara, T.; Ohgaki, K. "Pressure Dependence of Small-Cage Occupancy in the Cyclopropane Hydrate System", *Chemical Engineering Science* **56**, 2063-2067 (2001).
- [19] Dyadin, Y. A.; Aladko, E. Y.; Larionov, E. G. "Decomposition of Methane Hydrates up to 15 kbar," *Medeleev Communication*, 34-35 (1997)
- [20] Hirai, H.; Hasegawa, M.; Yagi, T.; Yamamoto, Y.; Nagashita, K.; Aoki, K.; Kikegawa, T. "Methane Hydrate, Amoeba or a Sponge Made of Water Molecules ", *Chemical Physics Letters*, **325**, 490-498 (2000).
- [21] Chou, I. M.; Sharma, A.; Burruss, R. C.; Shu, J.; Mao, H.-K.; Hemley, R. J.; Goncharov, A. F.; Stern, L. A.; Kirby, S. H. "Transformations in Methane Hydrates", *Proceedings of the National Academy of Sciences of the United States of America* , **97**,13484-13487 (2000).
- [22] Loveday, J. S.; Nelmes, R. J.; Guthrie, M.; Belmonte, S. A.; Allan, D. R.; Klug, D. D.; Tse, J. S.; Handa, Y. P. "Stable Methane Hydrate above 2 GPa and the Source of Titan's Atmospheric Methane", *Nature*, **410**, 661-663 (2000).
- [23] Shimizu, H.; Kumazaki, T.; Kume. T.; Sasaki, S. "In Situ Observations of High-Pressure Transformations in a Synthetic Methane Hydrate", *Journal of Physical Chemistry B*, **106**, 30-33 (2002).
- [24] Hirai, H.; Uchihara, Y.; Fujihisa, H.; Sakashita, M.; Katoh, E.; Aoki, K.; Nagashima, K.; Yamamoto, Y.; Yagi, T. "High-Pressure Structure of Methane Hydrate Observed up to 8 GPa at Room Temperature", *Journal of Chemical Physics*, **115**, 7066-7070 (2001).
- [25] Hirai, H; Tanaka, T; Kawamura, T.; Yagi, T. "Structural Changes in Gas Hydrates and Existence of a Filled Ice Structure of Methane Hydrate above 40 GPa", *Journal of Physics and Chemistry of Solid*, **65**, 1555-1559 (2004)

- [26] Kuhs, W. F. Chazallon, B.; Radaelli, P. G.; Pauer, F. "Cage Occupancy and Compressibility of Deuterated N₂-Clathrate Hydrate by Neutron Diffraction", *Journal of Inclusion Phenomena*, **29**, 65-77 (1997).
- [27] Dyadin, Y. A.; Bondaryuk, I. V.; Zhurko, F. V. "Inclusion Compounds Vol. 5 Chapter 7, Inorganics and Physical Aspects of Inclusion" , (Atwood, J. L.; Davies, J. E. D.; MacNichol, D. D., eds.), OXFORD UNIVERSITY PRESS (1991)
- [28] Subramanian, S.; Kini, R. A.; Dec, S. F; Sloan, E. D. "Evidence of Structure II Hydrate Formation from Methane + Ethane Mixtures", *Chemical Engineering Science*, **55**, 1981-1999 (2000).
- [29] Hashimoto, S; Sasatani, A.; Matsui, Y.; Sugahara, T.; Ohgaki, K. "Isothermal Phase Equilibria for Methane + Ethane + Water Ternary System Containing Gas Hydrates", *The Open Thermodynamics Journal*, **2**, 100-105 (2008).
- [30] Makino, T.; Tongu, M.; Sugahara, T.; Ohgaki, K. "Hydrate Structural Transition Depending on the Composition of Methane + Cyclopropane Mixed Gas Hydrate", *Fluid Phase Equilibria*, **233**, 129- 133 (2005).
- [31] Kunita, Y.; Makinio, T.; Sugahara, T.; Ohgaki, K. "Raman Spectroscopic Studies on Methane + Tetrafluoromethane Mixed-Gas Hydrate System", *Fluid Phase Equilibria*, **251**, 145-148 (2007).

Chapter-I: Thermodynamic Stability and Structure of N₂ Hydrate Crystal

Abstract

Stability boundary for the N₂ hydrate system has been investigated in a temperature range of (285 to 310) K and pressure range up to 440 MPa. The present experimental results show that nitrogen hydrates form structure-II without any solid-solid phase transition under the present experimental conditions. The strong pressure dependence of intermolecular O–O vibration reveals that hydrate cage is shrunk by pressurization.

Introduction

There are two kinds of gas hydrates in the nature; natural gas hydrates and air hydrates. Recently, the former have attracted much attention as a potential energy resource. For this reason, the methane hydrate system has been widely studied. The latter entrapped in the sedimentary ice of circumpolar region also have been of considerable interest because the paleoclimatic changes can be speculated from composition analysis of guest species. According to Hondoh et al. (1990) [1] the structure of air hydrates (N₂ and oxygen guest molecules in clathrate hydrates) in the ice core from Greenland (Dye-3) has identified as the structure-II (s-II).

The N₂ molecule is regarded to generate the s-II hydrate because of its smaller van der Waals diameter as well as argon and oxygen in the moderate pressure region. And N₂ molecule occupies both the S- and L-cages. According to van Hinsberg and Schouten (1994) [2], the N₂ hydrate lattice belongs to the s-II in a pressure range up to 750 MPa. On the other hand, Kuhs et al. (1997) [3] have reported that two N₂ molecules would be able to occupy both the L-cage of the s-II hydrate lattice and the M-cage of the structure-I (s-I) hydrate lattice (metastable) in a pressure range up to 250 MPa. The thermodynamic stability boundary for N₂ hydrate system has been reported by many investigators, such as van Cleeff and Diepen (1960) [4], Marshall et al. (1964) [5], Jhaveri et al. (1965) [6], and Dyadin et al. (2001) [7].

The thermodynamic stability usually depends on the pressure-temperature conditions. Dyadin et al. (2001, 1997) [7, 8] have stated that not only the N₂ hydrate but also the methane hydrate has the structural phase transition points under the certain pressure-temperature conditions. The discontinuity of dp/dT on the stability boundary is one of the most important index information in order to identify the structural phase transitions.

It is the main subject in this chapter to clarify the thermodynamic stability and the structure of pure N₂ hydrate at a pressure up to 500 MPa by use of Raman spectroscopy.

I-1 Experimental

I-1-1 Material

Research grade N₂ of purity 99.9995 mol % was purchased from Neriki Gas Co. Ltd. The distilled water was obtained from Yashima Pure Chemicals Co. Ltd. Both of them were used without further purification.

I-1-2 Experimental Apparatus

The experimental apparatus were essentially the same as that used previously (Nakano et al. 1998 [9]). Schematic diagram of the high-pressure optical cell used in this chapter is shown in **Figure I-1**. The cell made of stainless steel, SUS630), a mixing ball, a high-pressure pump for supplying and/or pressurizing the samples, an intensifier, pressure gauges, a temperature control system, and a charge-coupled device (CCD) camera. The cell was designed and manufactured to establish the equilibrium conditions for measuring the three-phase coexisting curve and to prepare the hydrate single crystal for performing in situ laser Raman spectroscopic analysis, simultaneously. The inner volume of the cell is approximately 0.2 cm³ and the maximum working pressure is 500 MPa. A pair of sapphire window (thickness was 5.5 mm) was set at both sides of the internal space. Each window was sealed with a packing made of Teflon type material. The depth and diameter of the internal space, which was enveloped in both windows, were 4.5 mm and 7 mm, respectively. A ruby ball of 2 mm in diameter was enclosed with the sample to agitate the system by vibration from outside. The system temperature was controlled by the thermostated water circulating from a thermocontroller (EYELA NCB-3100) through the jacket in the cell.

I-1-3 Experimental Procedure

A desired amount of Ar was introduced into the evacuated and cooled cell. The contents were pressurized up to the desired pressure by successive supply of water. After the formation of Ar hydrate, in order to establish the three-phase (hydrate + aqueous + gas) equilibrium, the system temperature was gradually increased and the contents were agitated intermittently. The phase behavior of the system was observed by the CCD camera through the sapphire window. The equilibrium temperature was measured within a reproducibility of 0.02 K using a thermistor probe (Takara D-641) calibrated by a Pt resistance thermometer (25 Ω) into the water bath or a hole in the cell wall. For pressure measurement, two different pressure gauges were used according the working pressure. A pressure transducer (NMB STD-5000K) and digital peak holder (NMB CSD-819) was used with an estimated maximum uncertainty of 2 MPa.

After the preparation of single crystal at the three-phase coexisting equilibrium under several pressure conditions, the Raman spectra were measured. The largest single crystal was aged more than a couple of weeks. (According to Nakano et al. (1998) [9], it is necessary to establish an annealing method for obtaining clear single crystals of gas hydrates for the Raman spectroscopy. The generated gas hydrate was annealed with a temperature cycle method (0.05 K one cycle per day) during a few days in the present experiment. In a higher pressure region, quite larger single crystals of gas hydrates were formed.). In several equilibrium conditions, N₂ hydrate crystals were analyzed using a laser Raman microprobe spectrometer with a multichannel CCD detector (Jobin Yvon Ramanor T64000). The laser beam from the object lens irradiated the sample through the upper sapphire window. The backscatter of the opposite direction was taken in with the same lens. The argon ion laser beam of 514.5 nm and 100 mW was condensed to 2 μm spot diameter. The spectral resolution was about 1 cm^{-1} . The integration time was varied within the range 60 to 300 sec, depending on the intensity of light scattering.

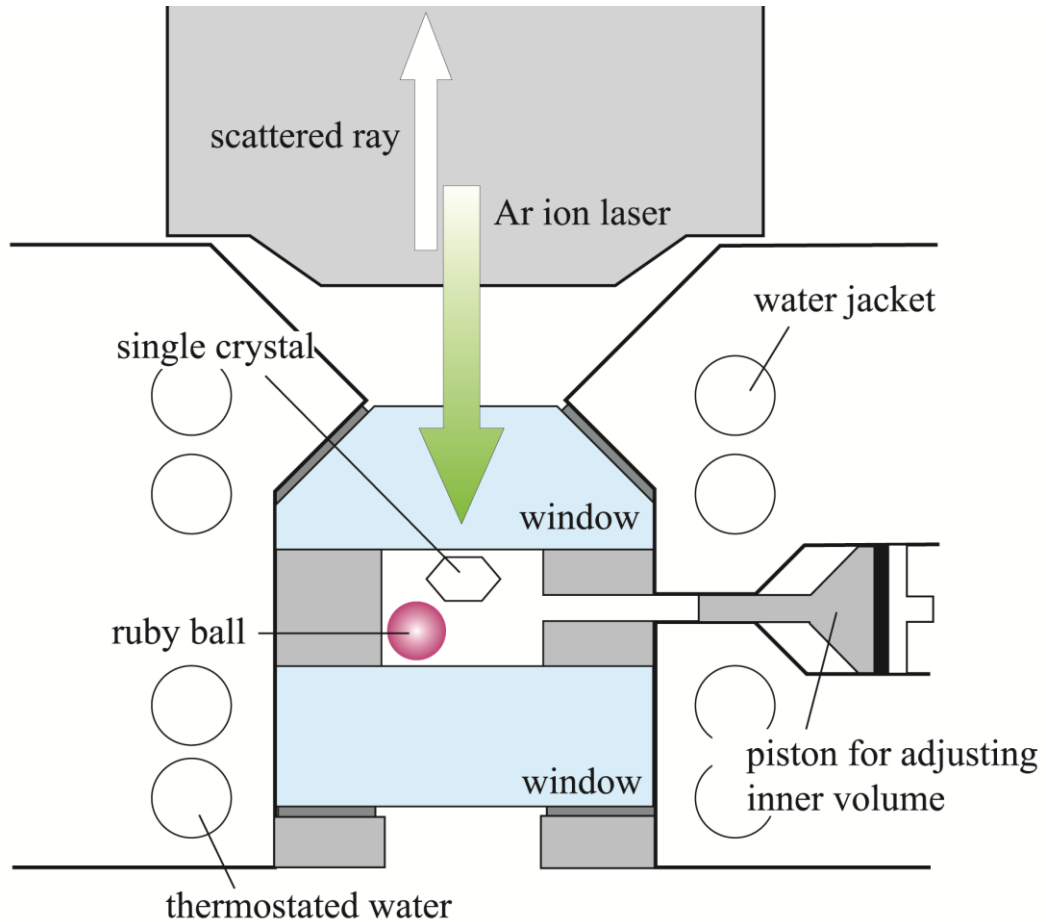


Figure I-1 Schematic illustration of the high-pressure cell (Maximum pressure; 500 MPa).

I-2 Results and discussion

The stability boundary (three-phase coexisting) curve for the N₂ hydrate system is listed in **Table I-1** and plotted on the plane of pressure versus temperature in **Figure I-2**. The experimental data obtained in the present study are in good agreement with the data of Marshall et al. (1964) [5], van Cleeff and Diepen (1960) [4], while the data of Dyadin et al. (2001) [7] slightly increase in the decomposition temperature at low pressures compared to the present study. Dyadin et al. (2001) [7] stated that the first structural phase transition point of the N₂ hydrate lattice has been observed at 314.65 K and 650 MPa, but they didn't mention about the next lattice structure for N₂ hydrate after the structural transition. The smoothness of the three-phase coexisting curve reveals that the crystal structure of N₂ hydrate never changes in the pressure range up to 440 MPa.

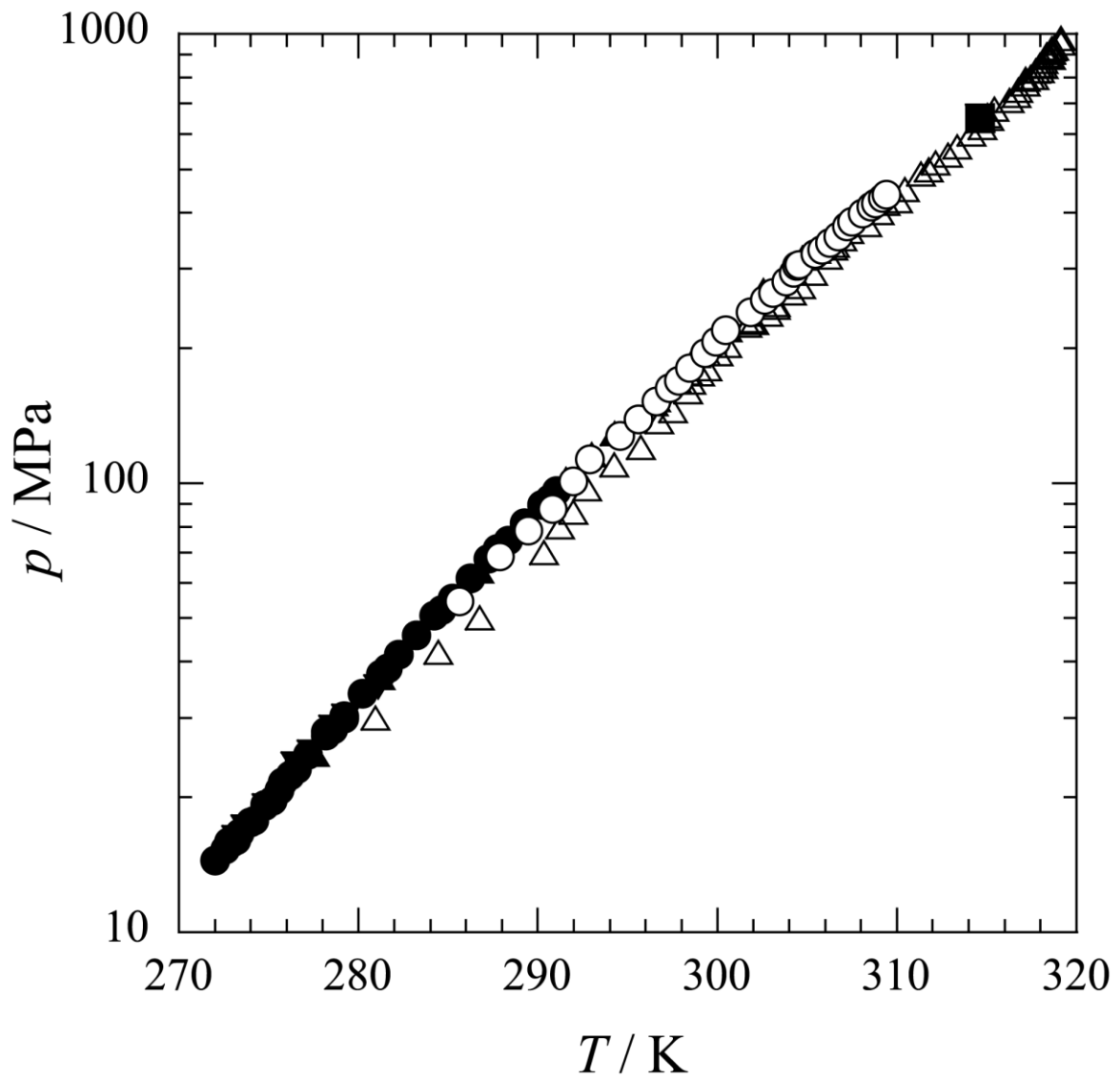


Figure I-2 Three-phase coexisting curve for the N_2 hydrate system: \circ , present study; \blacktriangledown , Jhaveri and Robinson (1965) [6]; \bullet , van Cleeff and Diepen (1960) [4]; \blacktriangle , Marshall et al. (1964) [5]; \triangle , Dyadin et al. (2001) [7]; \blacksquare , Structural phase transition point (Dyadin et al. 2001 [7]).

Table I-1 Three-phase coexisting curve for the N₂ hydrate system.

T / K	p / MPa	T / K	p / MPa
285.63	55	303.08	265
287.87	69	303.82	280
289.47	78	304.23	294
290.80	88	304.43	304
291.96	101	304.56	306
292.90	113	305.46	324
294.60	127	305.85	331
295.61	139	306.26	342
296.62	152	306.74	354
297.32	162	307.21	373
297.86	169	307.50	383
298.47	180	308.09	398
299.31	195	308.57	412
299.92	206	308.82	420
300.49	219	309.21	431
301.86	240	309.43	439
302.64	256		

A sufficient scale crystal is very important for *in situ* Raman spectroscopy, because the focal point of laser beam and its surroundings should be kept away from the fluid phase, otherwise the N₂ molecule in the fluid phase would give direct effects upon the Raman spectra. The N₂ hydrate is one of the most difficult substances to generate the clear single crystal. Gas hydrates normally grow to the single crystal easily in a high-pressure region of several hundreds MPa (Nakano et al. 1998 [9]). However, a large scale of N₂ hydrate crystal is not obtained with an ordinary aging method of our previous experiments. A typical

photograph of hydrate crystals is shown in **Figure I-3**. The largest crystal (*ca.* 0.5 mm) among them, which was aged more than a couple of weeks at 283 K and 270 MPa, shows clear crystal form. As it is still unclear now what interrupts the crystal growth of N₂ hydrate, all I can do is to spend much time on aging procedures.

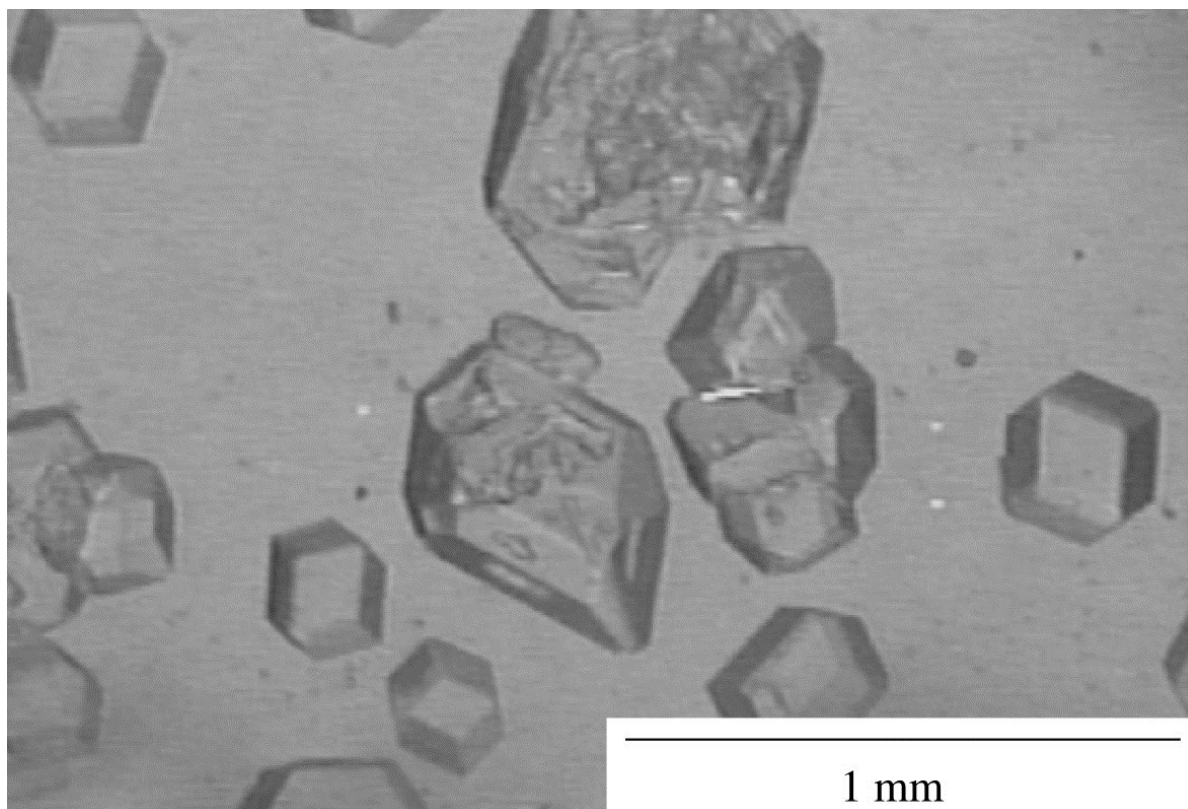


Figure I-3 A photo of single crystals of N₂ hydrate at 283 K and 270 MPa.

The N₂ molecule has only one Raman-active vibration mode. According to Hinsberg et al. (1993) [10] a single Raman peak was detected around 2325 cm⁻¹ for the symmetric N–N stretching vibration in the N₂ hydrate phase. A Raman peak is detected around 2324 cm⁻¹ and its pressure dependency is quite small. Kuhs et al. (1997) [3] stated that two N₂ molecules are able to occupy the L-cage of the s-II hydrate lattice at pressures below 30 MPa. However, I am not able to obtain positive evidence of “double occupancy”. The present experimental results show that there is no structural phase transition in the present pressure region.

The Raman spectrum of intermolecular O–O vibration mode of water is observed 210 cm⁻¹ in the N₂ hydrate crystal at 100 MPa. The pressure effect on the O–O vibration in the N₂ hydrate is shown in **Figure I-4** accompanied with the results of CO₂ (Nakano et al. 1998 [9]), methane (Nakano et al. 1999 [11]), ethane (Morita et al. 2000 [12]), ethylene (Sugahara et al.

2000 [13]), cyclopropane (Suzuki et al. 2001 [14]). The pressure dependence of the O–O vibration in the N₂ hydrate is similar to those of methane and CO₂ hydrates. And the O–O vibration energies of s-II N₂ hydrate are higher than those of s-I hydrates. The gas hydrates which consist of small guest species show considerably strong pressure dependency, that is, the hydrate cage entrapping small guest species is easily shrunk on pressurizing. The sufficient free volume for N₂ in the S-cage as well as the L-cage is supported by the following fact; the Raman shift for the symmetric N–N stretching vibration mode shows very weak pressure dependency in the present experimental conditions. In other words, the N₂ molecule is so small that the symmetric N–N vibration is not repressed in the compressed S-cage.

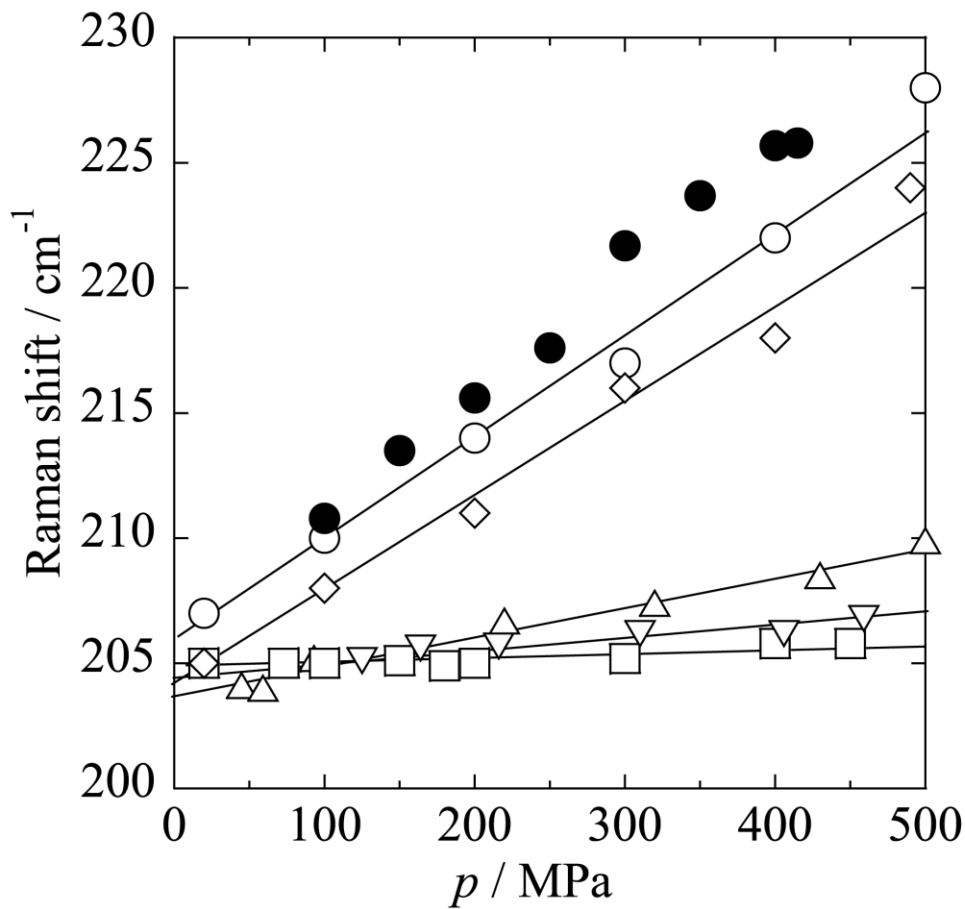


Figure I-4 Pressure effect on the O–O vibration in the N₂, CO₂, methane, ethane, ethylene, and cyclopropane hydrate systems: ●, N₂ hydrate; ○, methane hydrate (Nakano et al. 1999 [11]); ◇, CO₂ hydrate (Nakano et al. 1998 [9]); □, ethane hydrate (Morita et al. 2000 [12]); △, ethylene hydrate (Sugahara et al. 2000 [13]); ▽, cyclopropane hydrate (Suzuki et al. 2001 [14]).

Summary

The three-phase coexisting curve for the N₂ hydrate system has been determined in the temperature range of (285 to 310) K and pressure range up to 440 MPa. The single crystal of N₂ hydrate has been analyzed by use of Raman spectroscopy.

The present study on the N₂ hydrate phase reveals that the N₂ hydrate crystal belongs to the s-II lattice in the pressure range up to 440 MPa. The behavior of the three-phase coexisting curve also supports that the crystal structure of N₂ hydrate never changes in the present experimental conditions.

The Raman shift for the O–O vibration on the N₂ hydrate shows strong pressure dependence, that is, the N₂ hydrate cage is easily shrunk by pressurization. In contrast, the Raman shift for the symmetric N–N stretching vibration shows very weak pressure dependence. These results suggest that the N₂ molecule is so small that the symmetric N–N vibration is not affected by pressurization.

Nomenclature

p = pressure [Pa]

T = temperature [K]

Literature Cited

- [1] Hondoh, T.; Anzai, H.; Goto, A.; Mae, S.; Higashi, A.; Langway, Jr, C.C. "The Crystallographic Structure of the Natural Air-Hydrate in Greenland Dye-3 Deep Ice Core" *Journal of Inclusion Phenomena and Molecular Recognition in Chemistry*, **8**, 17-24 (1990).
- [2] van Hinsberg, M. G. E.; Schouten, J. A. "The Phase Diagram of Nitrogen Clathrate Hydrate" *AIP Conference Proceedings*, **309**, 271-274 (1994).
- [3] Kuhs, W. F. Chazallon, B.; Radaelli, P. G.; Pauer, F. "Cage Occupancy and Compressibility of Deuterated N₂-Clathrate Hydrate by Neutron Diffraction" *Journal of Inclusion Phenomena*, **29**, 65-77 (1997).
- [4] van Cleeff A.; Diepen, G. A. M. "Gas Hydrates of Nitrogen and Oxygen" *Recueil des Travaux Chimiques des Pays-Bas*, **79**, 582-586 (1960).
- [5] Marshall, D. R.; Saito, S.; Kobayashi, R. "Hydrates at High Pressures: Part I. Methane-Water, Argon-Water, and Nitrogen-Water Systems" *American Institute of Chemical Engineers Journal*, **10**, 734-739 (1964).
- [6] Jhaveri, J.; Robinson, D. B. "Hydrates in the Methane-Nitrogen System" *Canadian Journal of Chemical Engineering*, **43**, 75-78 (1965).
- [7] Dyadin, Y. A.; Larionov, E. G.; Aladko, E. Y.; Zhurko, F. V. "Clathrate Nitrogen Hydrate at Pressures of up to 15 kbar" *Doklady Physical Chemistry*, **378**, 159-161 (2001).
- [8] Dyadin, Y. A.; Aladko, E. Y.; Larionov, E. G. "Decomposition of Methane Hydrates up to 15 kbar," *Medeleev Communication*, 34-35 (1997)

- [9] Nakano, S.; Moritoki, M.; Ohgaki, K. “High-Pressure Phase Equilibrium and Raman Microprobe Spectroscopic Studies on the CO₂ Hydrate System” *Journal of Chemical and Engineering Data*, **43**, 807-810 (1998).
- [10] van Hinsberg, M. G. E.; Scheerboom, M. I. M.; Schouten, J. A. “The Vibration Spectra of N₂ Clathrate-Hydrates: A New High-Pressure Phase Transition” *Journal of Chemical Physics*, **99**, 752-754 (1993).
- [11] Nakano, S.; Moritoki, M.; Ohgaki, K. “High-Pressure Phase Equilibrium and Raman Microprobe Spectroscopic Studies on the Methane Hydrate System” *Journal of Chemical and Engineering Data*, **44**, 254-257 (1999).
- [12] Morita, K.; Nakano, S.; Ohgaki, K. “Structure and Stability of Ethane Hydrate Crystal” *Fluid Phase Equilibria*, **169**, 167-175 (2000).
- [13] Sugahara, T.; Morita, K.; Ohgaki, K. “Stability Boundaries and Small Hydrate-Cage Occupancy of Ethylene Hydrate System” *Chemical Engineering Science*, **55**, 6015-6020 (2000)
- [14] Suzuki, M.; Tanaka, Y.; Sugahara, T.; Ohgaki, K. “Pressure Dependence of Small-Cage Occupancy in the Cyclopropane Hydrate System” *Chemical Engineering Science*, **56**, 2063-2067 (2001).

Chapter-II: High-Pressure Phase Equilibrium and Raman Spectroscopic Studies on N₂O Hydrate System

Abstract

Thermodynamic stability boundaries of N₂O hydrate and Raman spectra of the N₂O and host water molecules in the N₂O hydrate system have been investigated in a temperature range of (275.20 to 298.19) K and a pressure range up to 305 MPa. Two three-phase coexisting curves of (hydrate + aqueous + gas) and (hydrate + aqueous + liquid N₂O) originate from the quadruple point of (hydrate + aqueous + liquid N₂O + gas) located at (285.15±0.05) K and (4.2±0.1) MPa. The phase behavior of N₂O hydrate system is similar to that of carbon dioxide (CO₂) hydrate system up to 100 MPa, while the stability boundaries of N₂O hydrate system are shifted parallel to 2-3 K higher temperature side than that of CO₂ hydrate. Raman peak splitting of the intramolecular vibration mode for the nitrous oxide molecule in hydrate phase indicates the occupancy of nitrous oxide molecule in both small and large cages of structure-I, and this observation is also corroborated by the pressure-induced Raman shift of lattice mode.

Introduction

N₂O (0.51 nm) is one of guest species forming structure-I (s-I) hydrate. N₂O hydrate has a long history, the existence of N₂O hydrate was found by Villard (1888) [1]. After that, the thermodynamic stability boundary was reported in a lower pressure region than the quadruple point (Q₂) of (hydrate + aqueous + liquid N₂O + gas) (Villard 1897 [2], von Tammann and Krige 1925 [3]). Recently, Mohammadi and Richon (2009) [4] reported the phase relations of N₂O hydrate accompanied with CO₂ hydrate. N₂O has the similar molecular mass and similar critical constants to CO₂. The largest van der Waals diameter of N₂O (0.51 nm) is slightly larger than that of CO₂ (0.50 nm) and it is almost the same as the void size of S-cage of s-I. In the CO₂ hydrate system, it had been believed that the CO₂ molecule can not occupy the S-cage, However, the occupancy of CO₂ in both S- and M-cages is confirmed by the single crystal X-ray diffraction (Udachin et al. (2001) [5]) and FTIR (Prasad et al. 2006 [6]) measurements.

Therefore, it is very important to investigate the S-cage occupancy of N₂O as well as the phase equilibrium relation of N₂O hydrate system.

In this chapter, I have investigated the thermodynamic stability boundaries of N₂O hydrate system in a temperature range of (275.20 to 298.19) K and a pressure range up to 305 MPa. In addition, the S-cage occupancy of N₂O molecule and the pressure effect of lattice mode of N₂O hydrate have been briefly discussed from the Raman spectra of the intra- and inter-molecular vibration modes.

II-1 Experimental

II-1-1 Material

Research grade N₂O (purity is higher than 99.9 %) was purchased from Neriki Gas Co. Ltd. The distilled water was obtained from Yashima Pure Chemicals Co. Ltd. Both were used without further purification.

II-1-2 Experimental Apparatus

I used three types of high-pressure cells depending on the experimental pressure. For precise measurement at a pressure up to 20 MPa, I have used the high-pressure cell as shown in **Figure II-1**. The inner volume and the maximum working pressure of the cell were *ca.* 100 cm³ and 20 MPa, respectively. The system temperature was controlled by circulating thermostated water from a thermocontroller (EYELA NCB-3100) through the jacket of cell. In the pressure range of (20 to 75 MPa), I have used another high-pressure cell, the same as previous one (Ohgaki and Hamanaka 1995 [8]), as shown in **Figure II-2**. The cell had inner volume of approximately 1 cm³ and the maximum working pressure was about 75 MPa. A pair of sapphire window, whose thickness and diameter were 4 mm and 16 mm, respectively, was set on both sides of the internal space. Each window was sealed with a packing made of Tefron type material. A stainless ball of 5 mm in diameter was enclosed with the sample to agitate the system by vibration from outside. The system temperature was controlled by the thermostated water circulating from a thermocontroller (TAITEC CL80 + TAITEC PU-9) through the jacket in the cell. Over 75 MPa, I have used the high-pressure optical cell as shown in **Figure II-3**. The high-pressure optical cell has a couple of sappier windows (4 mm).

The inner volume and maximum working pressure of the high-pressure cell were 0.2 m³ and 400 MPa, respectively. The cell was made of stainless steel (SUS630), a thermal insulating material, a mixing ball, a high pressure pump for supplying and/or pressurizing the samples, an intensifier, pressure gauges, temperature control system, and a charge-coupled device (CCD) camera.

II-1-3 Experimental Procedure

The single crystals of the N₂O hydrates prepared under the various three-phase coexisting conditions in the high-pressure optical cell were analyzed using a laser Raman microprobe spectrometer. The experimental procedure is essentially same as described in Chapter-I-1-3. For pressure measurement, two different pressure gauges were used according the working pressure. Up to 75 MPa, a pressure gauge (Valcom VPRT) calibrated by a Ruska quartz Bourdon tube gauge was used with an estimated maximum uncertainty of 0.02 MPa. Over 75 MPa, a pressure transducer (NMB STD-5000K) and digital peak holder (NMB CSD-819) was used with an estimated maximum uncertainty of 2 MPa.

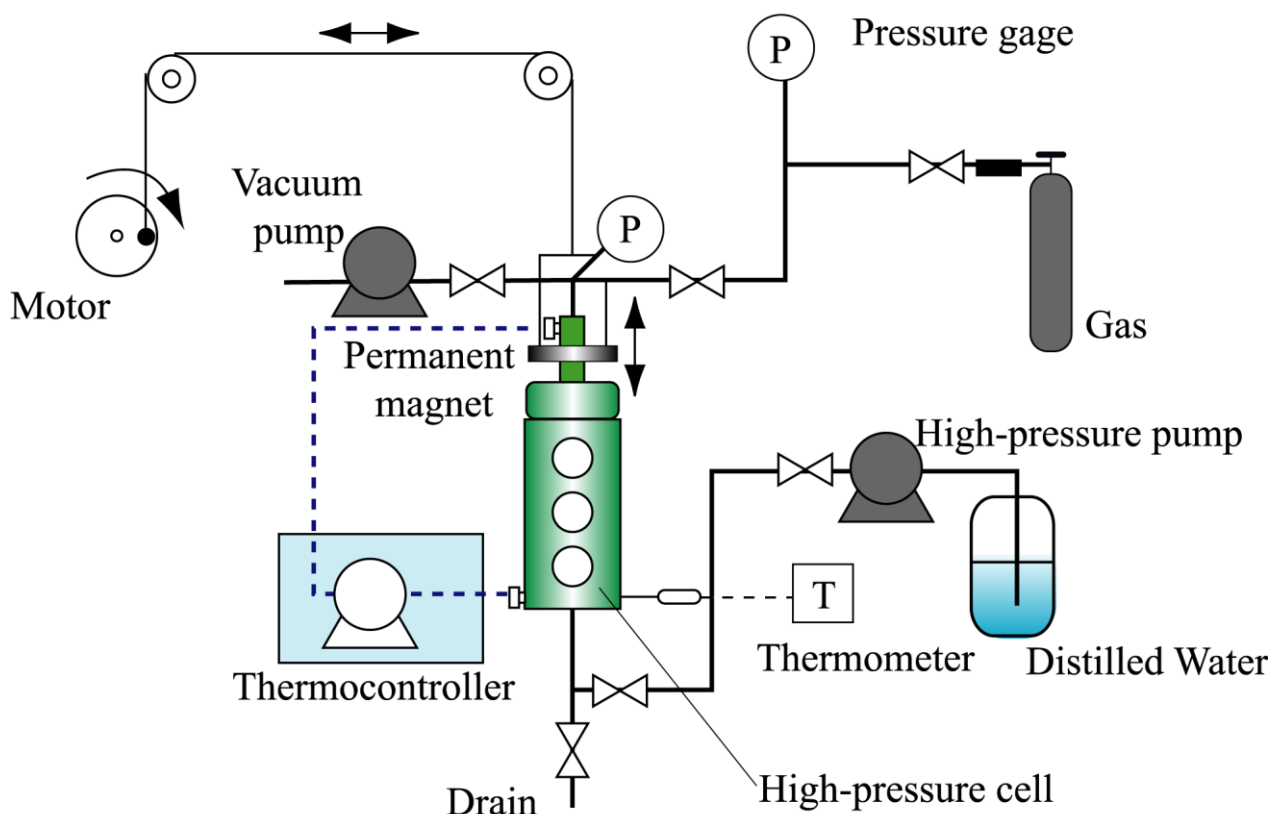


Figure II-1 Schematic illustration of the high-pressure cell (Maximum pressure; 20 MPa).

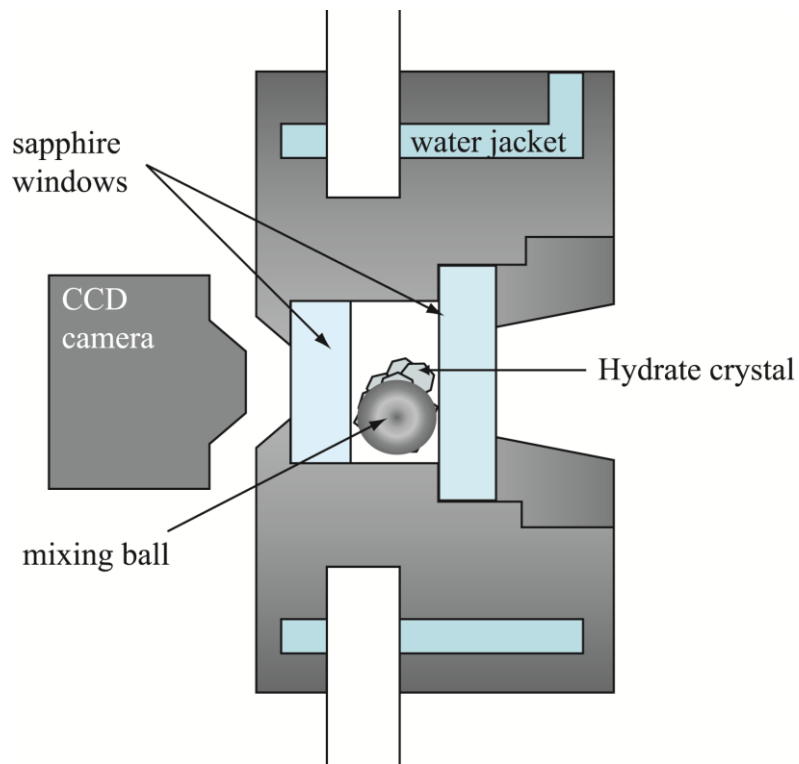


Figure II-2 Schematic illustration of the high-pressure cell (Maximum pressure; 75 MPa).

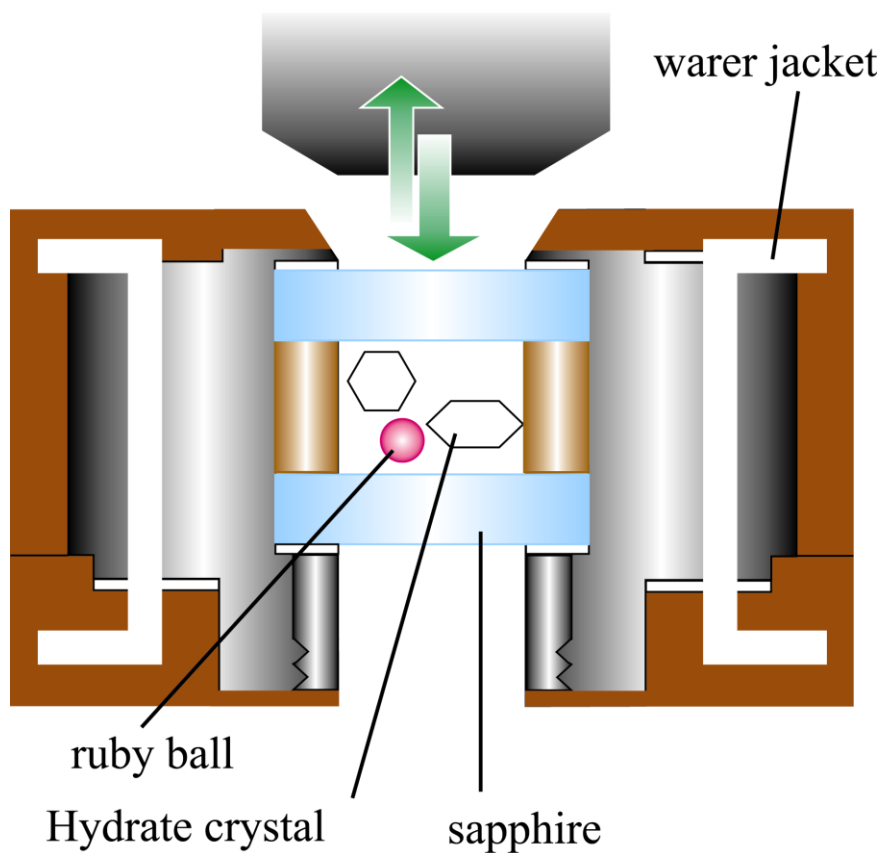


Figure II-3 Cross sectional illustration of the high-pressure cell (Maximum pressure; 400 MPa).

II-2 Results and discussion

The thermodynamic stability boundaries of N₂O hydrate are listed in **Table II-1** and plotted in **Figure II-4**. It is also compared with that of CO₂ hydrate (Nakano et al. 1998 [7], Ohgaki and Hamanaka (1995) [8]). The quadruple point Q₂ of (hydrate + aqueous + liquid N₂O + gas) phases, which was determined by the extrapolation of two three-phase coexistence curves, is located at 285.15 K and 4.2 MPa. The stability boundary in the lower pressure range than the Q₂ agrees well with the references (Villard 1888, 1897 [1, 2], von Tammann and Krige (1925) [3], Mohammadi and Richon 2009 [4]). The equilibrium temperature of N₂O hydrate is 2-3 K higher than that of CO₂ hydrate at the same pressure conditions below 100 MPa. Above 100 MPa, the temperature difference becomes gradually large, it is 4.5 K at around 300 MPa.

From the slope of equilibrium curve (dp/dT), the overall enthalpy change $\Delta_{\text{hyd}}H$ was obtained by using the Clapeyron equation:

$$\left(\frac{dp}{dT} \right)_{\text{equal.}} = \frac{\Delta_{\text{hyd}}H}{\Delta_{\text{hyd}}v \cdot T} \quad (\text{II-1})$$

The total volume change $\Delta_{\text{hyd}}v$ is defined by equation (II-2):

$$\Delta_{\text{hyd}}v = v_{\text{N}_2\text{O}} + \lambda \cdot v_{\text{water}} - v^{\text{H}} \quad (\text{II-2})$$

Where v^{H} was calculated from the lattice constant of 1.20 nm (von Stackelberg 1949 [14]) and $v_{\text{N}_2\text{O}}$ was obtained from the Soave-Redlich-Kwong equation of state (Soave 1972 [9]) and v_{water} was evaluated from equation of Saul and Wanger (1989) [15]. The hydration number λ was assumed to be 5.75 (ideal hydrate assumption of structure-I (s-I)). The average value of $\Delta_{\text{hyd}}H = (65 \pm 4)$ kJ/mol shows good agreement with the literature value of 61.5 kJ/mol (von Stackelberg and Meinhold 1954 [10]).

Table II-1 Thermodynamic stability boundaries (Temperature T , Pressure p) of (hydrate + aqueous + gas) and (hydrate + aqueous + liquid N₂O) in the N₂O hydrate system.

T / K	p / MPa	T / K	p / MPa
hydrate + aqueous + gas		hydrate + aqueous + liquid N ₂ O	
275.20	1.20	285.80	10.56
276.25	1.32	286.34	16.12
277.01	1.45	286.35	16.25
277.71	1.58	286.43	17.01
278.39	1.70	286.51	17.75
279.18	1.87	286.74	20.36
279.94	2.04	287.03	23.58
280.73	2.26	287.30	26.72
281.51	2.48	287.35	27.31
282.39	2.79	287.45	28.28
282.79	2.94	287.60	30.21
283.19	3.12	288.03	35.35
283.47	3.24	288.38	39.57
283.67	3.34	288.79	44.89
283.87	3.41	289.11	49.21
284.06	3.54	289.31	52.38
284.37	3.76	289.52	55.43
284.58	3.91	289.71	58.10
284.76	3.99	289.98	61.67
284.97	4.15	291.85	91
		292.83	107
		296.26	202
		298.19	305

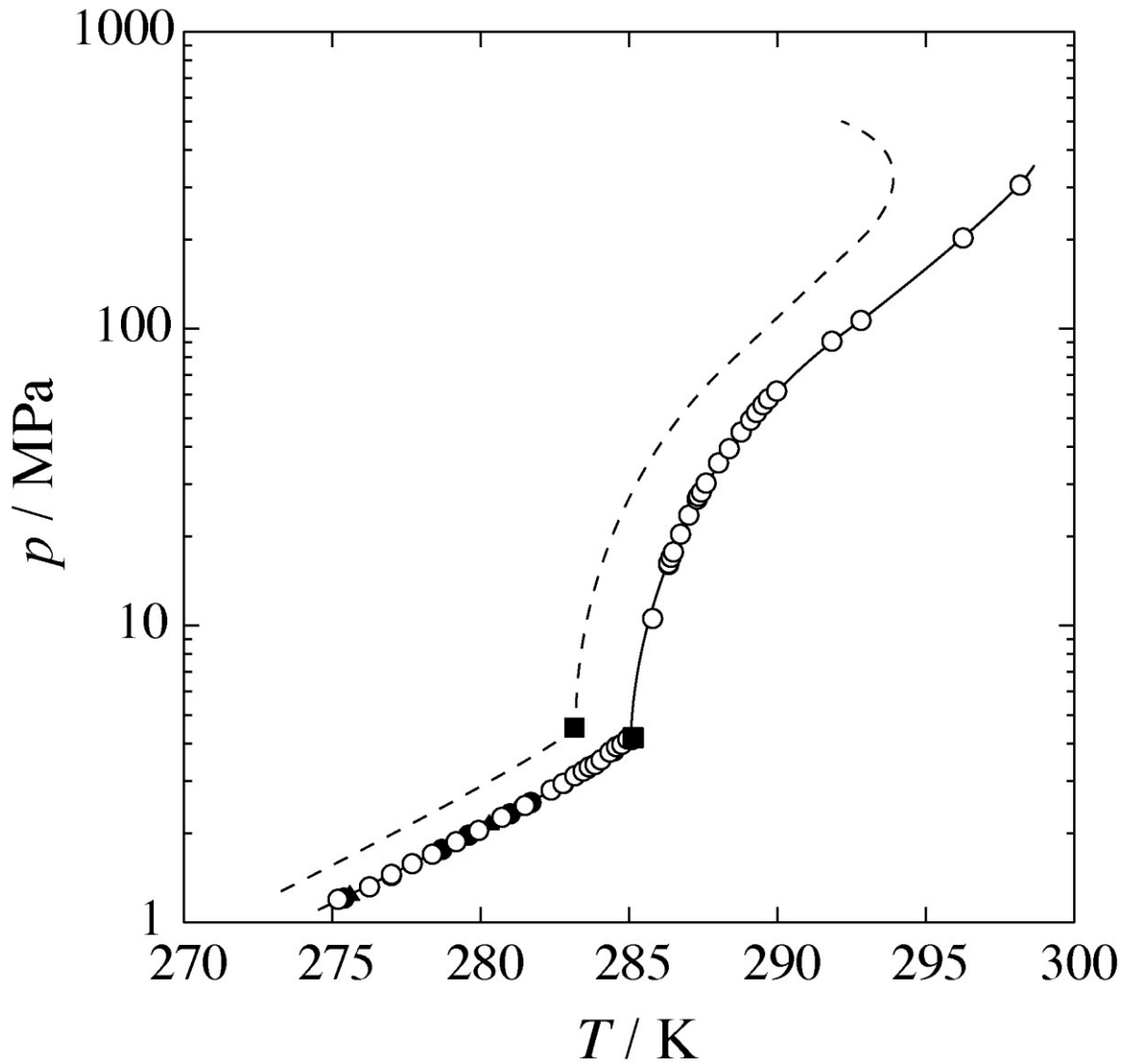


Figure II-4 Thermodynamic phase boundaries of N_2O (\circ , present study; \blacktriangle , Villard (1897) [2]; \bullet , Mohammadi and Richon (2009) [4]) and CO_2 (broken lines, Nakano et al. 1998 [7], Ohgaki and Hamanaka (1995) [8]) hydrate systems. The closed square symbols stand for the quadruple point Q_2 of hydrate + gas + liquid guest + aqueous phases.

The N₂O molecule has three Raman-active vibration modes, N–O stretching vibration (around 1285 cm⁻¹), N–N stretching vibration (around 2230 cm⁻¹) and N–N–O bending vibration (around 580 cm⁻¹). The Raman peak of N–O stretching vibration mode is the most intensive of three Raman-active modes. **Figure II-5** shows the typical in situ Raman spectra corresponding to N–O vibration of N₂O molecule in the hydrate, liquid N₂O and aqueous phases on the thermodynamic stability boundary at 40 MPa and 288.43 K. The spectrum splits into a doublet (1283 cm⁻¹ and 1290 cm⁻¹) in the N₂O hydrate phase, while a single peak is detected in both the liquid N₂O (1285 cm⁻¹) and aqueous (1287 cm⁻¹) phases. The shoulder at the higher wave number side of the Raman peak in the liquid N₂O phase is the overlap of the peak in the aqueous phase, because small N₂O droplets are dispersed in the aqueous phase. The split of the Raman peak in the hydrate phase indicates that the N₂O molecules occupy both the S- and M-cages. The stronger peak (1283 cm⁻¹) corresponds to N₂O entrapped in the M-cages, and the weaker one (1290 cm⁻¹) to the S-cages. This is also supported by the peak intensity ratio of N₂O in M-cage to S-cage, which is close to the cage-constituent ratio of s-I hydrate. The Raman spectrum in hydrate phase reveals that, even at 40 MPa, most of S-cages are occupied by the N₂O molecules.

There are two types of the pressure dependence on the Raman shift of the intermolecular O–O vibration between water molecules in the s-I hydrate systems. One is strong pressure dependence (methane (Nakano et al. 1999 [11]), CO₂ (Nakano et al. 1998 [7]) and so on, Type A). The other is very weak pressure dependence (ethane (Morita et al. 2000 [12]), cyclopropane (Suzuki et al. 2001 [13]) and so on, Type B). The Raman peak of the O–O vibration in the N₂O hydrate crystal (not shown) is located at (204±2) cm⁻¹ (40 MPa and 288.23 K) and (210±2) cm⁻¹ (203 MPa and 296.39 K). The larger deviation than the original accuracy of Raman spectrometer is caused by the low signal to noise ratio, because it is more difficult than other hydrate systems to prepare a single crystal of N₂O hydrate along the thermodynamic stability boundary. Nevertheless, I can barely distinguish the pressure effect of Raman shift. The pressure dependence of the O–O vibration energy in the N₂O hydrate is similar to that in the CO₂ hydrate system, that is, it belongs to the Type A group of s-I. The stronger pressure-dependence would indicate a higher shrinkage of the hydrogen-bonded cage or the larger free volume for the N₂O molecule.

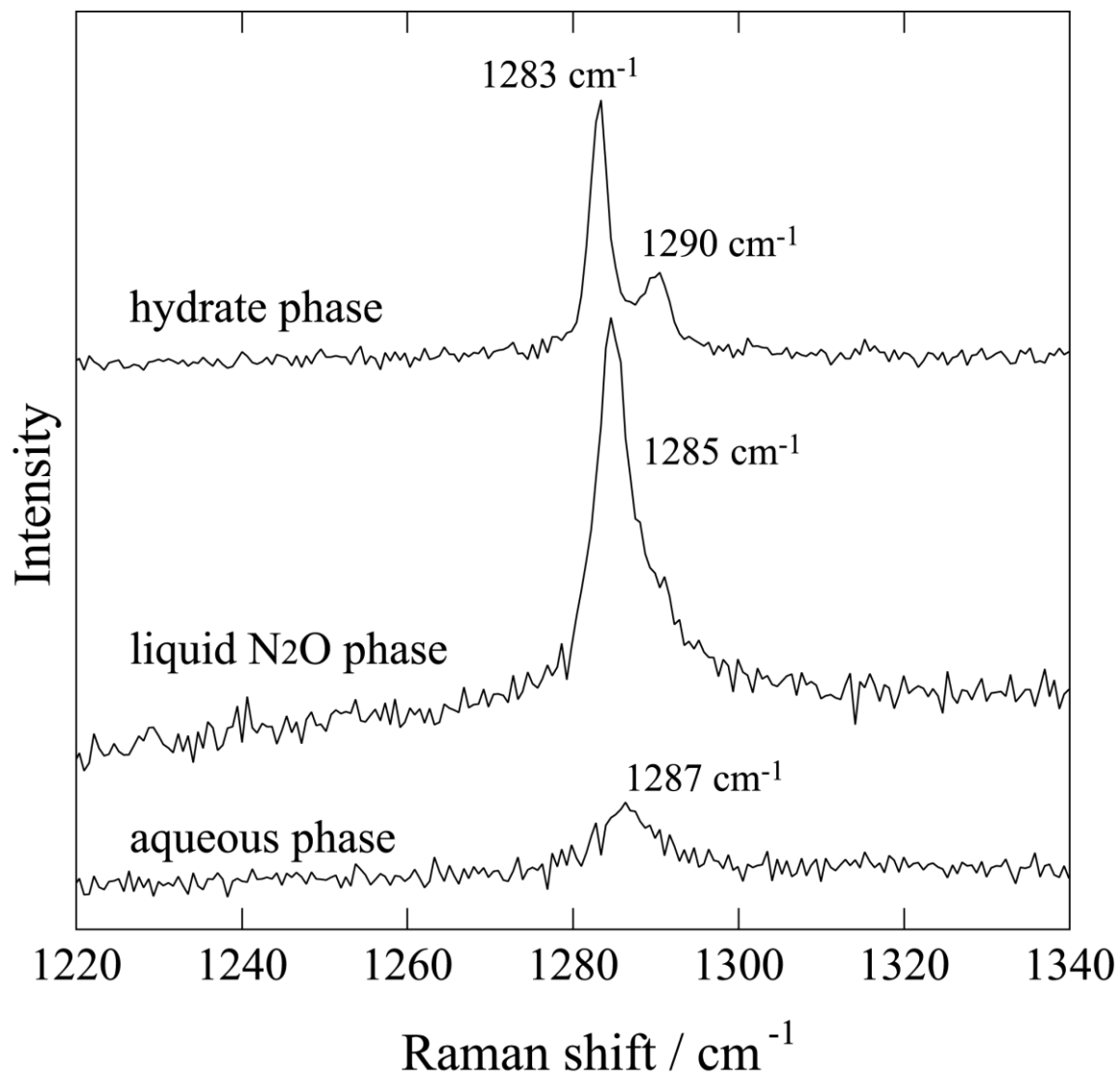


Figure II-5 In situ Raman spectra corresponding to N–O vibration mode of N₂O molecule in N₂O hydrate, liquid N₂O, and aqueous phases at 40 MPa and 288.43 K.

Summary

The thermodynamic stability boundaries of N₂O hydrate system were measured in a pressure range up to 305 MPa. The phase behavior of N₂O hydrate system is qualitatively similar to that of CO₂ hydrate system up to 100 MPa. One of the most important findings is that N₂O molecules can easily occupy both S- and M-cages of the s-I hydrate. The peak intensity ratio of N₂O in the S-cage to M-cage at 40 MPa and 288.15 K is close to the cage-constituent ratio (1:3) of s-I.

Nomenclature

H = enthalpy of the hydration	[J/mol]
p = pressure	[Pa]
T = temperature	[K]
ν = molar volume	[m ³ /mol]

<Greek>

λ = hydration number	[-]
------------------------------	-------

<Subscript>

hyd = hydration

Literature Cited

- [1] Villard, M. “Sur Quelques Nouveaux Hydrates de Gaz”, *Comptes rendus de l'Académie des Sciences*, **106**, 1602-1603 (1888).
- [2] Villard, M. “Etude Experimentale des Hydrates de Gaz”, *Annales de chimie et de physique*, **11**, 289-394 (1897).
- [3] von Tammann, G.; Krige, G. J. R. “Die Gleichgewichtsdrucke von Gashydraten”, *Zeitschrift für anorganische und allgemeine Chemie*, **146**, 179-195 (1925).
- [4] Mohammadi, A. H.; Richon, D. “Equilibrium Data of Nitrous Oxide and Carbon Dioxide Clathrate Hydrates”, *Journal of Chemical and Engineering Data*, **54**, 279-281 (2009).
- [5] Udachin, K. A.; Ratcliffe, C. I.; Ripmeester, J. A. “Structure, Composition, and Thermal Expansion of CO₂ Hydrate from Single Crystal X-ray Diffraction Measurements”, *Journal of Physical Chemistry B*, **105**, 4200-4204 (2001).
- [6] Prasad, P. S. R.; Prasad, K. S.; Thakur, N. K. “FTIR Signatures of Type-II Clathrates of Carbon Dioxide in Natural Quartz Veins”, *Current Science*, **90**, 1544-1547 (2006).
- [7] Nakano, S.; Moritoki, M.; Ohgaki, K. “High-Pressure Phase Equilibrium and Raman Microprobe Spectroscopic Studies on the CO₂ Hydrate System”, *Journal of Chemical and Engineering Data*, **43**, 807-810 (1998).
- [8] Ohgaki, K.; Hamanaka, T. “Phase-Behavior of CO₂ Hydrate-Liquid CO₂-H₂O System at High Pressure.”, *Kagaku Kogaku Ronbunshu*, **21**, 800-803 (1995).
- [9] Soave, G. “Equilibrium Constants from a Modified Redlich-Kwong Equation of State”, *Chemical Engineering Science*, **27**, 1197–1203 (1972).

- [10] von Stackelberg, M.; Meinhold, W. "Feste GasHydrate III: Mischhydrate", *Zeitschrift für Elektrochemie*, **58**, 40-45 (1954).
- [11] Nakano, S.; Moritoki, M.; Ohgaki, K. "High-Pressure Phase Equilibrium and Raman Microprobe Spectroscopic Studies on the Methane Hydrate System", *Journal of Chemical and Engineering Data*, **44**, 254-257 (1999).
- [12] Sugahara, T.; Morita, K.; Ohgaki, K. "Stability Boundaries and Small Hydrate-Cage Occupancy of Ethylene Hydrate System", *Chemical Engineering Science*, **55**, 6015-6020 (2000).
- [13] Suzuki, M.; Tanaka, Y.; Sugahara, T.; Ohgaki, K. "Pressure Dependence of Small-Cage Occupancy in the Cyclopropane Hydrate System", *Chemical Engineering Science*, **56**, 2063-2067 (2001).
- [14] Stackelberg, V. M. "Feste Gashydrate", *Die Naturwissenschaften*, **36**, 327-333 (1949).
- [15] Saul, A.; Wanger, W. "A Fundamental Equation for Water Covering the Range from the Melting Line to 1273 K at Pressures up to 25000 MPa", *Journal of Physical Chemistry Reference Data*, **18**, 1537-1564 (1989).

Chapter-III: Thermodynamic and Raman Spectroscopic Studies on Kr and Xe Hydrates

Abstract

The thermodynamic stability boundaries for two noble gas (Kr and Xe) hydrates have been investigated in a pressure range up to 445 MPa and a temperature range of (274.4 to 320.0) K for the Kr hydrate system or (324.4 to 345.3) K for the Xe hydrate system. The Raman spectrum of intermolecular O–O stretching vibration mode has been evaluated for each hydrate single crystal along with the three-phase coexisting curve. The slope change on the boundary curve and the pressure dependence on the Raman shift for the Kr hydrate crystal reveal that a structural phase transition point exists at (414 ± 1) MPa and (319.2 ± 0.1) K, while the Xe hydrate crystal of structure-I exhibits no phase transition.

Introduction

The noble gas hydrates are not necessarily essential for practical applications. How the noble gases, having a spherical shape and characteristic properties, affect the hydrate stability, however, is fundamental for a thermodynamic understanding of gas hydrates. Some important findings have been reported on the noble gas hydrate systems, for example, Kurnosov et al. (2001) [1] found that the 14-hedral cavity ($4^25^86^4$) doubly-occupied by Ar generates the tetragonal structure hydrate at very high pressures, and Ohgaki et al. (2000) [2] stated that the Xe hydrate system is the border system which does not have a high-temperature quadruple point in a series of critical temperatures of guest species.

Moreover, it seems to be that the hydrate cage occupied by the small and spherical guest molecules are easily shrunk by pressurization. The Raman spectrum of intermolecular O-O stretching vibration mode of water molecules gives an important information on the constriction as well as structural transition of hydrate by pressurization.

In this chapter, the three-phase coexisting curves for two noble gas (Kr and Xe) hydrate systems have been investigated, and the pressure dependence of the Raman O–O vibration shifts has been evaluated along with the equilibrium curve.

III-1 Experimental

III-1-1 Material

Kr was purchased from the Neriki Gas Co. Ltd., having a stated minimum purity of 99.999 mol %. Distilled water was obtained from Yashima Pure Chemicals Co. Ltd. Xe was purchased from the Daido Hoxan Inc., having a stated minimum purity of 99.995 mol %. The majority of the impurity was Kr at 3.78 ppm. Distilled water was obtained from Yashima Pure Chemicals Co. Ltd. All of them were used without further purification.

III-1-2 Experimental Apparatus

The experimental apparatus used in this study was essentially the same as the previous one as shown in **Figure I-1**, **Figure II-1** and **Figure II-2**. For precise measurement at a pressure up to 20 MPa, I have used other high-pressure cell as shown in **Figure II-1** in the Kr hydrate system. The inside volume and the maximum working pressure of cell were *ca.* 100 cm³ and 20 MPa, respectively. The system temperature was controlled by circulating thermostated water from a thermocontroller (EYELA NCB-3100) through the jacket of cell.

III-1-3 Experimental Procedure

The single crystals of the Kr and Xe hydrates prepared in the high-pressure optical cell under several three-phase coexisting conditions were analyzed using a laser Raman microprobe spectrometer. The experimental procedure is essentially same as described in Chapter-I-1-3 and Chapter-II-1-3.

III-2 Results and discussion

The experimental data obtained in the present study for the Xe and Kr hydrate systems are listed in **Tables III-1** and **Table III-2**, respectively. **Figure III-1** shows the pressure temperature relations of two noble-gas hydrate systems accompanied with the literature values [3, 6, 8].

The "S-shape" curve of Xe hydrate system is the characteristic behavior caused by the differential p - v - T relation around the critical end point not because of hydrate structural changes. The critical end point (the gas and liquid phases become identical in the presence of hydrate phase) for the Xe hydrate system is at 299.76 K and 5.86 MPa (Ohgaki et al. 2000 [2]), which is very close to the three-phase coexisting curve. The equilibrium curve obtained in the present study (over 75 MPa) is smoothly extrapolated to the previous results in the low-pressure region (Ohgaki et al. 2000 [2]). Over all, the discrepancy between the present results and the literature values (Dyadin et al. 1997 [3]) is less than 5 % in pressure.

From the slope of equilibrium curve (dp/dT), the overall enthalpy change $\Delta_{\text{hyd}}H$ was obtained using the Clapeyron equation (II-1) as shown in Chapter-II. The total volume change $\Delta_{\text{hyd}}v$ is defined by equation (III-1):

$$\Delta_{\text{hyd}}v = v_G + \lambda \cdot v_{\text{water}} - v^{\text{H}} \quad (\text{III-1})$$

Where v^{H} was calculated from the lattice constant of 1.20 nm (von Stackelberg 1949 [12]) and v_G of Xe was obtained from the Lee-Kesler equation of state (Reid et al. 1987 [4]) and v_{water} was evaluated from equation of Saul and Wanger (1989) [13]. The hydration number λ was assumed to be 5.75 (ideal hydrate assumption of structure-I (s-I)). The average value of $\Delta_{\text{hyd}}H = (65 \pm 6)$ kJ/mol shows good agreement with previous value of 65 kJ/mol (Ohgaki et al. 2000 [2], Ewing and Ionescu 1974 [5], Shimada et al. 2003 [11]). A large deviation at high temperatures was mainly caused by the uncertainty of volumetric properties of Xe fluid at high pressure.

The Kr hydrate system exhibits curious behavior as shown in **Figure III-1**. In the present study, the structural phase-transition point was determined at 414 MPa and 319.20 K along with the thermodynamic stability boundary. Dyadin et al. (1997) [6] have reported the

structural change (structure-II (s-II) to s-I) around 415 MPa. On the other hand, Desgreniers et al. (2003) [7] have stated that the s-II Kr hydrate changes to s-I near 300 MPa and to the hexagonal structure (structure-H, s-H) near 600 MPa at room temperature. However, there was no unusual pressure-temperature relation around 300 MPa caused by the hydrate structural change. It is possible that the s-I hydrate near 300 MPa corresponds to the metastable state because the latter's measurements were not performed in the three-phase equilibrium conditions. Around 10 MPa and 295 K, the present data show large disagreement with the literature (Dyadin et al. 1997 [6], Berecz and Balla-Achs 1983 [8]). The literature values indicate a structural phase transition at 10 MPa. However, careful measurement around this point shows a smooth curve in the present study. The average value of $\Delta_{\text{hyd}}H$ is evaluated with the almost same procedure to Chapter-II; Equation (II-1). The total volume change $\Delta_{\text{hyd}}V$ is defined by equation (III-1). The hydration number λ was assumed to be 5.67 (ideal hydrate assumption of s-II). A value of $\Delta_{\text{hyd}}H = (57 \pm 2)$ kJ/mol in a temperature range of (275 to 305) K is in good agreement with the literature value of 56.2 kJ/mol at 273 K (Handa 1986 [9]).

The Raman spectrum of intermolecular O–O stretching vibration mode of water was detected around 210 cm^{-1} in the s-II N_2 hydrate system at low pressures [Chapter-I]. The typical Raman peaks of Kr hydrate are shown in **Figure III-2**. The peak corresponding to the hydrate cage structured by hydrogen bonds is a peculiar spectrum of the hydrate lattice. Some small peaks at lower than 140 cm^{-1} were not taken up because it was difficult to specify the meaning peak from noises on the shoulder of Rayleigh scattering. The Raman peaks show the blue shift in proportion to pressure up to 414 MPa. Over 414 MPa, the peak becomes broad and shifts to a low energy vibration. The pressure effect on the O–O vibration mode in the Xe and Kr hydrate crystals is shown in **Figure III-3**. In both systems, the O–O vibration energy increases with pressure, that is, the hydrate cage constructed of water molecules shrinks gradually by pressurization.

The pressure dependence of the O–O vibration in the N_2 and CO_2 hydrate crystals is also shown for comparison in **Figure III-3**. The N_2 and CO_2 hydrates are well-known as typical crystals of s-II and s-I hydrates in the pressure region of the present study respectively. They show a common pressure-dependence on the O–O vibration, however, the N_2 hydrate [Chapter-I] exhibits a vibration energy higher than the CO_2 hydrate (Nakano et al. 1998 [10]) at the same pressure. The distinction proceeds from a size-difference of the pentagonal

dodecahedron hydrate cages, that is, the dodecahedron cage of s-II hydrate is slightly smaller than that of s-I hydrate. The Xe hydrate system shows good agreement with the CO₂ hydrate system (dotted line). On the other hand, the Kr hydrate system agrees well with the N₂ hydrate system (solid line) up to 414 MPa. Above the pressure, it shows a discontinuous line and the O–O vibration energy becomes lower than that of s-I hydrates. This fact reveals that the structural phase transition in the Kr hydrate crystal occurs around 400 MPa and the average ridge-line length of hydrate cages becomes longer than that of s-I hydrates.

The pressure-dependence in the Xe and Kr hydrates indicates the shrinkage of the hydrogen-bonded cage or the large free volume in the hydrate cage for these guest molecules. It is also important that the s-I Xe hydrate crystal never changes the structure at a pressure up to 445 MPa while the s-II Kr hydrate exhibits the structural change around 400 MPa. The hydrate structure observed over 414 MPa would be s-H as speculated by Desgreniers et al. (2003) [7].

Table III-1 Three-phase coexisting data for the Xe hydrate system.

T / K	p / MPa
324.40	106
326.67	129
329.79	163
332.15	193
334.19	221
335.96	247
337.35	271
338.68	294
340.06	320
341.29	345
342.54	368
343.59	391
344.45	416
345.32	440

Table III-2 Three-phase coexisting data for the Kr hydrate system.

<i>T</i> / K	<i>p</i> / MPa	<i>T</i> / K	<i>p</i> / MPa
274.49	1.62	300.89	35.21
275.84	1.82	301.70	39.33
277.15	2.10	302.46	44.23
278.14	2.30	303.04	49.23
278.87	2.51	303.94	56.09
279.77	2.70	305.16	67.57
280.09	2.80	306.20	78
280.75	2.98	307.22	88
281.73	3.28	307.51	89
282.21	3.43	308.37	98
283.22	3.83	309.72	113
284.18	4.23	310.81	129
285.11	4.60	312.04	148
285.62	4.87	313.01	166
286.58	5.36	313.96	180
286.59	5.39	314.86	199
287.59	6.02	315.69	218
288.57	6.68	315.96	226
289.58	7.44	316.55	249
290.57	8.31	317.19	270
291.56	9.31	317.40	285
292.46	10.19	317.90	309
294.26	12.70	318.26	330
295.48	15.10	318.86	353
296.65	17.74	319.00	376
297.39	19.93	319.29	399
298.39	23.34	319.20	414*
299.47	27.41	319.37	433*
300.26	31.09	320.02	445*

*new hydrate structure

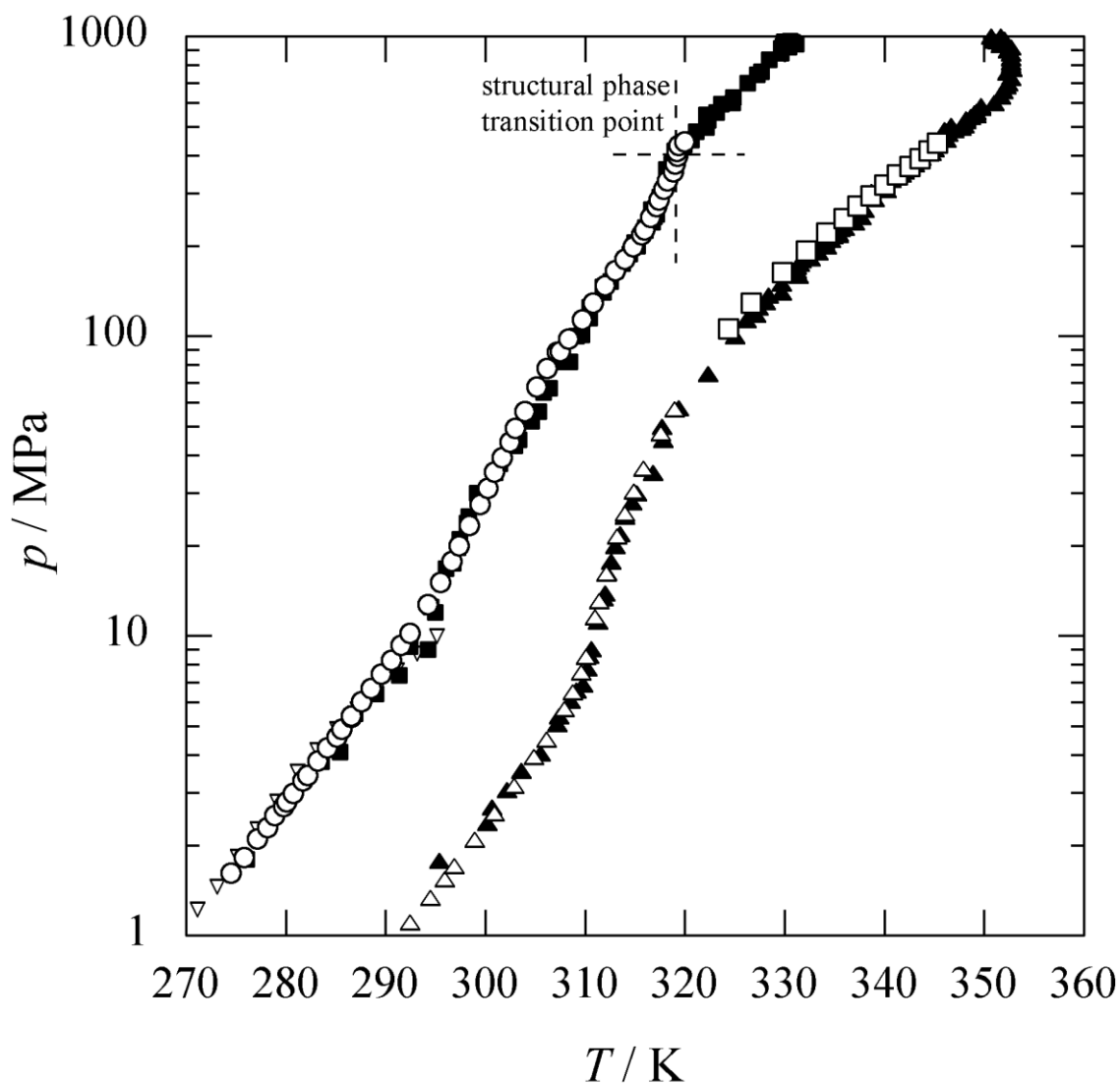


Figure III-1 Pressure - temperature relations of hydrate stability boundaries: \square , three-phase coexisting curve of Xe hydrate (present study); \blacktriangle , Dyadin et al. (1997) [3]; \triangle , Ohgaki et al. (2000) [2]; \circ , three-phase coexisting curve of Kr hydrate (present study); ∇ , Berez and Balla-Achs (1983) [8]; \blacksquare , Dyadin et al. (1997) [6]. The structural phase transition point exists at 414 MPa and 319.20 K for the Kr hydrate system.

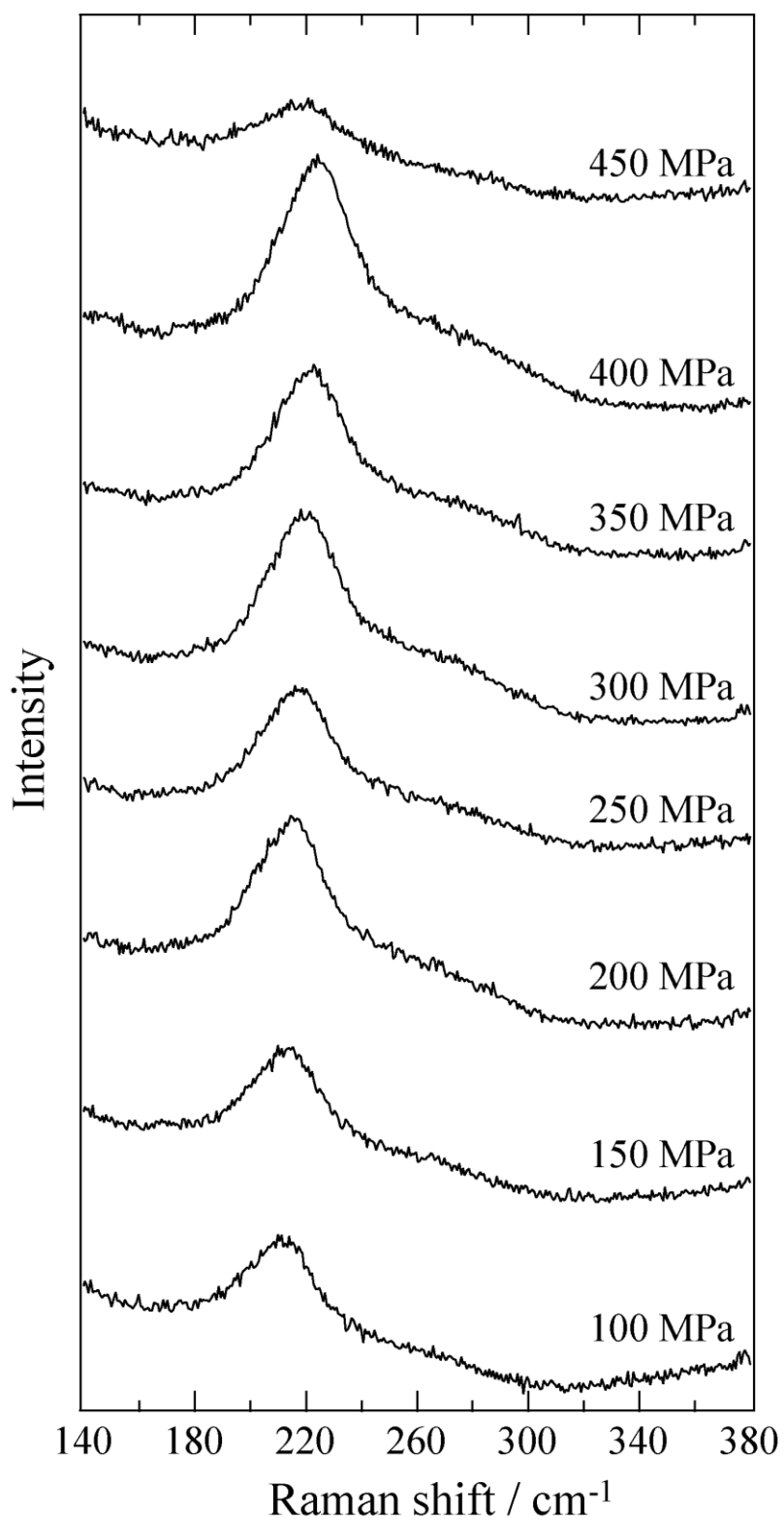


Figure III-2 Raman spectra of the O–O stretching vibration for the Kr hydrate crystal on the thermodynamic stability boundary curve.

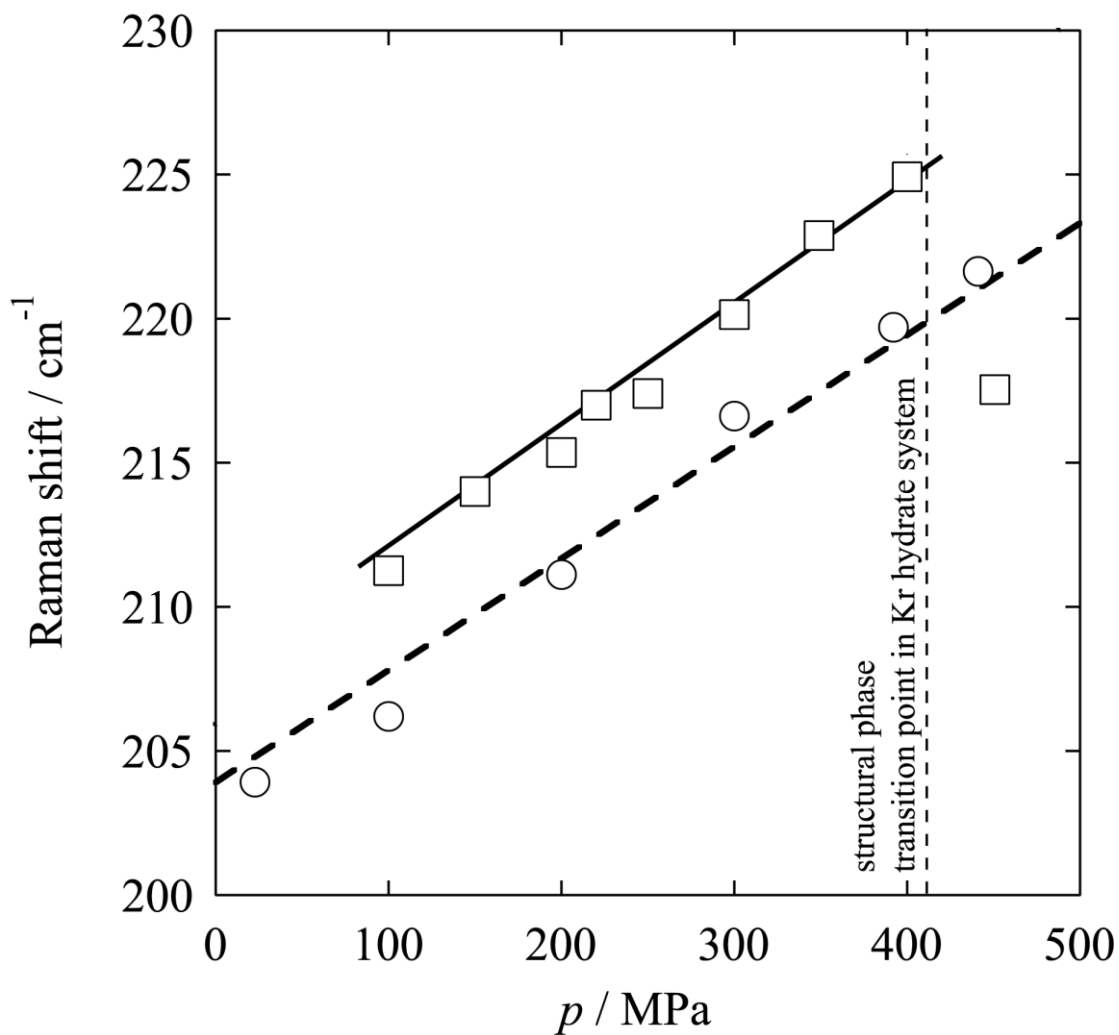


Figure III-3 Pressure dependence on the Raman shift corresponding to the O–O stretching vibration for the Xe and Kr hydrate systems: ○, Xe hydrate; □, Kr hydrate; solid line, N₂ hydrate (s-II) [Chapter-I]; dotted line, CO₂ hydrate (s-I) (Nakano et al. 1998 [10]). Xe hydrate crystal belongs to the s-I hydrate in the whole experimental region. In the Kr hydrate system, the s-II hydrate crystal exists up to 414 MPa and changes to a different structure.

Summary

The three-phase coexisting curves of Xe and Kr hydrate systems were obtained up to 445 MPa by use of a high-pressure optical cell. Each single crystal of Xe and Kr hydrates was analyzed *in situ* by use of laser Raman spectroscopy. The pressure dependence of the intermolecular O–O stretching vibration mode reveals that the Xe hydrate crystal belongs to the s-I hydrate over the whole experimental region. For the Kr hydrate system, the s-II hydrate crystal exists up to 414 MPa and changes to a different structure (probably s-H). Both noble-gas hydrate crystals indicate a considerable shrinkage of the hydrate cage by pressurization.

Nomenclature

H = enthalpy of the hydration	[J/mol]
p = pressure	[Pa]
T = temperature	[K]
ν = molar volume	[m ³ /mol]

<Greek>

λ = hydration number	[–]
------------------------------	-------

<Subscript>

hyd = hydration

G = guest species

Literature Cited

- [1] Kurnosov, A. K.; Manakov, A. Y.; Komarov, V. Y.; Voronin, V. I.; Teplykh, A. E.; Dyadin, Y. A. A “New Gas Hydrate Structure”, *Doklady Physical Chemistry*, **381**, 303-305 (2001).
- [2] Ohgaki, K.; Sugahara, T.; Suzuki, M.; Jindai, H. “Phase Behavior of Xenon Hydrate System”, *Fluid Phase Equilibria*, **175**, 1-6 (2000).
- [3] Dyadin, Y. A.; Larionov, E. G.; Mirinslij, D. S.; Mikina, T. V.; Alakado, E. Y.; Starostina, L. I. “Phase Diagram of the Xe-H₂O System up to 15 kbar”, *Journal of Inclusion Phenomena and Molecular Recognition in Chemistry*, **28**, 271-285 (1997).
- [4] Reid, R. C.; Prausnitz, J. M.; Poling, B. E. “*The Properties of Gases and Liquids, 4th Ed.*”, McGraw-Hill, New York, 1986, pp. 47-49.
- [5] Ewing, G. J.; Ionescu, L. G. “Dissociation Pressure and Other Thermodynamic Properties of Xenon-Water Clathrate”, *Journal of Chemical and Engineering Data*, **19**, 367-369 (1974).
- [6] Dyadin, Y. A.; Larionov, E. G.; Mikina, T. V.; Starostina, L. I. “Clathrate Formation in Kr-H₂O and Xe-H₂O Systems under Pressures up to 15 kbar”, *Mendeleev Communication*, 74-76 (1997).
- [7] Desgreniers, S.; Flacau, R.; Klug, D. D.; Tse, J. S. Dense Noble Gas Hydrates: Phase Stability and Crystalline Structures. *Proceeding of SMEC Conference*, Florida (2003).
- [8] Berez, E.; Balla-Achs, M. “*Gas Hydrate, Studies in Inorganic Chemistry, Vol. 4*”, Elsevier, Amsterdam, 1983, pp. 174-182.

- [9] Handa, Y. P. “Calorimetric Determinations of the Compositions, Enthalpies of Dissociation, and Heat Capacities in the Range 85 to 270 K for Clathrate Hydrates of Xenon and Krypton”, *Journal of Chemical Thermodynamics*, **18**, 891-902 (1986).
- [10] Nakano, S.; Moritoki, M.; Ohgaki, K. “High-Pressure Phase Equilibrium and Raman Microprobe Spectroscopic Studies on the CO₂ Hydrate System”, *Journal of Chemical and Engineering Data*, **43**, 807-810 (1998).
- [11] Shimada, N.; Sugahara, K.; Sugahara, T.; Ohgaki, K. “Phase Transition from Structure-H to Structure-I in the Methylcyclohexane + Xenon Hydrate System”, *Fluid Phase Equilibria*, **205**, 17-23 (2003).
- [12] Stackelberg, V. M. “Feste Gashydrate”, *Die Naturwissenschaften*, **36**, 327-333 (1949).
- [13] Saul, A.; Wanger, W. “A Fundamental Equation for Water Covering the Range from the Melting Line to 1273 K at Pressures up to 25000 MPa”, *Journal of Physical Chemistry Reference Data*, **18**, 1537-1564 (1989).

Chapter-IV: Thermodynamic and Raman Spectroscopic Studies of Ar Hydrate System

Abstract

The three-phase coexisting curve (hydrate + aqueous + gas) of Ar has been investigated in a pressure range up to 485 MPa and a temperature range of (279.57 to 305.32) K. The Raman spectrum of intermolecular O–O stretching vibration mode has been measured for Ar hydrate crystal along the stability boundary curve. Both the discontinuity of slope of the three-phase coexisting curve and the pressure dependence of the Raman shift reveal that two structural phase transition points exist at (281±1) MPa and (302.7±0.1) K, and (456±1) MPa and (304.6±0.1) K in a pressure range up to 485 MPa for the Ar hydrate system.

Introduction

Ar hydrate was found out by Villard in 1896 [1], and it has been widely studied by many investigators. It has been well known that Ar hydrate belongs to structure-II (s-II) hydrate (Davidson 1984 [2]) as well as Kr, O₂, and N₂ hydrates. Structure-II hydrate is composed of the two types of hydrogen-bonded water cages, S-cage and L-cage.

Thermodynamic stability boundary for the Ar hydrate system at high pressures has been reported by several investigators. Dyadin et al. (1997) [3] have reported the stability boundary of hydrate formation in the Ar and H₂O system under pressure up to 1500 MPa. They have indicated that two structural transition points are located at 720 MPa and 960 MPa. Lotz and Schouten (1999) [4] have stated that s-II Ar hydrate changes to structure-I (s-I) around 620 MPa from the decomposition curve originated from new quadruple point (620 MPa and 304.6 K). Manakov et al. (2001) [5] measured the stability boundary in a pressure range up to 1000 MPa. They have stated that there are three structural phase transition points from the discontinuity of dp/dT on the stability boundary, and discovered that the s-II Ar hydrate changes to the structure-H (s-H) type hydrate ($P6/mmm$) at 460 MPa, which is similar to the low-pressure's one discovered by Ripmeester et al. (1987) [6]; the s-H is composed of three S-cages, two S'-cages, and one U-cage. The most important finding by Kurnosov et al. (2001)

[7] is that the tetragonal hydrate structure ($P4_2/mmm$) consists of two 14-hedral cavities ($4^25^86^4$) in the unit lattice and two Ar atoms occupy a 14-hedral cavity in a pressure range of (770 to 960) MPa. Hirai et al. (2002) [8] confirmed the tetragonal structure by X-ray diffraction studies at room temperature, but they couldn't find s-H Ar hydrate around 500 MPa. Loveday et al. (2003) [9] supported those findings of Manakov et al. (2001) [5] and Kurnosov et al. (2001) [7], and they clarified that the Ar hydrate changes to so called "filled-ice" above 960 MPa.

Shimizu et al. (2003) [10] have reported that the Raman spectra of interatomic Ar–Ar interaction are detected around 150 cm^{-1} in the pressure range from (160 to 970) MPa at room temperature. They have stated that this Raman spectrum corresponds to the multioccupancy of Ar atoms in the L-cage of s-II. The double occupancy of Ar hydrate system has been predicted by many simulation approaches (Tanaka et al. 2004 [11], Inerbaev et al. 2004 [12], Malenkov et al. [13]). Based on the neutron diffraction experiments at 293 K, Manakov et al. (2004) [14] have reported the multioccupancy of Ar in the s-II Ar hydrate in at a pressure range from (340 to 430) MPa.

Many investigators have studied the Ar hydrate system, but the most of them have carried out by use of Diamond Anvil Cell at room temperature, which is away from three-phase coexisting conditions (hydrate + aqueous + gas). Unless the investigation is carried out along the three-phase coexisting condition, any varied structure might emerge as a metastable structure depending on the composition. In this chapter, the three-phase coexisting curve (hydrate + aqueous + gas) for Ar hydrate system in a temperature range of (279.57 to 305.32) K and a pressure range up to 485 MPa has been precisely measured. The pressure dependence of the intermolecular O–O vibration along the three-phase coexisting curve has been analyzed by use of laser Raman spectroscopy.

IV-1 Experimental

IV-1-1 Material

Research grade Ar was purchased from the Neriki Gas Co. Ltd., having a stated minimum purity of 99.9999 mol %. Distilled water was obtained from Yashima Pure Chemicals Co. Ltd. Both were used without further purification.

IV-1-2 Experimental Apparatus

Two types of high-pressure cell that are appropriate for the experimental pressure region were used in the present study. The experimental apparatus were essentially the same as shown in **Figure I-1** and **Figure II-2**.

IV-1-3 Experimental Procedure

After the preparation of single crystal at the three-phase coexisting equilibrium under several pressure conditions, Raman spectra were measured. A typical photograph of Ar hydrate crystals is shown in **Figure IV-1**. The largest single crystal was aged more than a couple of weeks. The details procedure were same as Chapter-I-1-3 and Chapter-II-1-3.

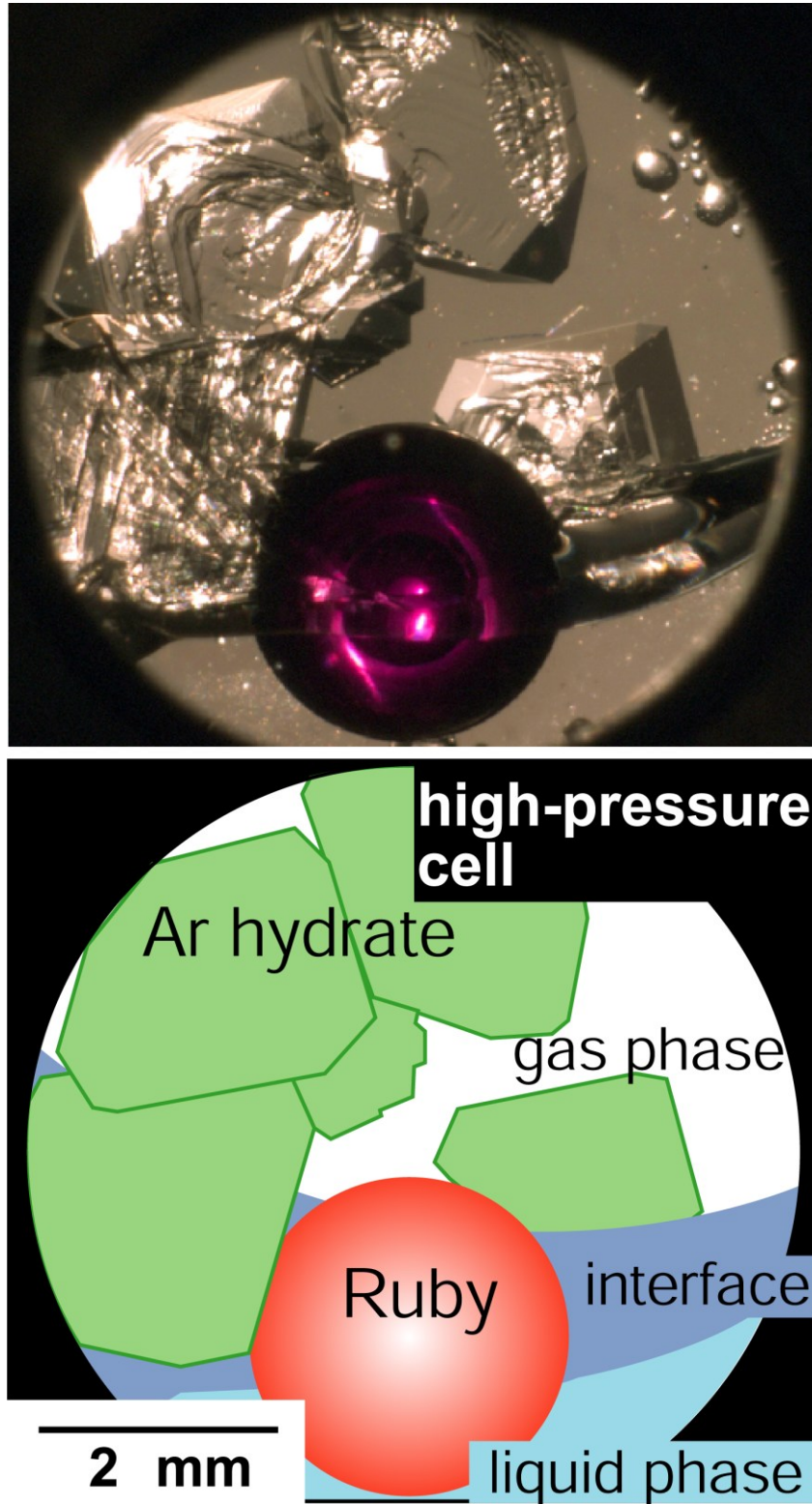


Figure IV-1 Photo (upper) and schematic drawing (bottom) of single crystals of Ar hydrate under three-phase coexisting condition of hydrate + liquid (aqueous) + gas at 284 MPa and 302.75 K. A spherical ruby of 2.5 mm in diameter is trapped in the high-pressure cell in order to stir the contents.

IV-2 Results and discussion

The three-phase coexisting data obtained in the present study for the Ar hydrate system are listed in **Table IV-1**. **Figure IV-2** shows the pressure temperature relations of Ar hydrate system accompanied with the literature values (Dyadin et al. 1997 [3], Marshall et al. 1964 [15]). In the low-pressure region (up to 200 MPa), the present data are in good agreement with Marshall's ones (1964) [15]. Moreover, except less than 20 MPa, the present data are in almost agreement with Dyadin's ones (1997) [3].

Table IV-1 Three-phase coexisting data for the Ar hydrate system.

T / K	p / MPa	T / K	p / MPa
279.57	17.72	293.95	98
280.55	19.81	294.70	108
281.64	22.23	296.10	129
282.64	24.44	297.17	147
283.95	28.17	297.99	169
284.72	31.93	299.44	199
284.84	32.38	300.39	226
285.25	32.60	301.65	258
286.15	38.29	302.75	284 (s-I)
287.16	42.86	303.09	322 (s-I)
288.16	48.82	303.60	358 (s-I)
288.66	51.70	304.10	409 (s-I)
289.65	57.96	304.57	447 (s-I)
290.68	66.22	305.05	464 (s-H)
291.06	69.40	305.19	474 (s-H)
292.07	77	305.21	476 (s-H)
293.18	89	305.32	485 (s-H)

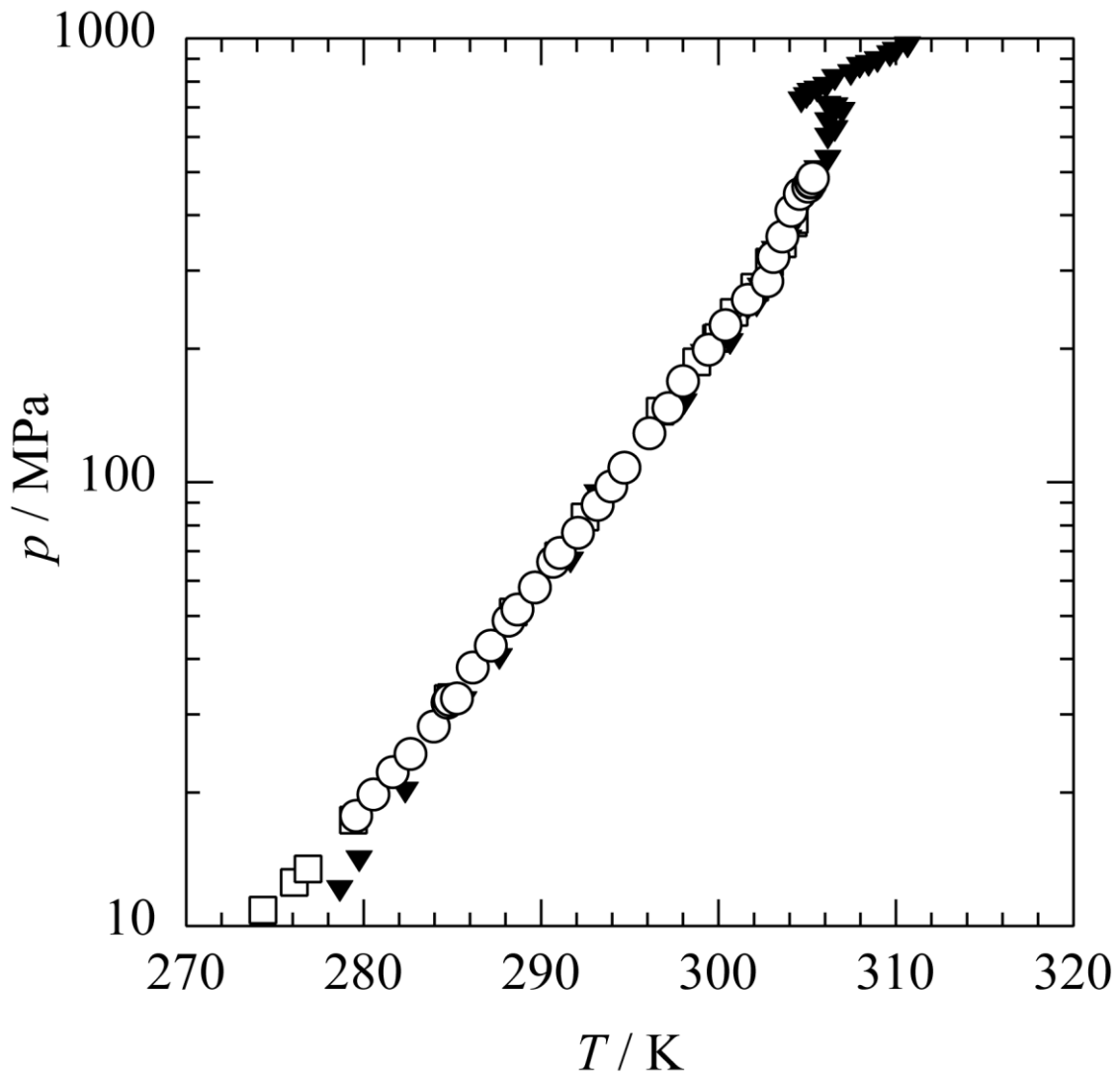


Figure IV-2 Pressure - temperature relations of Ar hydrate stability boundaries: ○, three-phase coexisting curve of Ar hydrate (present study); □, Marshall et al. (1964) [15]; ▼, Dyadin et al (1997) [3]. From my experimental data (up to 485 MPa), Ar hydrate has two structural transition points located at 281 MPa and 456 MPa. Dyadin et al. (1997) [3] have stated that the discontinuous slope changes around 460 MPa and 770 MPa are caused by structural transitions to s-H (Manakov et al. 2001 [5]) and to tetragonal structure (Kurnosov et al.2001[7]), respectively.

Figure IV-3 shows the extended figure (the pressure ranges from 200 MPa to 500 MPa) of the thermodynamic stability boundary for the Ar hydrate system in the present study. The stability boundary changes greatly in the slope at 281 MPa and 302.7 K, and 456 MPa and 304.6 K, respectively. Generally, the large slope change of dp/dT means the structural phase transition point. Manakov et al. (2001) [5] have reported the structural change (s-II to s-H) around 460 MPa. On the other hand, no investigator has reported about the structural change point around 280 MPa. We have divided the three-phase coexisting curve to the three regions. The region A corresponds to the pressure range up to 281 MPa. The pressure range from 281 to 456 MPa is region B, and over 456 MPa defined as region C. Especially, in the region B, the present data show the large discrepancies with the literature (Dyadin et al. 1997 [3], Marshall et al. 1964 [15]).

The Raman spectrum of intermolecular O–O stretching vibration mode of water molecules was detected around 210 cm^{-1} in the s-II gas hydrate systems as N_2 hydrate systems [chapter-I]. The peak corresponding to the hydrate cage structured by hydrogen bonds is a peculiar to the structure of hydrate lattice. In the present study, the Raman shift of the O–O stretching vibration for the Ar hydrate crystal at 46 MPa and 288 K is detected at 209 cm^{-1} . The typical Raman spectra of the intermolecular O–O vibration mode in the Ar hydrate crystals in each region of **Figure IV-3** are shown in **Figure IV-4**. The O–O vibration energy increases with pressure (along the three-phase coexisting curve), that is, the hydrate cage shrinks gradually by pressurization.

Figure IV-5 shows the pressure dependence of the Raman shift corresponding to the O–O stretching vibration for the Ar hydrate system, which measured along the three-phase coexisting curve. For comparison, my results of the Kr (s-II) and Xe (s-I) hydrate crystals measured along the three-phase coexisting curves [Chapter-III] are also shown in **Figure IV-5**. I have speculated in Chapter-III that the s-II Kr hydrate changes to s-H at 414 MPa based on the slope change of three-phase coexisting curve and the Raman spectrum.

The pressure dependence of the O–O vibration in the Ar hydrate system up to 281 MPa (correspond to region A of **Figure IV-3**) agrees well with the s-II Kr hydrate system. Therefore, the s-II Ar hydrate is stable in the region A.

From the pressure range from (281 to 456) MPa (correspond to region B), the results of the O–O vibration are almost the same tendency of the Xe hydrate system [Chapter-III]. The fact

suggests that Ar hydrate crystal may be the s-I lattice in the region B. Moreover, the slope change of the stability boundary (**Figure IV-3**) also supports structural phase transition of Ar hydrate crystal. However, Shimizu et al. (2003) [10] have evaluated the multi occupancy of Ar atoms by the Raman spectra of Ar–Ar interatomic stretching vibration around 150 cm^{-1} . Manakov et al. (2004) [14] has suggested the double occupancy of the s-II Ar hydrate in the pressure region from (340 to 440) MPa based on neutron diffraction experiments at 293 K. Tanaka et al. (2004) [11] reported that double occupancy dominated over single occupancy above 270 MPa from van der Waals Platteuw theory. In the present study, those were not taken up because it was difficult to clarify the meaning Raman peak from noises on the shoulder of Rayleigh scattering. Therefore, we cannot discuss about the double occupancy of Ar atoms in the Ar hydrate system by the Raman peaks of the present study. On the other hand, Lotz and Schouten (1999) [4] suggested that s-II Ar hydrate changes to s-I at the high-pressure region. Thus, it might be thought that there are the following two possibilities about the phenomenon around 280 MPa; the structural phase transition of Ar hydrate and/or the change of cage occupancy. I speculate that, around 280 MPa, an Ar atom occupied in the large cage (M-cage) of s-I may be more comfortable than two Ar atoms occupied in the L-cage (double occupancy) of s-II. As a result of that, the structural change from s-II Ar hydrate to s-I would occur in the region B.

At 459 MPa (correspond to region C), the O–O vibration energy of Ar hydrate becomes lower than that of s-I hydrate [Chapter-III] (Xe hydrate system). The similar discontinuity of the pressure dependence has shown in the Kr hydrate system (**Figure IV-5**); the Raman shift of Ar hydrate is slightly (3 cm^{-1}) higher than that of the Kr hydrate at almost the same pressure; in this pressure range, the Kr hydrate is s-H [Chapter-III]. Moreover, there is a drastic slope change of three-phase coexisting curve of Ar hydrate around 456 MPa in the present study (**Figure IV-3**). They show good agreement with Manakov et al. (2001) [5] (460 MPa). Those facts strongly support that the structural phase transition in the Ar hydrate crystal occurs around 456 MPa, and that the structure of Ar hydrate observed over 456 MPa (region C) would be s-H as reported by Manakov et al. (2001) [5] and Manakov et al. (2004) [14] and Loveday et al. (2003) [9]. Additionally, in the high-pressure region (760 to 960 MPa), the tetragonal Ar hydrate would be stable as Kurnosov et al. (2001) [7] have reported.

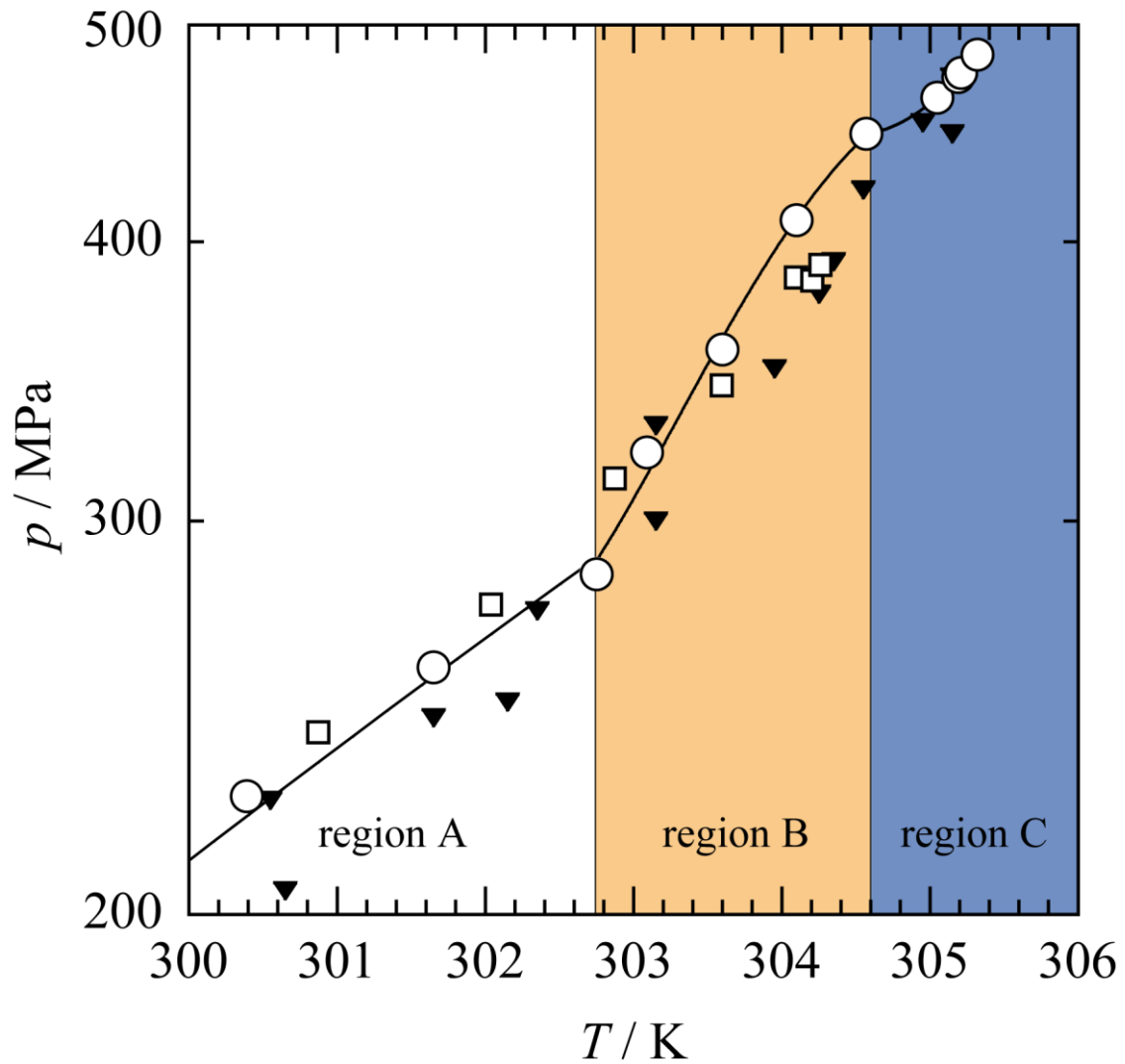


Figure IV-3 Enlarger data (the pressure ranges from 200 MPa to 500 MPa) of **Figure IV-2**: \circ , present study; \square , Marshall et al. (1964) [15]; \blacktriangledown , Dyadin et al. (1997) [3]. The stable structure in each region is as follows; region A, s-II; region B, s-I; region C, s-H.

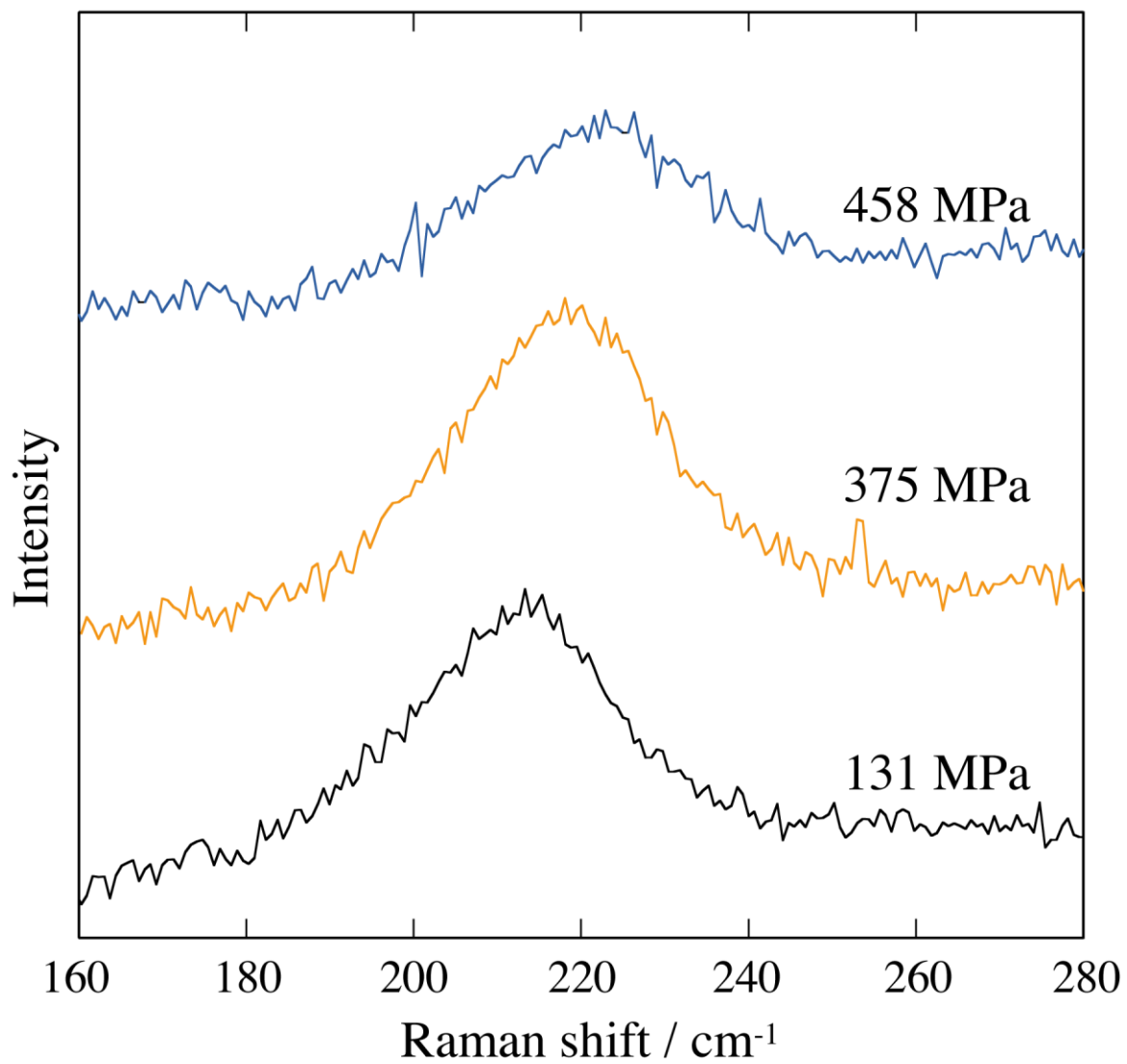


Figure IV-4 Raman spectra of the intermolecular O–O vibration mode in the Ar hydrate crystals at 131 MPa (s-II), 375 MPa (s-I), and 458 MPa (s-H).

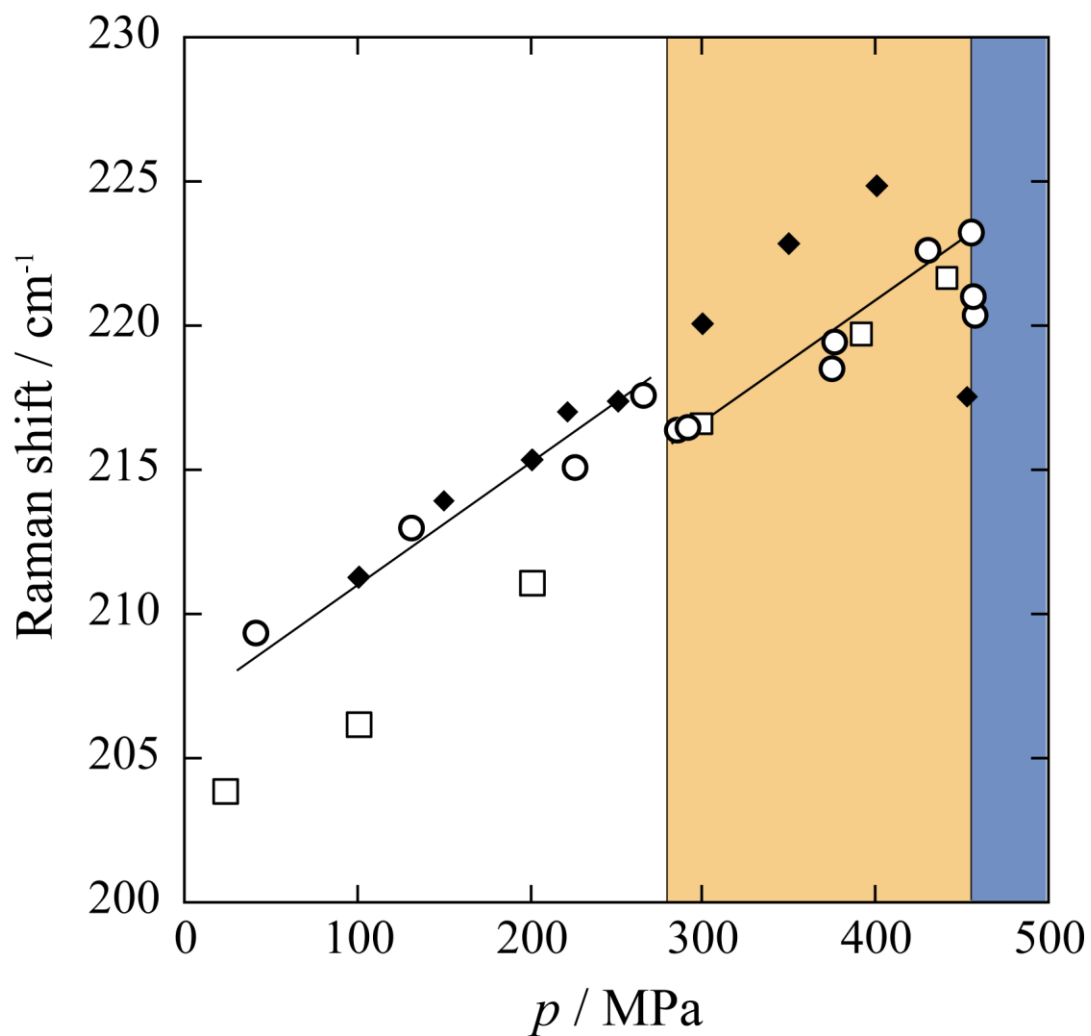


Figure IV-5 Pressure dependence of the Raman shift corresponding to the O–O stretching vibration for the Ar hydrate system along the three-phase coexisting curve: ○, Ar hydrate; ◆, Kr hydrate (s-II: up to 414 MPa; s-H: over 414 MPa) [Chapter-III] ; □, Xe hydrate (s-I) [Chapter-III].

Summary

The three-phase coexisting curve of Ar hydrate system was obtained up to 485 MPa. Single crystals of Ar hydrate were analyzed in situ by use of laser Raman spectroscopy along the three-phase coexisting curve. The slope changes of dp/dT on the boundary curve and the pressure dependence of the intermolecular O–O stretching vibration mode of the Ar hydrate system reveal that two structural phase transition points exist at 281 MPa and 302.7 K, 456 MPa and 304.6 K, respectively. For the Ar hydrate system, the s-II hydrate crystal exists up to 281 MPa and changes to s-I in the pressure region from 281 to 456 MPa. Finally, Ar hydrate changes to s-H around 456 MPa.

Nomenclature

p = pressure [Pa]

T = temperature [K]

Literature Cited

[1] Villard, P, “Combination de l’argon avec l’eau”, *Comptes Rendus Hebdomadaires des Seances de l’Academie des Sciences*, **123**, 377-380 (1896).

[2] Davidson, D. W.; Handa, Y. P.; Ratcliffe, C. I.; Tse, J. S.; Powell, B. M. “The Ability of Small Molecules to Form Clathrate Hydrates of Structure II”, *Nature*, **311**, 142-143 (1984).

[3] Dyadin, Y. A.; Larionov, E. G.; Mirinski, D. S.; Mikina, T. V.; Starostina, L.I. “Clathrate Formation in the Ar-H₂O Systems under Pressures up to 15000 bar”, *Mendeleev Communucation*, **7**, 33-34 (1997).

[4] Lotz, H. T.; Schouten, J. A. “Clathrate Hydrate in the System H₂O-Ar Pressures and Temperatures up to 30 kbar and 140 °C”, *Journal of Chemical Physics*, **111**, 10242-10247 (1999).

[5] Manakov, Y. A.; Voronin, A, V; Kurnosov, A. V.; Teplykh, A. E.; Larionov, E. G.; Dyadin, Y. A. “Argon Hydrates: Structural Studies at High Pressures”, *Doklady Physical Chemistry*, **378**, 148-151 (2001).

[6] Ripmeester, J. A.; Tse, J. S.; Ratcliffe, C. I.; Powell, B. M. “A New Clathrate Hydrate Structure”, *Nature*, **325**, 135-136 (1987).

[7] Kurnosov, A. V.; Manakov, A. Y.; Komarov, V. Y.; Voronin, V. I.; Teplykh, A. E.; Dyadin, Y. A. “A New Gas Hydrate Structure”, *Doklady Physical Chemistry*, **381**, 303-305 (2001).

[8] Hirai, H.; Uchihara, Y.; Nishimura, Y.; Kawamura, T.; Yoshimoto, Y.; Yagi, T. “Structural Changes of Argon Hydrate under High Pressure”, *Journal of Physical Chemistry B*, **106**, 11089-11092 (2002).

- [9] Loveday, J. S.; Nelmes, R. J.; Klug, D. D.; Tse, J. S.; Desgraniers, S. "Structural Systematics in the Clathrate Hydrates under Pressure", *Canadian Journal of Physics*, **81**, 539-544 (2003).
- [10] Shimizu, H.; Hori, S.; Kume, T.; Sasaki, S. "Optical Microscopy and Raman Scattering of A Single Crystalline Argon Hydrate at High Pressures", *Chemical Physics Letter*, **368**, 132-138 (2003).
- [11] Tanaka, H.; Nakatsuka, T.; Koga, K. "On the Thermodynamic Stability of Clathrate Hydrates IV: Double Occupancy of Cages", *Journal of Chemical Physics*, **121**, 5488-5493 (2004).
- [12] Inerbaev, T. M.; Belosludov, V. R.; Belosludov, R. V.; Sluiter, M.; Kawazoe, Y.; Kudoh, J. "Theoretical Study of Clathrate Hydrates with Multiple Occupation", *Journal of Inclusion Phenomena and Macrocyclic Chemistry*, **48**, 55-60 (2004).
- [13] Malenkov, G. G.; Zheligovskaya, E. A. "Dynamics of Some He and Ar Clathrate Hydrates. Computer Simulation Study", *Journal of Inclusion Phenomena and Macrocyclic Chemistry*, **48**, 45-54 (2004).
- [14] Manakov, A. Y.; Voronin, V. I.; Kurunosov, A. V.; Teplykh, A. E.; Komarov, Y. V.; Dyadin, Y. A. "Structural Investigations of Argon Hydrates at Pressure up to 10 kbar", *Journal of Inclusion Phenomena and Macrocyclic Chemistry*, **48**, 11-18 (2004).
- [15] Marshall, D. R.; Saito, S.; Kobayashi, R. "Hydrates at High Pressures: Part I. Methane-Water, Argon-Water, and Nitrogen-Water Systems", *American Institute of Chemical Engineers Journal*, **10**, 202-205 (1964).

Chapter-V: High-Pressure Phase Behavior and Cage Occupancy for the CF₄ Hydrate System

Abstract

Three-phase coexisting curve of CF₄ hydrate + aqueous + fluid CF₄ and Raman spectra for the CF₄ hydrate system have been investigated in a temperature range of (276 to 317) K and pressure up to 454 MPa. The present experimental results show that the CF₄ molecule occupies both the S- and M-cages at high-pressure region (above 70 MPa) as well as cyclopropane hydrate system. The pressure independence of intermolecular O–O vibration reveals that the CF₄ hydrate cage is hardly shrunk by pressurization.

Introduction

The cage occupancy by the guest molecule is one of the most important information for the property of gas hydrates. It has been extensively regarded that the molecular size of guest species has an effect upon the hydrate structure and cage occupancy. For example, the methane molecule generates the structure-I (s-I) hydrate and occupies both the S- and M-cages. On the other hand, it has been argued that some molecules such as ethane, ethylene and cyclopropane could not occupy the S-cage since they have larger molecular sizes than the S-cage. However, it has been reported that the direct evidence of S-cage occupancy by ethane (Morita et al. 2000 [1]), ethylene (Sugahara et al. 2000 [2]), and cyclopropane (Suzuki et al. 2001 [3]) from the Raman spectroscopic analysis for the intramolecular vibration in a pressure range up to 500 MPa under the three-phase (hydrate + aqueous + liquid guest) coexisting conditions. Tanaka (1994) [4] has predicted that the CF₄, whose size is similar to ethane, can occupy the S-cage at relatively moderate pressure region from the van der Waals Platteau theory. In Jeffrey's book (1984) [5], the CF₄ molecule constructs s-I hydrate. However the information of CF₄ cage-occupancy is not mentioned there.

The thermodynamic stability boundary for CF₄ hydrate system has been reported by several investigators (Miller et al. 1969 [6], Garg et al. 1975 [7], Mooijer-van den Heuvel et al. 2000

[8]). However all of them are limited to the low-pressure region. The thermodynamic stabilities of gas hydrates at high-pressures (above 100 MPa) are informative and important for the understanding of gas hydrate properties, for example, the structural-phase transition as described in I-3-3. In this chapter, I have measured the three-phase coexisting state (CF_4 hydrate (H) + aqueous (L_1) + fluid CF_4 (F)) for the CF_4 hydrate system in a temperature range of (276 to 317) K and pressure up to 454 MPa. The intramolecular symmetric C–F stretching vibration of CF_4 in each phase and the intermolecular O–O vibration of hydrate cage were measured by use of laser Raman spectroscopy under the three-phase coexisting (H + L_1 + F) conditions. In addition, the pressure dependences were also analyzed in a pressure range up to approximately 400 MPa.

V-1 Experimental

V-1-1 Material

Research grade CF_4 of purity 99.999 mol % was purchased from Neriki Gas Co. Ltd. The distilled water was obtained from Yashima Pure Chemicals Co. Ltd. Both of them were used without further purification.

V-1-2 Experimental Apparatus

The experimental apparatus used in this study were essentially the same as the previous one as shown in **Figure II-2** and **Figure I-1**.

V-1-3 Experimental Procedure

The single crystals of the CF_4 hydrates prepared in the high-pressure optical cell under several three-phase coexisting conditions were analyzed using a laser Raman microprobe spectrometer. The experimental procedure is essentially same as described in Chapter-I-1-3 and Chapter-II-1-3.

V-II Results and Discussion

The stability boundary curve (H + L₁ + F) for the CF₄ hydrate system is listed in **Table V-1** and plotted on the plane of logarithmic pressure versus temperature in **Figure V-1** accompanied with the methane hydrate system (Nakano et al. 1999 [10], Oghaki and Hamanaka 1995 [11]). As the present experimental equipment is not suitable for measuring phase equilibrium at the temperature below the ice point (273 K), we could not compare with some literature values (Milkler et al. 1969 [6], Garg et al. 1975 [7]). The data of Mooijer-van den Heuvel (2000) [8] in the lower pressure region up to 13 MPa are located at the slightly higher-temperature region than that of the present study. Compared with the methane hydrate system, the stability zone of the CF₄ hydrate system exists higher-pressure (lower temperature) region than the methane hydrate system, and the equilibrium pressures increase monotonically and moderately with temperatures. The smoothness of the three-phase coexisting curve suggests that there is no structural phase-transition point in the experimental region of the present study, that is, the CF₄ hydrate is still s-I at even high-pressure region of about 500 MPa.

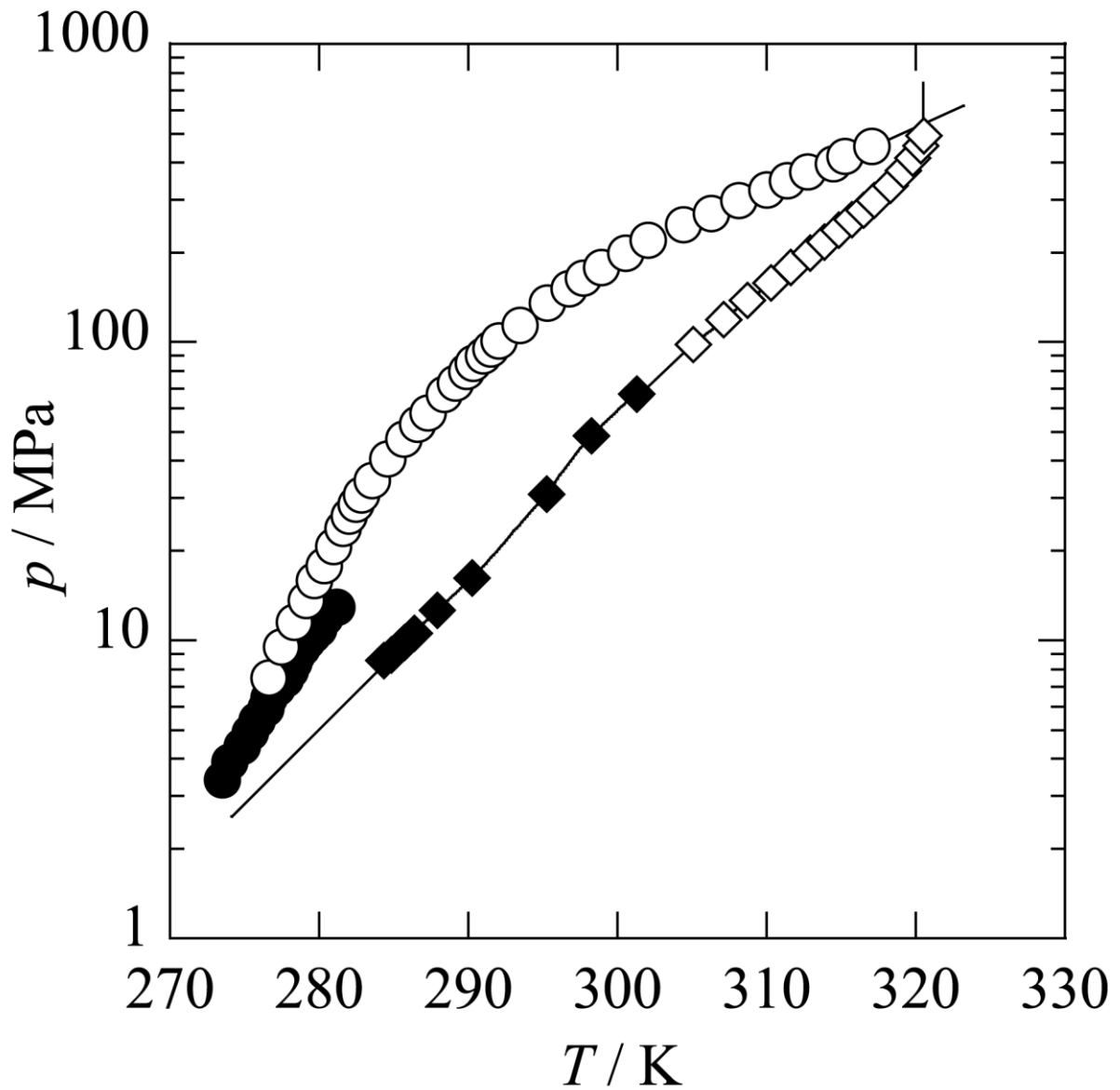


Figure V-1 Three-phase coexisting curve for the CF₄ hydrate system (circular keys) accompanied with methane hydrate system (lozenge keys): ○, present study; ●, Mooijervanden Heuvel et al. (2000) [8]; ◇, Nakano et al. (1998) [10]; ◆, Ohgaki and Hamanaka (1995) [11].

Table V-1 Three-phase coexisting curve for the CF₄ hydrate system.

T / K	p / MPa	T / K	p / MPa
276.62	7.48	291.00	90
277.47	9.49	291.51	95
298.34	11.48	292.05	101
279.11	13.60	293.46	114
279.68	15.84	295.31	135
280.34	17.79	296.76	151
280.95	20.67	297.71	164
281.60	23.78	298.92	178
281.99	26.14	300.55	199
282.46	28.62	302.06	220
282.84	30.75	304.43	248
283.56	34.41	306.28	270
285.68	47.41	308.15	299
286.60	53	310.00	324
287.30	58	311.39	349
288.37	67	312.76	372
289.15	73	315.27	420
289.89	80	317.05	454
290.35	85		

The CF₄ molecule has four Raman active vibration modes. In the present study, we noticed the symmetric C–F vibration mode (ν_1 : detected at 908.5 cm⁻¹ at atmospheric pressure (Monosrori and Weber 1960 [12])) because it exhibits sharp and highly intensive. The Raman spectrum of the symmetric C–F vibration for CF₄ hydrate crystal was single peak (around 908 cm⁻¹) below 70 MPa. Typical Raman spectrum observed in the CF₄ hydrate crystal at 50 MPa is shown in **Figure V-2 (a)**. The Raman spectrum of the symmetric C–F vibration mode for the fluid CF₄ phase was single peak (around 909 cm⁻¹) and slightly higher frequency than the hydrate phase. Unfortunately, we could not analyze the Raman peak for aqueous phase because it was very weak. As the system pressure increases, an additional Raman peak is detected around 918 cm⁻¹ in the CF₄ hydrate phase as shown in **Figure V-2 (b)** (at 150 MPa). The split of Raman peak reveals that the CF₄ molecules are entrapped in two different cages, that is, the CF₄ molecule is able to occupy both the S- and M-cages. The Raman-peak area ratio of the CF₄ molecule in S-cage becomes larger at 400 MPa as shown in **Figure V-2 (c)**. The relative Raman-peak area of S-cage ($S_{S\text{-cage}}$) to M-cage ($S_{M\text{-cage}}$) versus pressure is shown in **Figure V-3**. The peak area ratio ($S_{S\text{-cage}}/S_{M\text{-cage}}$) increases in acceleration with pressure. It means that the CF₄ molecule shows peculiar cage occupancy so-called “pressure oppressive S-cage occupancy” as well as the cyclopropane [3]. The S-cage occupancy of CF₄ is higher than that of cyclopropane and has strong pressure dependency. Tanaka (1994) [4] has predicted that the CF₄ molecule could occupy both the S- and M-cages at relatively low-pressures. However, we have obtained single peak at low-pressures (**Figure V-2 (a)**). In addition, extrapolating the peak area ratio (**Figure V-3**), the S-cage occupancy of CF₄ molecule becomes zero around 70 MPa. These findings indicate that the CF₄ molecule occupies both the S- and M-cages of s-I hydrate at least above 70 MPa.

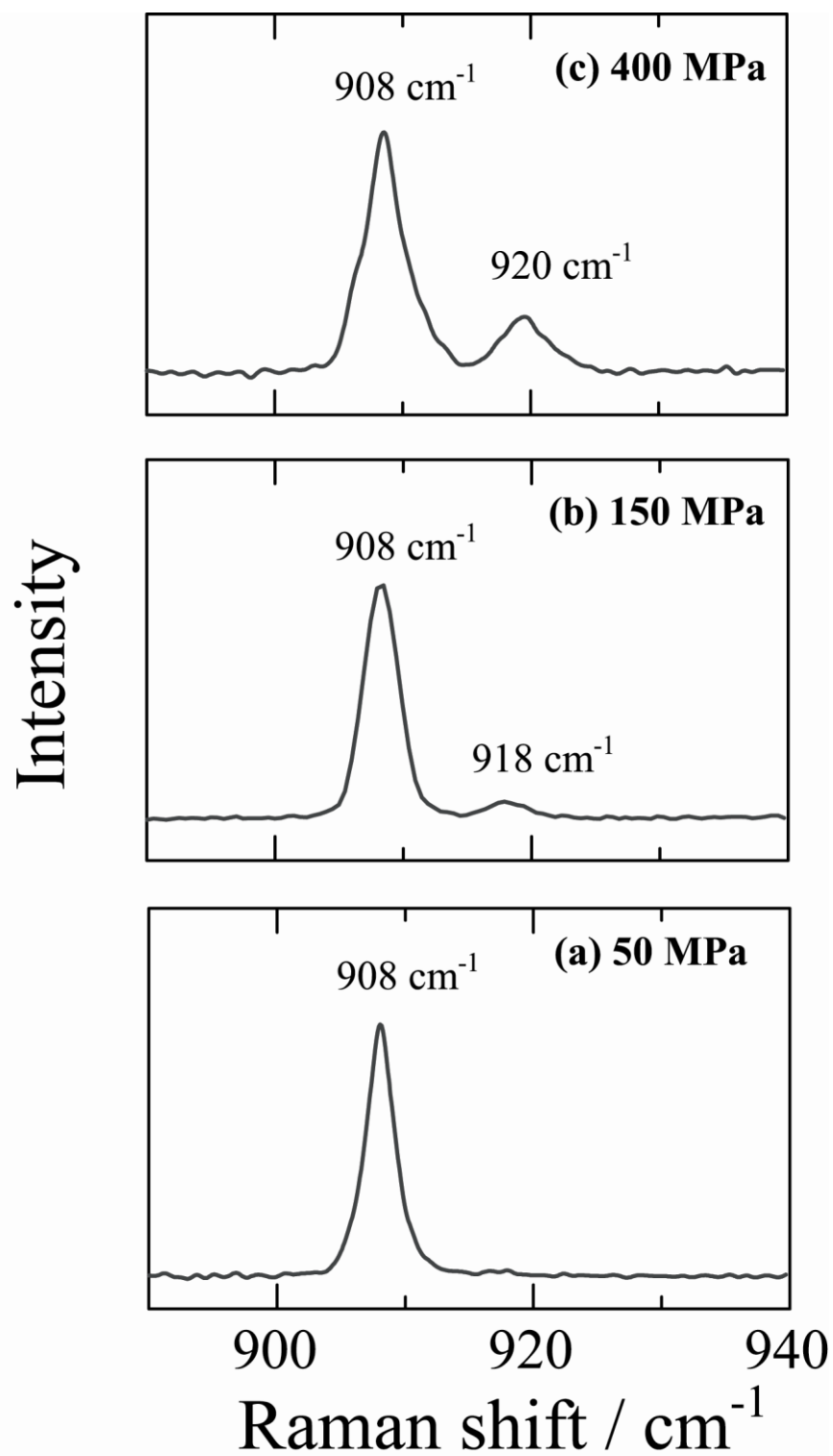


Figure V-2 Raman spectra of the symmetric C-F vibration mode of CF₄ in the CF₄ hydrate crystal. **(a)** 50 MPa, **(b)** 150 MPa, **(c)** 400 MPa.

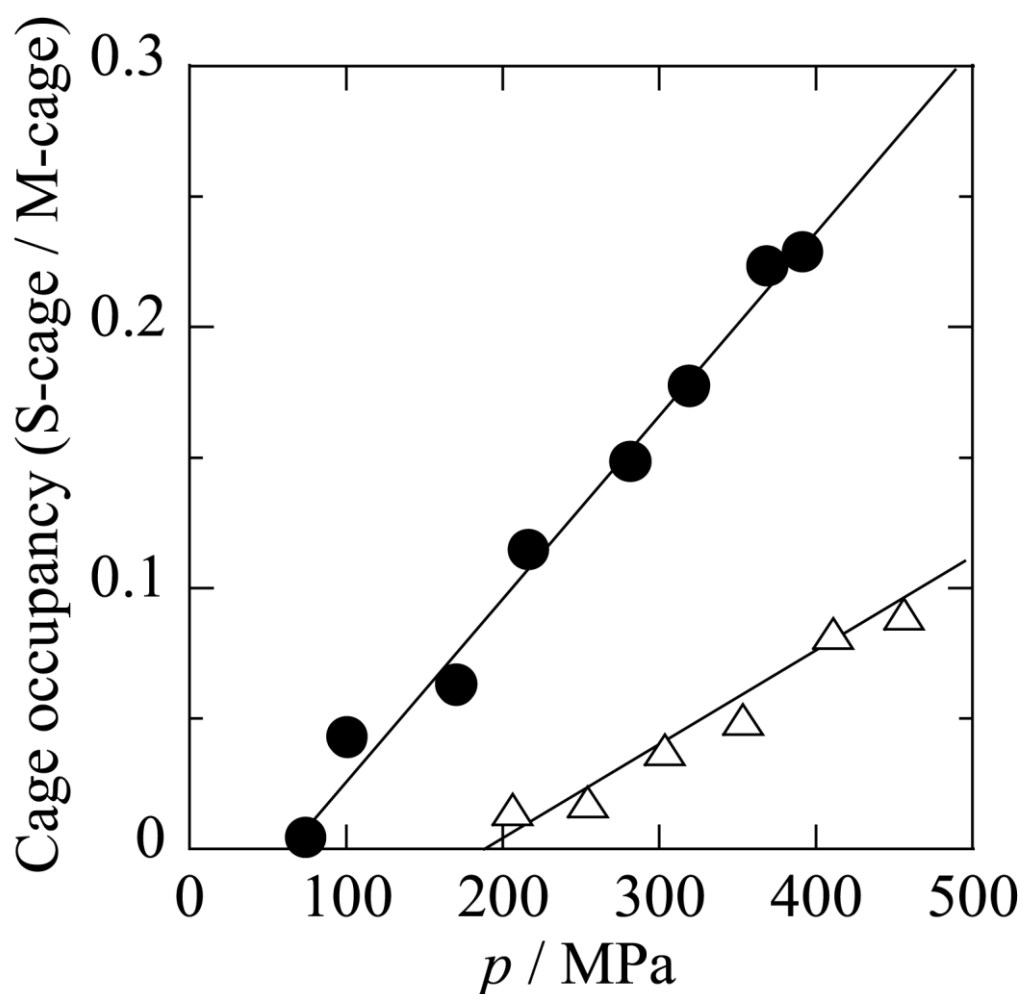


Figure V-3 Pressure effect on the cage occupancy of guest species: ●, CF₄; △, cyclopropane [3].

The pressure dependency of Raman shift for the symmetric C–F stretching vibration is shown in **Figure V-4**. The higher frequency peak for the S-cage shows weak pressure dependency ($0.5 \text{ cm}^{-1} / 100 \text{ MPa}$). On the other hands, the lower one for the M-cage is independent of pressure. Similar behavior is also observed in the results of some s-I hydrate systems (Morita et al. 2000 [1], Sugahara 2000 [2], Suzuki et al. 2001 [3], Nakano et al. 1998 [9], Nakano et al. 1999 [10]). It suggests that the inner volume of M-cage is still large enough for the CF₄ molecule even if the pressure is raised up to 500 MPa.

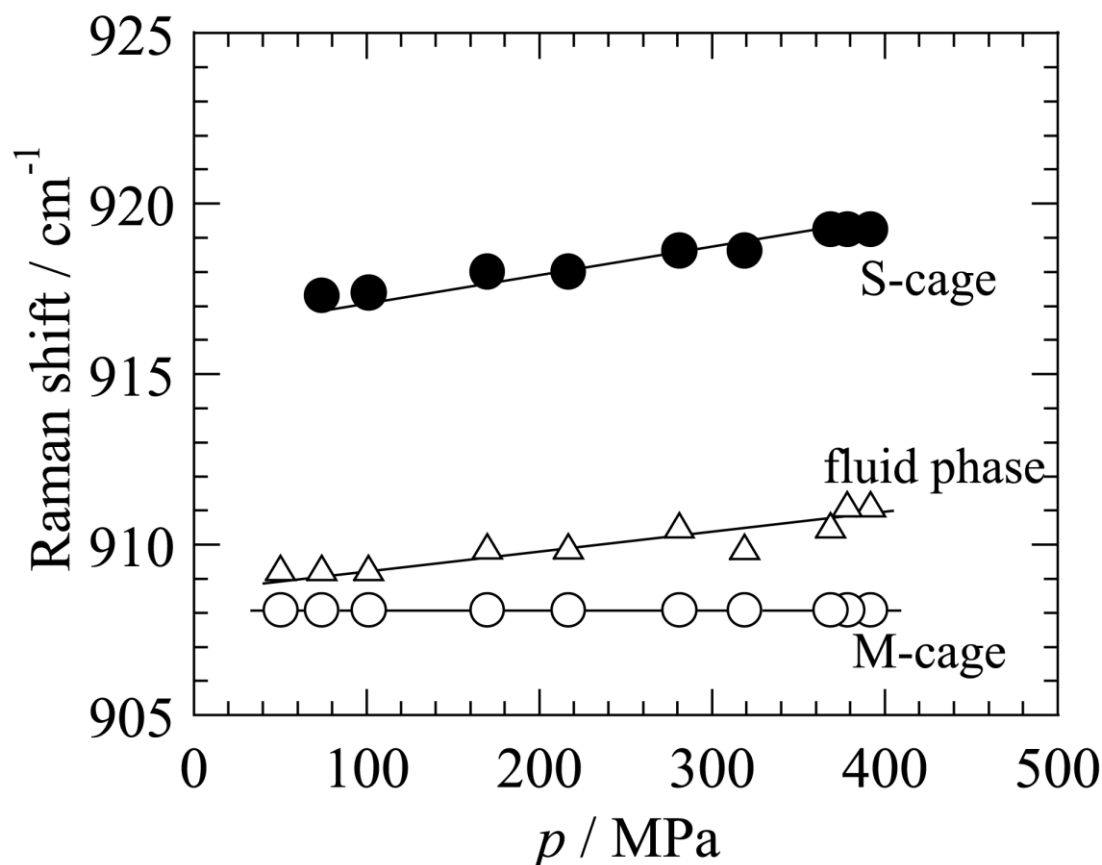


Figure V-4 Pressure effect on the symmetric C–F stretching vibration in the CF_4 hydrate system: ●, S-cage; ○, M-cage; △, fluid phase.

The intermolecular O–O vibration mode of the s-I hydrate crystal is usually detected around 205 cm^{-1} . The Raman spectrum of intermolecular O–O vibration mode in the CF_4 hydrate crystal at 400 MPa is detected at 206 cm^{-1} as shown in **Figure V-5**. The pressure effect on the O–O vibration in the CF_4 hydrate is shown in **Figure V-6** accompanied with the results of N_2 [Chapter-I], Kr [Chapter-III], CO_2 (Nakano et al. 1998 [9]), methane (Nakano et al. 1999 [10]), ethane (Morita et al. 2000 [1]), ethylene (Sugahara 2000 [2]), and cyclopropane (Suzuki et al. 2001 [3]) hydrate systems. The O–O vibration in the CF_4 hydrate crystal is almost independent of pressure and this behavior is similar to those of ethane, ethylene and cyclopropane hydrate systems, while nitrogen, CO_2 and methane hydrate systems show weak pressure dependency. The pressure independency for the CF_4 hydrate system means that the hydrate cages are hardly shrunk by pressurization.

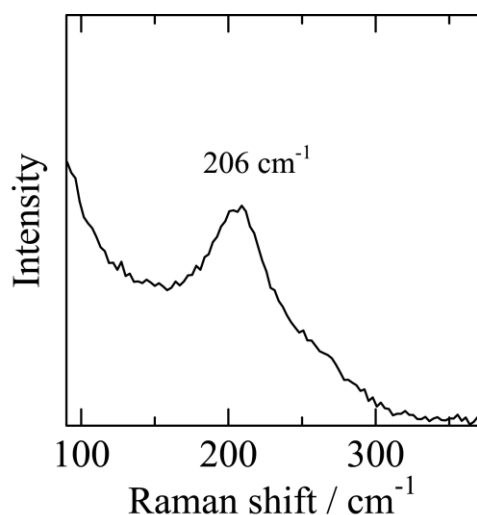


Figure V-5 Raman spectrum of the intermolecular O–O vibration mode in the CF₄ hydrate crystal at 400 MPa.

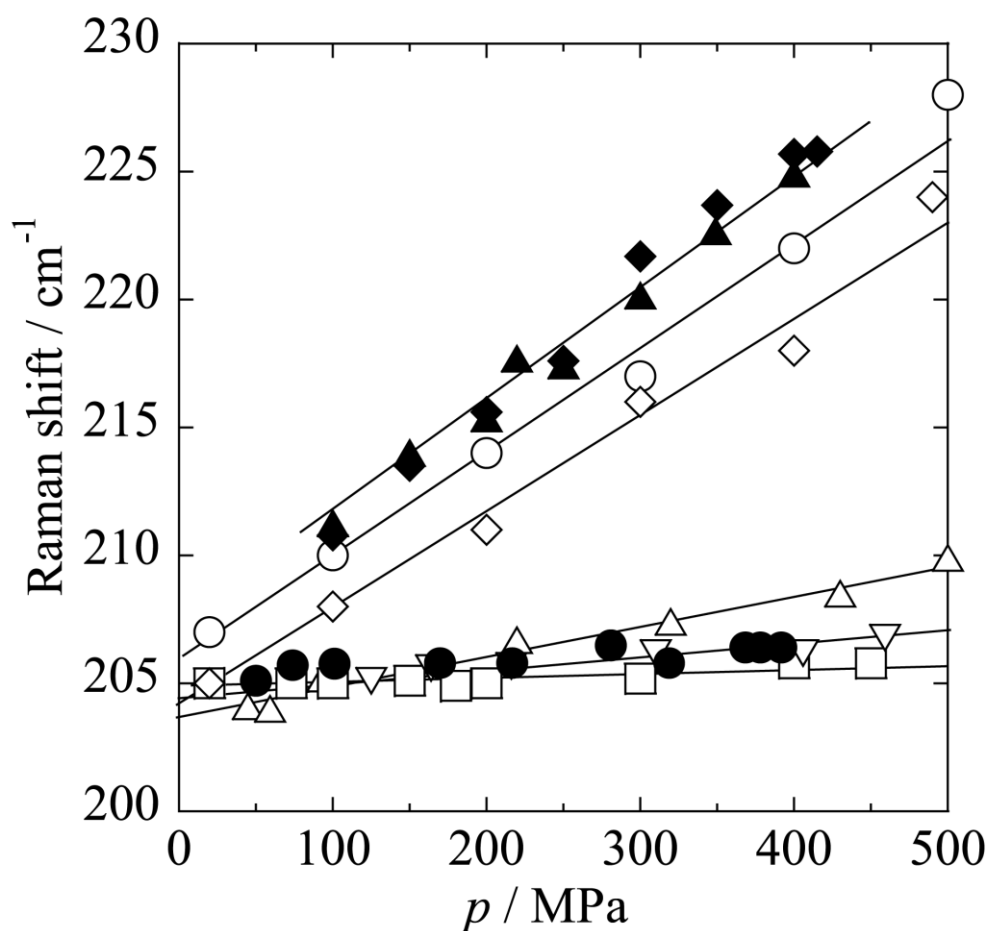


Figure V-6 Pressure effect on the O–O vibration in the hydrate systems: ●, CF₄; ◆, N₂ [Chapter-I]; ▲, Kr [Chapter-III]; ◇, CO₂ (Nakano et al. 1998 [9]); ○, methane (Nakano et al. 1999 [10]); □, ethane (Morita et al. 2000 [1]); △, ethylene (Sugahara et al. 2000 [2]); ▽, cyclopropane (Suzuki et al. 2001 [3]).

Summary

The three-phase coexisting curve of CF₄ hydrate + aqueous + fluid CF₄ was investigated up to 454 MPa by use of a high-pressure optical cell. The equilibrium pressure increases monotonically with temperature in the present experimental region. The behavior of the three-phase coexisting curve supports that the s-I CF₄ hydrate never changes any other lattice structure in the present experimental conditions.

The Raman spectra of the intramolecular symmetric C–F stretching vibration of the CF₄ molecule and the intermolecular O–O vibration modes were observed in the pressure range up to approximately 400 MPa. The split of Raman spectra for the symmetric C–F vibration in the CF₄ hydrate phase is detected in the higher-pressure range than 70 MPa. This fact indicates that the CF₄ molecule occupies both the S- and M-cages of s-I hydrate in the high-pressure region above 70 MPa. In addition, the S-cage occupancy of the CF₄ molecule becomes larger with pressure increasing. The O–O vibration of the CF₄ hydrate crystal is almost independent of pressure.

Nomenclature

p = pressure [Pa]

T = temperature [K]

<Symbol>

F = fluid phase

H = hydrate phase

L = liquid phase

<Subscript>

1 = host component (water)

Literature Cited

- [1] Morita, K.; Nakano, S.; Ohgaki, K. "Structure and Stability of Ethane Hydrate Crystal", *Fluid Phase Equilibria*, **169**, 167-175 (2000).
- [2] Sugahara, T.; Morita, K.; Ohgaki, K. "Stability Boundaries and Small Hydrate-Cage Occupancy of Ethylene Hydrate System", *Chemical Engineering Science*, **55**, 6015-6020 (2000).
- [3] Suzuki, M.; Tanaka, Y.; Sugahara, T.; Ohgaki, K. "Pressure Dependence of Small-Cage Occupancy in the Cyclopropane Hydrate System", *Chemical Engineering Science*, **56**, 2063-2067 (2001).
- [4] Tanaka, H. "The Stability of Xe and CF₄ Clathrate Hydrates. Vibrational Frequency Modulation and Cage Distortion", *Chemical Physics Letters*, **202**, 345-349 (1993).
- [5] Jeffery, G. A. "Inclusion Compounds Vol.1 Chapter 5, Hydrate Inclusion Compounds", Academic Press: London (1984).
- [6] Miller, S. L.; Eger, E. I.; Lundgreen, C. "Anesthetic Potency of CF₄ and SF₆ in Dogs", *Nature*, **221**, 468-469 (1969).
- [7] Garg, S. K.; Gough, S. R.; Davidson, D. W. "A Wide-Line NMR Study of Reorientation of Some Spherical-Top Molecules Enclathrated in Water", *The Journal of Chemical Physics*, **63**, 1646-1654 (1975).
- [8] Mooijer-van den Heuvel, M. M.; Peters, C. J.; de Swaan Arons, J. "Influence of Water-Insoluble Organic Components on the Gas Hydrate Equilibrium Conditions of Methane", *Fluid Phase Equilibria*, **172**, 73-91 (2000).

- [9] Nakano, S.; Moritoki, M.; Ohgaki, K. “High-Pressure Phase Equilibrium and Raman Microprobe Spectroscopic Studies on the CO₂ Hydrate System”, *Journal of Chemical and Engineering Data*, **43**, 807-810 (1998).
- [10] Nakano, S.; Moritoki, M.; Ohgaki, K. “High-Pressure Phase Equilibrium and Raman Microprobe Spectroscopic Studies on the Methane Hydrate System”, *Journal of Chemical and Engineering Data*, **44**, 254-257 (1999).
- [11] Ohgaki, K.; Hamanaka, T. “Phase-Behavior of CO₂ Hydrate-Liquid CO₂-H₂O System at High Pressure”, *Kagaku Kougaku Ronbunshu*, **21**, 800-803 (1995).
- [12] Monostori, B.; Weber, A. “The Raman Spectrum of Gaseous CF₄”, *The Journal of Chemical Physics*, **33**, 1867-1868 (1960).

Chapter-VI: Thermodynamic and Raman Spectroscopic Studies on Pressure-Induced Structural Transition of SF₆ Hydrate

Abstract

The SF₆ hydrate system has been investigated by use of a laser Raman spectroscopic analysis in a temperature range from 274 K to 313 K and pressure up to 155 MPa. Two quadruple points have been determined at (286.6±0.1) K and (1.79±0.01) MPa (SF₆ hydrate + aqueous + liquid SF₆ + gas), and at (300.3±0.1) K and (131±1) MPa (SF₆ hydrate + aqueous + liquid SF₆ + solid SF₆), respectively. The structure-II SF₆ hydrate changes to the structure-I type hydrate around 33 MPa, which is a so-called "pressure-induced structural transition" of SF₆ hydrate crystal.

Introduction

Two types of guest species that generate the structure-II (s-II) hydrate are found. One is small guest species less than 0.41 nm, for example Ar, Kr, and N₂ and the other is large guest species (0.59 to 0.67) nm, propane (Sloan 2003 [1]) and THF (Manakov 2003 [2]) etc. It has been said that the smaller one occupies both cages. But large one occupies only L-cage because of its volume, whereas the S-cage is vacant. In Chapter-I, Chapter-III, and Chapter-IV, I have reported N₂, Kr and Ar hydrate systems in the pressure region up to 500 MPa, and revealed that Ar and Kr hydrate crystals change to new structure crystals at high-pressure region whereas N₂ hydrate still remains the s-II type within the experimental condition.

SF₆ hydrate belongs to s-II hydrate in the low-pressure region as well as propane hydrate system. The thermodynamic stability boundary for SF₆ hydrate system has been reported by several investigators (Dyadin et al. 2002 [3], Miller et al. 1969 [4], Sortland and Robinson 1964 [5]). But the thermodynamic stabilities of SF₆ hydrate at high-pressures (above 100 MPa) are reported only by Dyadin et al. (2000) [3]. In this chapter, the five three-phase coexisting curves of (SF₆ hydrate (H) + aqueous (L₁) + gas (G)), (SF₆ hydrate (H) + aqueous

(L₁) + liquid SF₆ (L₂)), (SF₆ hydrate (H) + liquid SF₆ (L₂) + gas (G)), (aqueous (L₁) + liquid SF₆ (L₂) + gas (G)), and (aqueous (L₁) + liquid SF₆ (L₂) + solid SF₆ (S₂)) for the SF₆ hydrate system in a temperature range of 274 K to 313 K and pressure up to 155 MPa have been measured. The intramolecular symmetric S–F stretching vibration of SF₆ in each phase and the intermolecular O–O vibration between the water molecules are measured using laser Raman spectroscopy under the three-phase coexisting (H + L₁ + L₂) conditions. In addition, their pressure dependences are also analyzed in a pressure range up to approximately 155 MPa.

VI-1 Experimental

VI-1-1 Material

Research grade SF₆ of mole fraction purity 99.999 % was obtained from Neriki Gas Co., Ltd. The distilled water was purchased from Yashima Pure Chemicals Co., Ltd. Both were used without further purification.

VI-1-2 Experimental Apparatus

According to the measurement pressure region, three types of high-pressure cells (Type A, Type B, and Type C) were used in the present study.

VI-1-2-1 Type A (Maximum pressure is 5 MPa)

The high-pressure cell made of tempered glass by TAIATU TECHNO was used. The inner volume and maximum working pressure were about 5 cm³ and 5 MPa, respectively. In the inside of the cell, a magnetic stirrer bar was controlled to agitate by a permanent magnet outside. The system temperature was controlled by the thermostated water circulating from a thermocontraller (TAITEC CL80 and TAITEC PU-9) to water bath. Schematic illustration of the high-pressure cell (Type A) is shown in **Figure VI-1**.

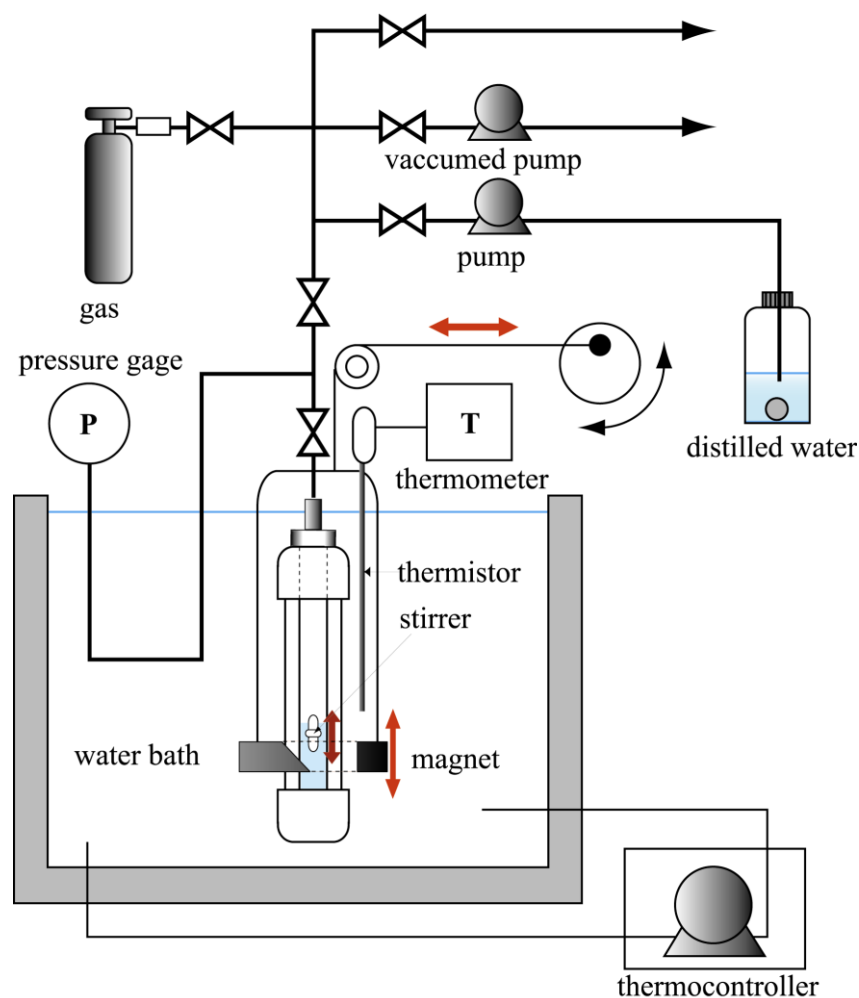


Figure VI-1 Schematic illustration of the high-pressure cell (Type A; 5 MPa).

VI-1-2-2 Type B (Maximum pressure is 75 MPa) and Type C (Maximum pressure is 400 MPa)

The experimental apparatus were the same as shown in **Figure II-2** (Type B) and **Figure II-3** (Type C).

VI-1-3 Experimental Procedure

The single crystals of the SF₆ hydrates prepared in the high-pressure optical cell (Type C) under several three-phase coexisting conditions were analyzed using a laser Raman microprobe spectrometer. The experimental procedure is essentially same as described in Chapter-I-1-3 and Chapter-II-1-3. The SF₆ molecule has three Raman active vibration modes. In the present study, I have noticed the symmetric S–F stretching vibration mode (ν_1 : detected at 774 cm⁻¹ at atmospheric pressure (Rubin et al. 1978 [6]) because it is sharp and intensive).

VI-2 Results and Discussion

The three-phase coexisting curves for the SF₆ hydrate system are listed in **Table VI-1** and plotted on the plane of logarithmic pressure versus temperature in **Figure VI-2** accompanied with the Dyadins' data (2003) [3]. The (H + L₂ + G) and (L₁ + L₂ + G) curves lie above the saturated vapor-pressure curve of SF₆. The (H + L₂ + G) curve intersects the (H + L₁ + G) curve at lower quadruple point Q₂ (H + L₁ + L₂ + G) of 286.6 K and 1.79 MPa. The (H + L₁ + L₂) curve originates from Q₂. Based on the discontinuity of dp/dT on the stability boundary (H + L₁ + L₂) around 33 MPa, the structural-phase transition point has also determined at 288.0 K and 33 MPa. According to Dyadin et al. (2002) [3], the structural-phase transition of SF₆ hydrate occurs at 288.2 K and 33 MPa. My datum agrees well with that of Dyadin et al. Based on the cross-point of (H + L₁ + L₂) and (L₁ + L₂ + S₂) curves, I have determined the higher quadruple point Q₃ (H + L₁ + L₂ + S₂) of 303.3 K and 131 MPa. Dyadin et al. have stated the second structural-phase transition point at 301.2 K and 132 MPa. It is very near to higher quadruple point (Q₃) in the present study. Unfortunately, our apparatus are not suitable to measure the three-phase coexisting (H + L₁ + S₂) and (H + L₂ + S₂) curves. Therefore, the second structural-phase transition point cannot be determined.

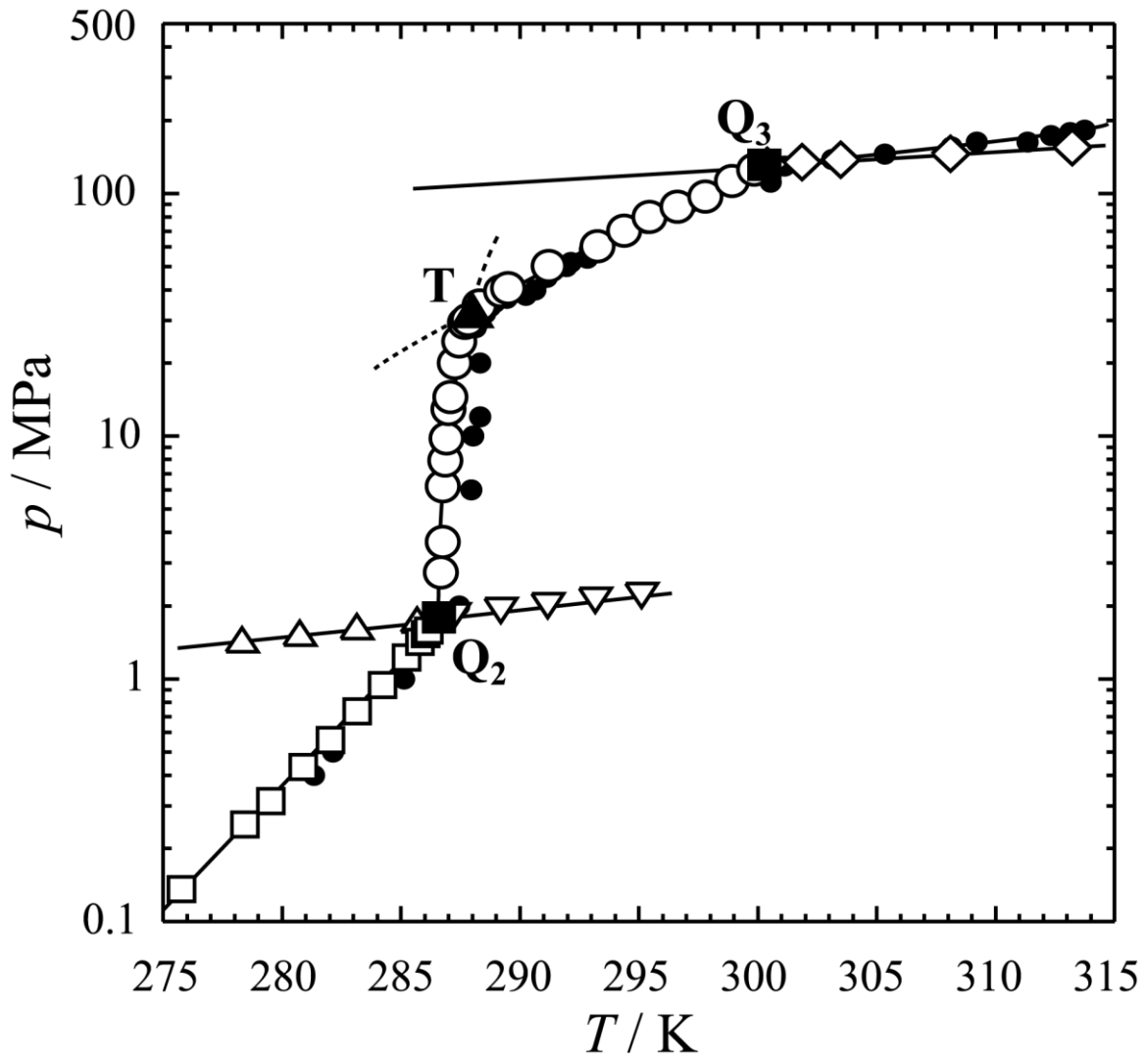


Figure VI-2 Three-phase coexisting curves for the SF₆ hydrate system: \square , H + L₁ + G; \triangle , H + L₂ + G; \circ , H + L₁ + L₂; ∇ , L₁ + L₂ + G; \diamond , L₁ + L₂ + S₂; \blacksquare , quadruple point; \blacktriangle , phase-transition point; \bullet , Dyadin et al. (2002) [3].

Table VI-1 Three-phase coexisting curves for the SF₆ hydrate system.

p / MPa	T / K	p / MPa	T / K
H + L ₁ + L ₂		H + L ₂ + G	
286.68	2.73	278.34	1.44
286.75	3.67	280.77	1.54
286.77	6.22	283.16	1.63
286.86	7.94	285.69	1.74
286.93	9.80	286.32	1.77
287.01	12.92		
287.08	14.48	L ₁ + L ₂ + G	
287.28	20.06	286.85	1.79
287.45	24.47	287.26	1.81
287.70	29.18	289.23	1.91
287.82	30.18	291.20	2.00
288.32	34.47	293.19	2.10
289.22	39.64	295.14	2.20
289.52	40.78		
291.23	50.18	L ₁ + L ₂ + S ₂	
293.27	60.69	313.25	155
294.38	70.12	308.12	145
295.45	80	303.51	137
296.64	88	301.89	134
297.80	97	300.41	131
298.92	113		
299.85	125		
H + L ₁ + G		Q ₂	
274.28	0.10	286.6	1.79
275.78	0.14		
278.45	0.25	Q ₃	
279.54	0.31	300.3	131
280.90	0.43		
282.04	0.56	Structural-transition point	
283.17	0.73	288	33
284.22	0.94		
285.24	1.22		
285.81	1.42		
286.05	1.53		
286.18	1.59		

Typical Raman spectra for the SF₆ hydrate system at 20 MPa are shown in **Figure VI-3**. The Raman peak of SF₆ molecules dissolved in the liquid aqueous phase cannot be analyzed because it is very weak. On the other hand, a single Raman peak is detected around 769 cm⁻¹ and 773 cm⁻¹ for the symmetric S–F stretching vibration in the SF₆ hydrate (**Figure VI-3 (a)**) and fluid SF₆ (**Figure VI-3 (b)**) phases, respectively. This result reveals that the SF₆ molecule occupies only the L-cage of the s-II unit lattice. Above 40 MPa, the single Raman peak in the SF₆ hydrate phase is detected around 772 cm⁻¹ as shown in **Figure VI-4**, and it is constant in the whole pressure region above 40 MPa.

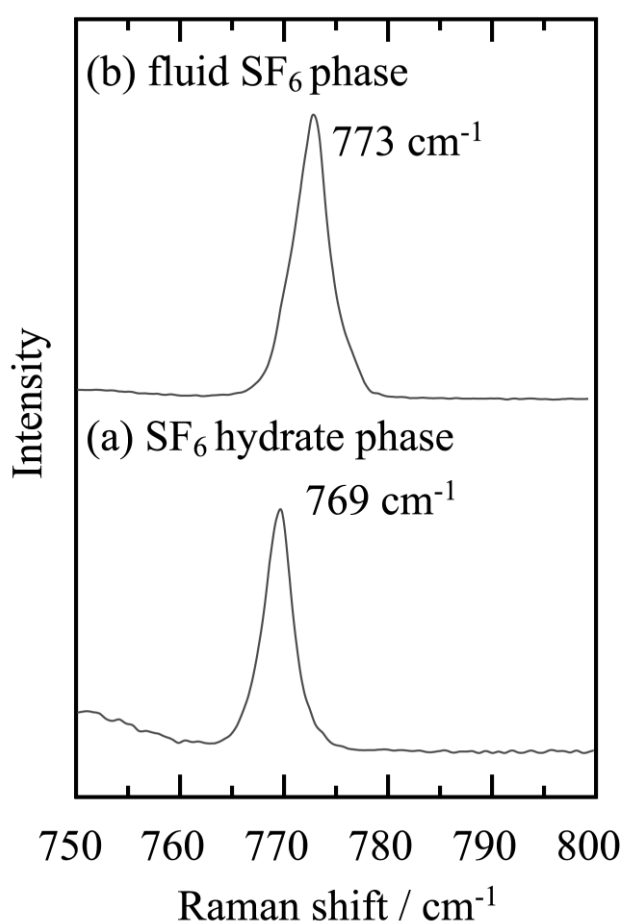


Figure VI-3 Raman spectra of the symmetric S–F stretching vibration mode of SF₆ molecules at 20 MPa. **(a)** SF₆ hydrate phase, **(b)** fluid SF₆ phase.

The pressure dependence of the Raman shift for the symmetric S–F stretching vibration is summarized in **Figure VI-5**. The Raman shift in the SF₆ fluid phase is detected at 773 cm⁻¹ in the whole pressure range of the present study. The Raman shift in the SF₆ hydrate phase is detected at 769 cm⁻¹ in the pressure range up to 30 MPa. While the Raman shift exhibits 3 cm⁻¹ blue shift above 33 MPa, that is, SF₆ hydrate changes the crystal lattice from the s-II to the structure-I (s-I) type near 33 MPa. According to the neutron diffraction experiment of Dyadin et al. (2002) [3], the s-II SF₆ hydrate changes to the s-I hydrate at 33 MPa. My results agree well with that of Dyadin et al. (2002) [3].

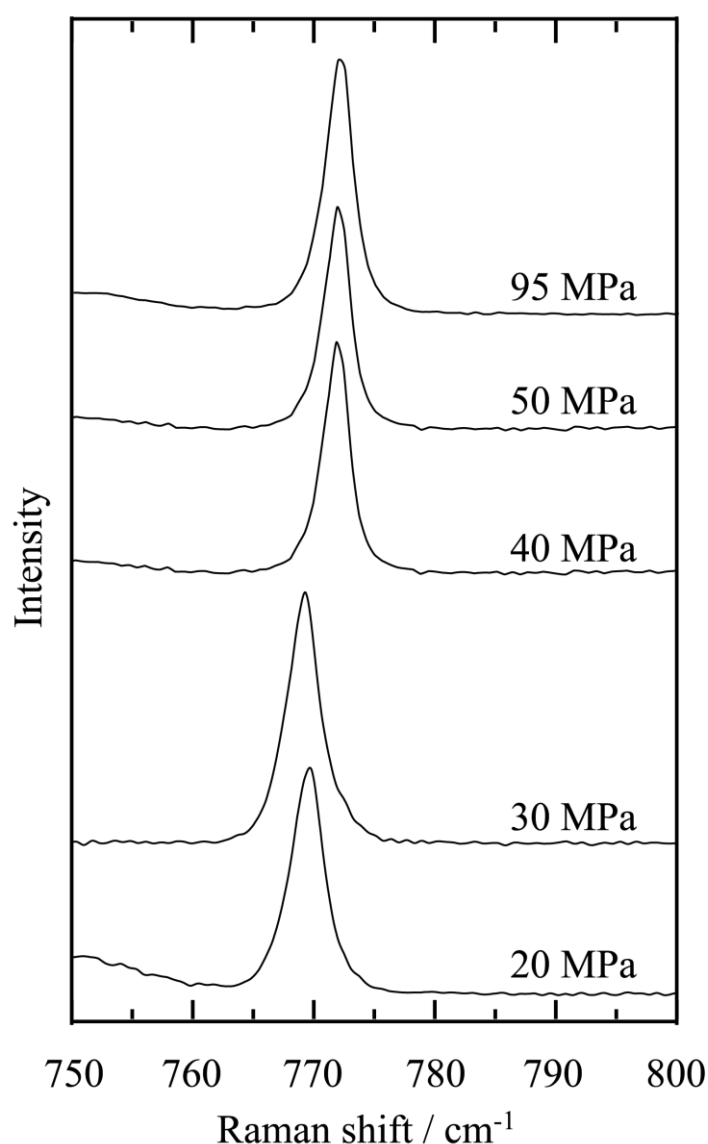


Figure VI-4 Raman spectra of the symmetric S–F stretching vibration in the SF₆ hydrate crystal on thermodynamic stability boundary.

The Raman shift of the intermolecular O–O stretching vibration mode of water molecules was usually detected around 205 cm^{-1} for s-I hydrate crystals in the low-pressure region (Nakano et al. 1998 [7], Nakano et al. 1999 [8], Morita et al. 2000 [9], Sugahara et al. 2000 [10], Suzuki et al. 2001 [11]). The Raman shift of the intermolecular O–O vibration mode in the SF_6 hydrate crystal is detected at 210 cm^{-1} as shown in **Figure VI-6** and agrees well with that of the s-II THF hydrate crystal in the similar pressure region (Takasu et al. 2003 [12]). The Raman shift of the O–O vibration for the N_2 [Chapter-I] and Kr [Chapter-III] hydrates, both belong to the s-II hydrate, is obtained around 209 cm^{-1} from the extrapolation of their pressure dependence. These facts reveal that the Raman shift of the O–O vibration of s-II hydrates exhibits 5 cm^{-1} higher frequencies than that of s-I regardless of S-cage occupancies.

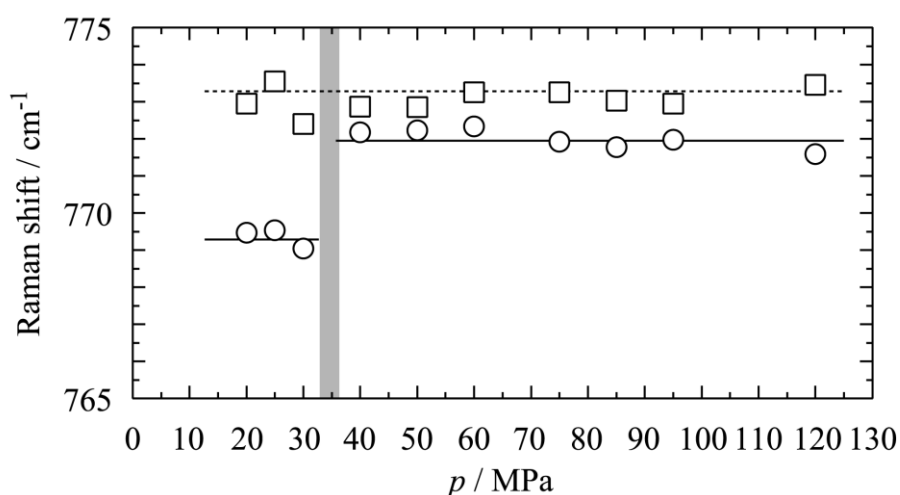


Figure VI-5 Pressure effect on the symmetric S–F stretching vibration in the SF_6 hydrate system: ○, hydrate phase; □, fluid phase.

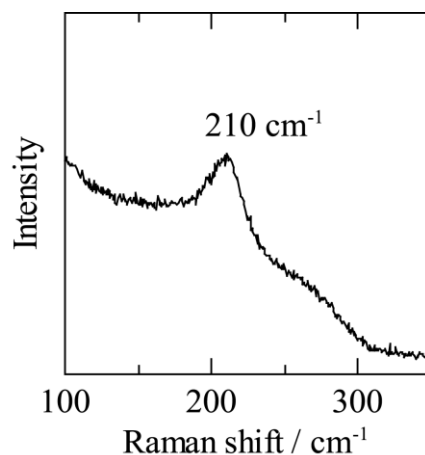


Figure VI-6 Raman spectrum of the intermolecular O–O vibration mode in the SF_6 hydrate crystal at 30 MPa.

Above 40 MPa, the SF₆ hydrate changes to the s-I. Therefore, it was supposed that the Raman peak of O–O vibration was detected around 205 cm⁻¹. However, the O–O vibration peak is vanished in a pressure region from 40 MPa to 120 MPa, even if the hydrate crystal seems to be apparently single crystal as shown in **Figure VI-7**. It is certain that the pressure where the Raman peak disappears coincides with the structural transition point. At the pressure, the SF₆ molecule is removed into the M-cage of s-I from the L-cage of s-II by pressurization. We speculate that the M-cage would be modified and distorted by taking the SF₆ molecule in forcibly. However, the peak disappearance is not interpreted sufficiently at the present time.

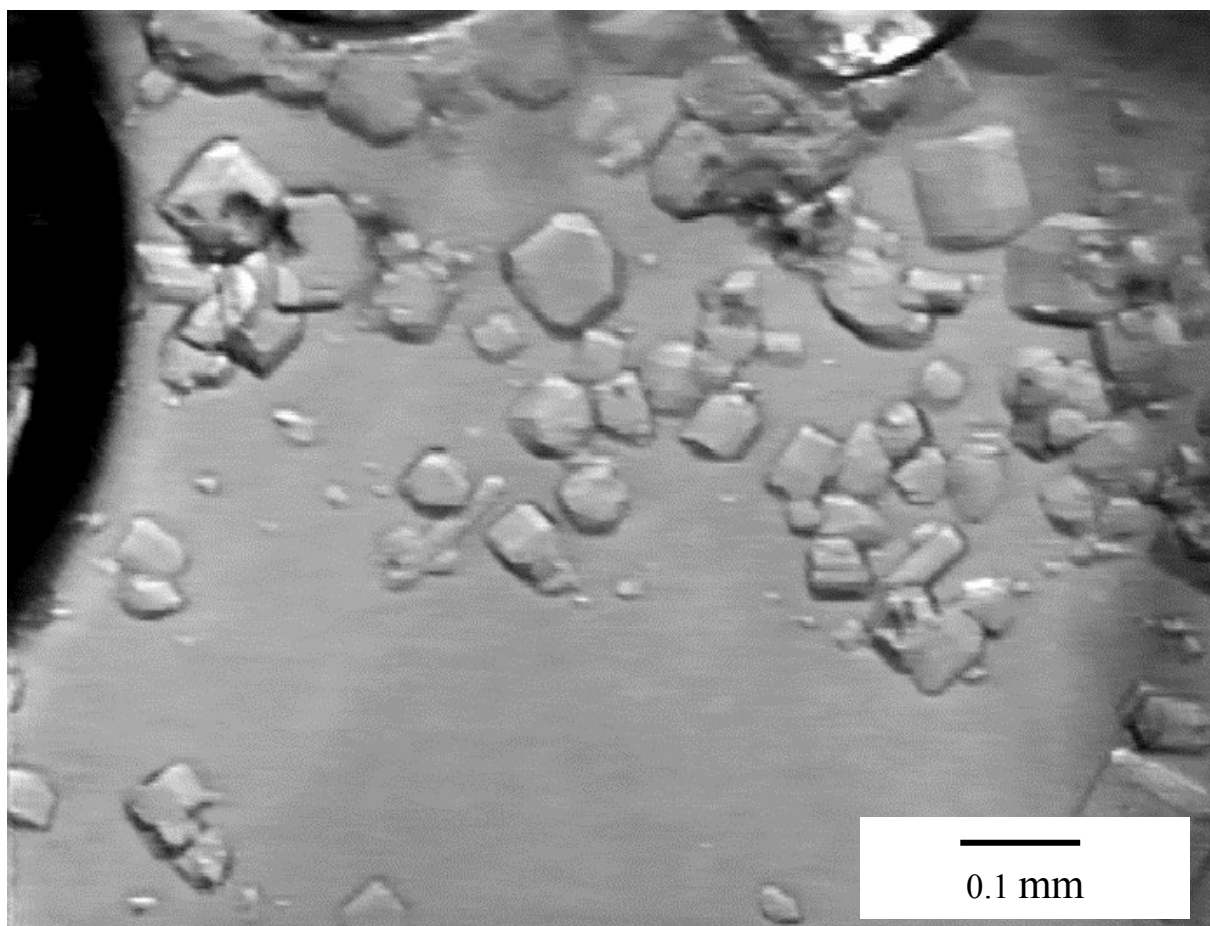


Figure VI-7 A photo of single crystals of SF₆ hydrate at 293 K and 60 MPa.

Summary

Three-phase coexisting curves of SF₆ hydrate system were obtained up to 155 MPa by use of high-pressure optical cell. Two quadruple points (four phases coexisting points; Q₂ and Q₃) were determined at 286.6 K and 1.79 MPa (Q₂; SF₆ hydrate + aqueous + liquid SF₆ + gas), and at 300.3 K and 131 MPa (Q₃; SF₆ hydrate + aqueous + liquid SF₆ + solid SF₆), respectively. Based on the discontinuity of dp/dT on the stability boundary at 33 MPa, the structural-phase transition point was also determined at 288 K and 33 MPa. The pressure dependence of the Raman shift for the symmetric S–F stretching vibrational mode also supports that the pressure-induced structural transition occurs in the pressure region near 33 MPa. These facts indicate that the s-II SF₆ hydrate changes to the s-I at the pressure.

Nomenclature

p = pressure [Pa]

T = temperature [K]

<Symbols>

F = fluid phase

G = gas phase

H = hydrate phase

L = liquid phase

S = solid phase

<Subscripts>

1 = host component (water)

2 = guest component (SF₆)

Literature Cited

- [1] Sloan, E. D., Jr. "Fundamental Principles and Applications of Natural Gas Hydrates", *Nature*, **426**, 353-359 (2003).
- [2] Manakov, A. Y.; Goryainov, S. V.; Kurnosov, A. V.; Likhacheva, A. Y.; Dyadin, Y. A.; Larionov, E. G. "Clathrate Nature of the High-Pressure Tetrahydrofuran Hydrate Phase and Some New Data on the Phase Diagram of the Tetrahydrofuran-Water System at Pressures up to 3 GPa", *Journal of Physical Chemistry B*, **107**, 7861-7866 (2003).
- [3] Dyadin, Y. A.; Larionov, E. G.; Manacov, A. Y.; Kurnosov, A. V.; Zhurko, F. V.; Aladko, E. Y.; Aladko, A. I.; Tolochko, B. P.; Sheromov, M. A. "Clathrate Hydrate of Sulfer Hexafluoride at High Pressures", *Journal of Inclusion Phenomena and Macrocyclic Chemistry*, **42**, 213-218 (2002).
- [4] Miller, S. L.; Eger, E. I.; Lundgreen, C. "Anasthetic Potency of CF_4 and SF_6 in Dogs", *Nature*, **221**, 468-469 (1969).
- [5] Sortland, L. D.; Robinson, D. B. "The Hydrates of Methane and Sulphur Hexafluoride" *Canadian Journal of Chemical Engineering*, **42**, 38-41 (1964).
- [6] Rubin, B.; McCubbin, T. K., Jr; Polp, S. R. "Vibrational Raman Spectrum of SF_6 ", *Journal of Moecular. Spectroscopy*, **69**, 254-259 (1978).
- [7] Nakano, S.; Moritoki,; M. Ohgaki, K. "High-Pressure Phase Equilibrium and Raman Microprobe Spectroscopic Studies on the CO_2 Hydrate System", *Journal of Chemical and Engineering Data*, **43**, 807-810 (1998).
- [8] Nakano, S.; Moritoki,; M. Ohgaki, K. "High-Pressure Phase Equilibrium and Raman Microprobe Spectroscopic Studies on the Methane Hydrate System", *Journal of Chemical and Engineering Data*, **44**, 254-257 (1999).

- [9] Morita, K.; Nakano, S.; Ohgaki, K. "Structure and Stability of Ethane Hydrate Crystal", *Fluid Phase Equilibria*, **169**, 167-175 (2000).
- [10] Sugahara, T.; Morita, K.; Ohgaki, K. "Stability Boundaries and Small Hydrate-Cage Occupancy of Ethylene Hydrate System", *Chemical Engineering Science*, **55**, 6015-6020 (2000).
- [11] Suzuki, M.; Tanaka, Y.; Sugahara, T.; Ohgaki, K. "Pressure Dependence of Small-Cage Occupancy in the Cyclopropane Hydrate System", *Chemical Engineering Science*, **56**, 2063-2067 (2001).
- [12] Takasu, Y.; Iwai, K.; Nishio, I. "Low Frequency Raman Profiles of Type-II Clathrate Hydrate of THF and Its Application for Phase Identification", *Journal of Physical Society of Japan*, **72**, 1287-1291 (2003).

General Conclusion

Through this thesis, I have revealed various interesting phenomena. I believe that these findings reported in this thesis are one of the most important fundamental data for understanding the scientific properties of pure gas hydrates and developing “attractive applications using gas hydrates”. The especially important discoveries are summarized as follows.

High-Pressure stability

Noble gas, having a simple and spherical shape, is the most appropriate guest species for investigating the relation between the thermodynamic stability and the molecular size. In Chapter-III and Chapter-IV, the stability boundaries of three noble gas (Ar, Kr, and Xe) hydrate systems were investigated in the pressure range up to approximately 500 MPa. The single crystals of each noble gas hydrate were analyzed under three-phase coexisting condition (hydrate + aqueous + gas) based on the Raman spectra of intermolecular O–O vibration energies. The stability boundaries of three noble gas hydrate systems depend on the molecular sizes of guest species. The equilibrium temperature becomes higher Ar (0.38 nm) < Kr (0.40 nm) < Xe (0.43 nm) in that order. The slight difference of molecular size results in a different trend of structural phase transition along the stability boundaries. The Ar hydrate crystal changes from the structure-II (s-II) to the structure-I (s-I) at 281 MPa and 302.7 K and from the s-I to structure-H (s-H) at 456 MPa and 304.6 K. The Kr hydrate crystal changes from the s-II to the s-H at 414 MPa and 319.2 K, whereas the s-I Xe hydrate exhibits no structural phase transition. In Chapter-VI, the stability boundaries of SF₆ hydrate system were investigated up to 155 MPa. Two quadruple points Q₂ (hydrate + liquid SF₆ + gas + aqueous) and Q₃ (hydrate + liquid SF₆ + solid SF₆ + aqueous) are located at 1.79 MPa and 286.6 K, 131 MPa and 300.3 K, respectively. Based on the discontinuity of dp/dT on the hydrate stability boundary and the results of Raman spectra of the symmetric S–F vibration, the s-II SF₆ hydrate crystals changed to the s-I at 33 MPa and 288 K. The pressure-induced structural phase transition to few vacant S-cage of s-I such a low pressure may be caused by the existence of many vacant S-cages of s-II SF₆ hydrate.

Pressure oppressive S-cage occupancy

In Chapter-V, the three-phase coexisting (hydrate + aqueous + fluid CF_4) curve of CF_4 hydrate system was investigated up to 454 MPa. The single crystals of CF_4 hydrates were analyzed under three-phase coexisting condition by use of a Raman spectrometer. The split of Raman spectra for the intramolecular symmetric C–F vibration in the CF_4 hydrate crystal is detected in the higher-pressure range than 70 MPa. This evidence indicates that the CF_4 molecule (0.52 nm) occupies both the S-cage (0.51 nm) and M-cage (0.58 nm) of s-I hydrate at a pressure above 70 MPa. In addition, the S-cage occupancy of the CF_4 molecule becomes larger with pressure increasing, because the peak area ratio ($S_{\text{S-cage}}/S_{\text{M-cage}}$) increases with pressure. It means that the CF_4 molecule shows peculiar cage occupancy so-called “pressure oppressive S-cage occupancy”. The ratio would approach to nearly one-third at approximately 600 MPa.

The relation between hydrate structures and the O–O vibration energies

In this thesis, the Raman shifts of O–O vibration energies were obtained in seven pure hydrate systems. The pressure dependences on the intermolecular vibrations based on the *in situ* Raman spectroscopy are clarified. The s-I hydrates that consist of a comparatively small guest molecule, Ar (from 281 to 456 MPa; Chapter-IV), Xe (Chapter-III), and N_2O (Chapter-II) showed a pressure dependence of O–O vibration energy (Type-A) along with methane and CO_2 hydrate systems. The relatively large molecule like CF_4 (Chapter-V), which occupies only M-cages, showed almost constant vibration energy (205 cm^{-1} ; Type-B) as well as ethane and cyclopropane hydrate systems. The O–O vibration energies in the s-II hydrates, Ar (below 281 MPa; Chapter-IV), Kr (Chapter-III), N_2 (Chapter-I), and SF_6 (Chapter-VI) are approximately 5 cm^{-1} higher than those of the Type-A s-I hydrates. Oppositely, the s-H hydrate, Ar (above 456 MPa; Chapter-IV) and Kr (above 414 MPa; Chapter-III), showed O–O vibration energies smaller than those of the Type-A s-I hydrates. These results indicate the hydrate lattice structure can be distinguished based on the relation between Raman shift of O–O vibration energy and pressure along the stability boundaries. According to the review (Ohgaki 2009 [1]), Raman shift of the O–O vibrations in low-pressure s-H hydrate systems is detected around 200 cm^{-1} . The relations between the hydrate structures and the pressure dependencies of the intermolecular O–O vibrations are shown in **Figure A**.

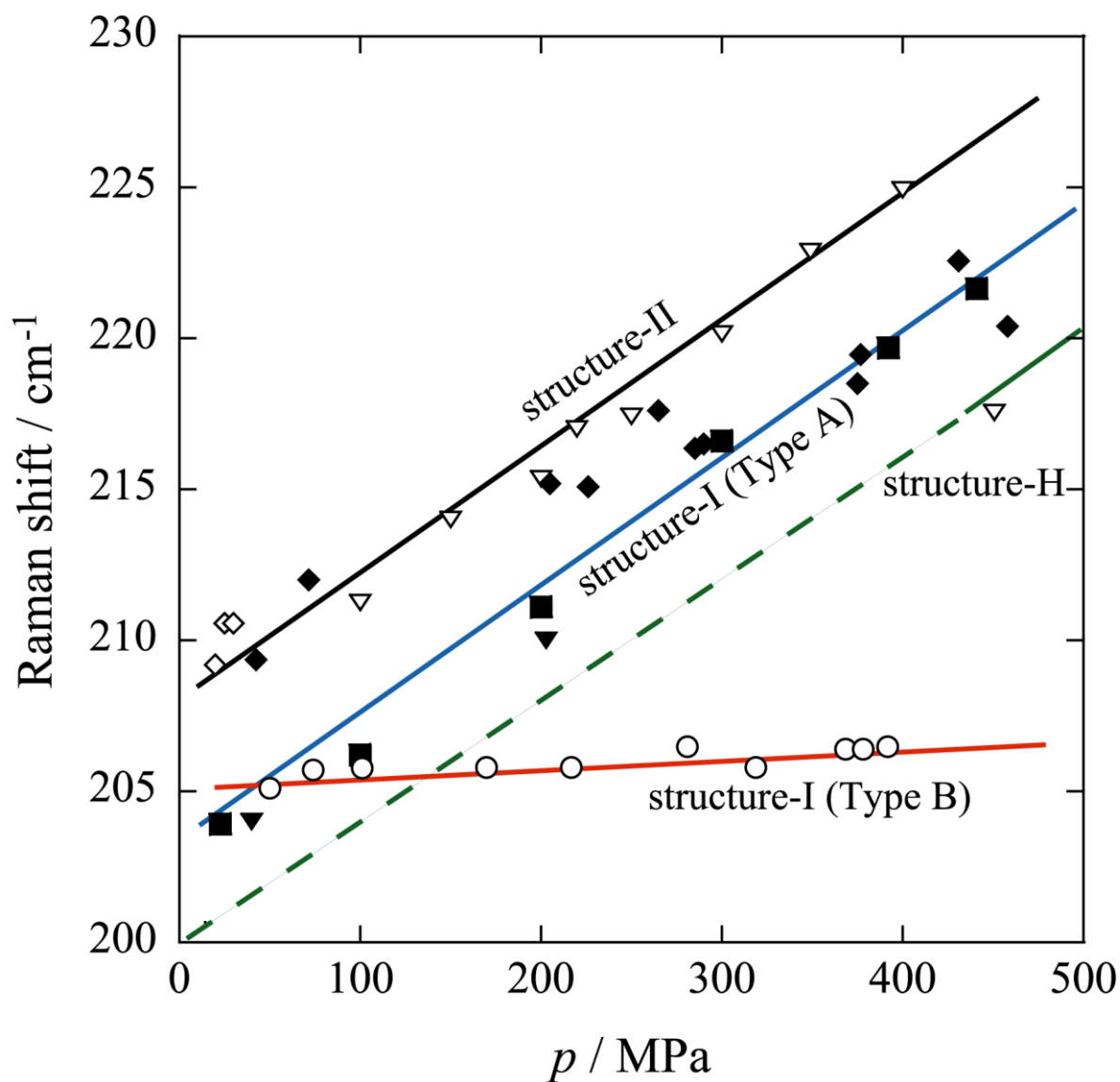


Figure A Pressure dependencies of the Raman peak corresponding to the intermolecular O–O vibrations under three-phase equilibrium conditions. \blacklozenge , Ar hydrate (Chapter-IV); ∇ , Kr hydrate (Chapter-III); \blacksquare , Xe hydrate (Chapter-III); \blacktriangledown , N₂O hydrate (Chapter-II); \circ , CF₄ hydrate (Chapter-V); \diamond , SF₆ hydrate (Chapter-VI).

Literature Cited

[1] Ohgaki, K. “Properties and Functions of Gas Hydrates (in Japanese)”, *The Review of High Pressure Science and Technology*, **19**, 148-155 (2009).

List of Publications and Presentations

Publications (papers)

Main works for this thesis

{1} Keisuke Sugahara, Yuuki Tanaka, Takeshi Sugahara, and Kazunari Ohgaki

“Thermodynamic Stability and Structure of Nitrogen Hydrate Crystal”

Journal of Supramolecular Chemistry, **2**(4-5), 365-368 (2002)

{2} Keisuke Sugahara, Masayoshi Yoshida, Takeshi Sugahara, and Kazunari Ohgaki

“High-Pressure Phase Behavior and Cage Occupancy for the CF₄ Hydrate System”

Journal of Chemical and Engineering Data, **49**(2), 326-329 (2004)

{3} Keisuke Sugahara, Takeshi Sugahara, and Kazunari Ohgaki

“Thermodynamic and Raman Spectroscopic Studies of Xe and Kr Hydrates”

Journal of Chemical and Engineering Data, **50**(1), 274-277 (2005)

{4} Keisuke Sugahara, Masayoshi Yoshida, Takeshi Sugahara, and Kazunari Ohgaki

“Thermodynamic and Raman Spectroscopic Studies on Pressure-Induced Structural Transition of SF₆ Hydrate”

Journal of Chemical and Engineering Data, **51**(1), 301-304 (2006)

{5} Keisuke Sugahara, Ryuji Kaneko, Arata Sasatani, Takeshi Sugahara, and Kazunari Ohgaki

“Thermodynamic and Raman Spectroscopic Studies of Ar Hydrate System”

The Open Thermodynamics Journal, **2**, 95-99 (2008)

{6} Takeshi Sugahara, Akira Kawazoe, Keisuke Sugahara, and Kazunari Ohgaki

“High-Pressure Phase Equilibrium and Raman Spectroscopic Studies on Nitrous Oxide Hydrate System”

Journal of Chemical and Engineering Data, **54**(8), 2301-2303 (2009)

Other works

{7} Takeshi Sugahara, Keisuke Sugahara, and Kazunari Ohgaki

“Phase Behavior for Pure and Mixed Gas Hydrate Systems (in Japanese)”

The Review of High Pressure Science and Technology, **12**(1), 34-39 (2002)

{8} Noriyuki Shimada, Keisuke Sugahara, Takeshi Sugahara, and Kazunari Ohgaki

“Phase Transition from Structure-H to Structure-I in the Methylcyclohexane + Xenon Hydrate System”

Fluid Phase Equilibria, **205**(1), 17-23 (2003)

Presentations (international conferences)

[1] Takeshi Sugahara, Keisuke Sugahara, and Kazunari Ohgaki

“Small Cage-Occupancy of Guest Species in the Ethane, Ethylene and Cyclopropane Hydrate Systems”

Proceedings of the Fourth International Conference on Gas Hydrates, Yokohama, Japan, Vol. 2 pp. 608-613, (2002)

[2] Keisuke Sugahara and Kazunari Ohgaki

“High-Pressure Phase Equilibrium and Raman Spectroscopic Studies on CHF_3 Hydrate System”

The 1st International 21 Century COE Symposium on Integrated EcoChemistry, Toyonaka, Japan (2003)

[3] Keisuke Sugahara and Kazunari Ohgaki

“High-Pressure Raman Spectroscopic Study for CF_4 Hydrate System”

The 2nd International 21 Century COE Symposium on Integrated EcoChemistry, Awaji Island, Japan (2003)

[4] Keisuke Sugahara and Kazunari Ohgaki

“High-Pressure Raman Spectroscopic Studies on Structure-I and -II Hydrates”

The 3rd International 21 Century COE Symposium on Integrated EcoChemistry, Suita, Japan (2004)

Acknowledgements

First of all, the author is greatly indebted to Professor Kazunari Ohgaki (Division of Chemical Engineering, Department of Materials Engineering Science, Graduate School of Engineering Science, Osaka University) for his significant guidance throughout his student life without whose guidance his study could not be successful.

The author is also grateful to Professor Yoshiro Inoue (Division of Chemical Engineering, Department of Materials Engineering Science, Graduate School of Engineering Science, Osaka University) and Professor Michio Matsumura (Research Center for Solar Energy Chemistry, Osaka University) for their helpful comments and suggestions to his study.

The author would also like to thank Associate Professor Hiroshi Sato (Division of Chemical Engineering, Department of Materials Engineering Science, Graduate School of Engineering Science, Osaka University) for his helpful advice on this study and to thank Dr. Masato Moritoki for his technical support of experiment apparatus. The author also expresses his thanks to Mr. Masao Kawashima for his helpful advice and assistance in the GHAS (Gas-Hydrate Analyzing System) room.

The author wishes to express his sincere appreciation to Assistant Professor Takeshi Sugahara (Division of Chemical Engineering, Department of Materials Engineering Science, Graduate School of Engineering Science, Osaka University) for innumerable assistances, guidance, and encouragements throughout his student life. The author would also like to thank Professor Naoshi Suzuki (Kansai University) and Assistant Professor Atsushi Tani (Department of Earth and Space Science, Graduate School of Science, Osaka University). Thanks are made to Dr. Shunichi Iida, Dr. Takashi Makino, Dr. Kei Takeya, and Dr. Shunsuke Hashimoto. In addition, thanks are given to his collaborators, Mr. Yuuki Tanaka, Mr. Noriyuki Shimada, Mr. Shu Saito, Mr. Toshiyuki Nakamura, Mr. Masayoshi Yoshida, Ms. Asami Asanoma, Mr. Michiharu Taniguchi, Mr. Ryuji Kaneko, Mr. Arata Sasatani, Mr. Akira Kawazoe, Mr. Takaaki Tsuda, Mr. Yuuki Matsumoto, and the other members of Ohgaki laboratory.

Finally, the author would like to thank his family, Toshio Sugahara, Emiko Sugahara, Rieko Shibata, and Kenji Sugahara for their continuous and hearty encouragements to him.

This work was supported by the center of excellence (21COE) program "Creation of Integral EcoChemistry" of Osaka University from 2002 to 2005.

Keisuke Sugahara